Sede Amministrativa: Università degli Studi di Padova

Dipartimento di

MEDICINA MOLECOLARE

CORSO DI DOTTORATO DI RICERCA IN: BIOMEDICINA

CURRICOLO: MEDICINA MOLECOLARE

CICLO XXIX

Insights into the functionality and druggability of the homodimerization of human papillomavirus E6 oncoprotein

Coordinatore: Ch.mo Prof. Stefano Piccolo

Supervisore: Ch.mo Prof.ssa Arianna Loregian

Dottorando: Lorenzo Messa

Table of Contents

Abstract

High-risk human papillomaviruses (HR-HPV), typified by HPV16 and HPV18, are the cause of several epithelial cancers, including cervical, oropharyngeal, and anogenital carcinomas. The mechanisms by which HR-HPV infections lead to malignant cell transformation rely mainly on the activities of two viral oncoproteins, E6 and E7, which synergistically act to transform and immortalize the infected cell. E6 is considered the main oncoprotein responsible for cellular transformation, since its sustained expression and transforming activity are key elements for tumor progression. Recent structural and mutational studies revealed the importance of a conserved alpha-helix (α2) in the N-terminal domain of E6 for the productive degradation of p53. Indeed, a few key residues of the α2-helix form a hydrophobic pocket on E6 protein surface which was shown to be crucially involved in the interaction with p53. Notably, the α2-helix was previously characterized to be important also for E6 self-association, an event poorly understood that involves the same amino acids important for the binding to p53. Thus, the hydrophobic pocket corresponding to the α2-helix of E6 seems to be important for different protein-protein interactions and represents a new attractive target for the development of anti-E6 compounds, since no specific anti-HPV drugs exist so far.

In the present PhD thesis we demonstrate that HPV16 E6 can dimerize not only *in vitro* but also in cells, and the dimerization is specifically driven by the α2-helix. In addition, our results suggest that the homodimerization of E6 is not required for the degradation of p53 and thus these two interactions, i.e., the binding of E6 to p53 and E6 self-association, likely occur independently of each other and probably in different cellular compartments. Furthermore, we observed that E6 induces the upregulation of TAZ which is, together with YAP, the main transducer of the Hippo signaling pathway, controlling organ size, tumorigenesis and metastasis. Strikingly, this process seems to require E6 self-association, since dimerization-defective E6 mutants are unable to upregulate TAZ in transfected cells. Finally, with the goal to develop dual inhibitors that could block the protein-protein interactions occurring on the α2-helix of the viral oncoprotein, we performed *in silico* drug screenings, taking advantage of the available structural models, and identified some candidate compounds fitting on the hydrophobic core of the α2-helix of E6. We then evaluated their ability to impair both E6 self-association and the E6-mediated degradation of p53. Strikingly, we identified one compound able to block both interactions, thus representing a candidate dual inhibitor, which could also induce the downregulation of E6 protein levels in parallel to its ability to rescue p53 in transfected cells. This compound also exhibited specific anti-proliferative and anti-clonogenic activities against HPV-positive cells. In conclusion, the present study successfully investigated and elucidated the potential role of E6 homodimerization with regard to the transforming activities of the viral oncoprotein, and demonstrated that targeting the α2-helix of high-risk E6 proteins may represent a novel fascinating strategy for the development of anti-E6 compounds.

Riassunto

I papillomavirus umani ad alto rischio (HR-HPV), rappresentati dai genotipi 16 e 18, sono causa di diversi tumori epiteliali, inclusi carcinomi della cervice uterina, dell'orofaringe e anogenitali. I meccanismi attraverso i quali le infezioni da HR-HPV portano alla trasformazione cellulare maligna, si basano sulle attività di due oncoproteine virali, E6 ed E7, le quali agiscono sinergisticamente per trasformare ed immortalizzare le cellule infettate. E6 è considerata la principale oncoproteina responsabile della trasformazione cellulare, in quanto la sua prolungata espressione ed attività trasformante sono elementi chiave per la progressione del tumore. Alcuni recenti studi strutturali e mutazionali hanno rivelato l'importanza di un'alfa elica (α2) nel dominio N-terminale di E6, altamente conservata tra i vari genotipi di HR-HPV, per la degradazione di p53. Infatti, è stato visto che alcuni residui chiave di quest'alfa elica formano una tasca idrofobica sulla superficie di E6 cruciale per l'interazione con p53. In più, era stato visto anche che quest'alfa elica media l'autoassociazione di E6, un processo che, sebbene poco caratterizzato, coinvolge gli stessi aminoacidi necessari per il legame a p53. Perciò, la tasca idrofobica corrispondente all'elica α2 di E6 sembra essere importante per diverse interazioni proteina-proteina e rappresenta un nuovo affascinante target per lo sviluppo di composti anti-E6, considerato che ad oggi non esistono ancora farmaci contro HPV.

In questa tesi di dottorato dimostriamo come E6 di HPV16 possa dimerizzare non solo *in vitro* ma anche nelle cellule, e come la dimerizzazione di E6 sia mediata specificamente dall'elica α2. Inoltre, i nostri risultati suggeriscono che la dimerizzazione di E6 non è necessaria per la degradazione di p53 e che quindi queste due interazioni proteina-proteina, cioè il legame di E6 a p53 e l'autoassociazione di E6, possano avvenire indipendentemente l'una dall'altra e probabilmente in compartimenti cellulari diversi. In aggiunta abbiamo osservato che E6 stabilizza i livelli di TAZ che, assieme a YAP, è il principale effettore della via di segnalazione Hippo, che regola la crescita degli organi ed anche i processi di tumorigenesi e di metastasi. Sorprendentemente, questo processo pare richiedere l'autoassociazione di E6, in quanto mutanti di E6 incapaci di dimerizzare, sono incapaci anche di stabilizzare TAZ in cellule trasfettate. Infine, con l'obiettivo di sviluppare inibitori duplici che possano bloccare entrambe le interazioni proteina-proteina che coinvolgono l'elica α2 dell'oncoproteina virale, abbiamo condotto degli screening *in silico* utilizzando i modelli strutturali disponibili in letteratura e abbiamo identificato alcuni composti in grado di legarsi al core idrofobico dell'elica α2 di E6. Abbiamo quindi valutato la loro capacità di interferire sia con l'autoassociazione di E6 che con la degradazione di p53 indotta da E6. Sorprendentemente, un composto si è rivelato capace di bloccare entrambe le interazioni, rappresentando quindi un potenziale inibitore duplice, e ha mostrato anche le capacità di indurre una diminuzione dei livelli di E6 in parallelo alla sua abilità di prevenire la degradazione di p53 in cellule trasfettate. In più, questo composto ha mostrato anche attività anti-proliferative e anti-clonogeniche specifiche contro cellule HPV-positive.

In conclusione, questo studio ha investigato con successo e chiarito il potenziale ruolo della dimerizzazione di E6 relativamente alle attività trasformanti dell'oncoproteina virale, e ha dimostrato che colpire l'elica α2 di E6 può rappresentare una strategia innovativa per lo sviluppo di composti anti-E6.

1. Introduction

1.1 Human papillomaviruses.

Human Papillomaviruses (HPVs) belong to the familiy of *Papillomaviridae*, which includes over 300 different papillomaviruses that infect a wide range of mammals and vertebrates. These viruses have evolved over millions of years to replicate themselves in epithelial tissues, with the ability to infect different anatomical sites, depending on the viral genotype involved [Egawa *et al.*, 2015].

Papillomaviruses are small, non-enveloped, ichosaedral DNA viruses of about 50-55 nm in diameter. In general, viral protein capsid is composed of 72 capsomeres, protecting a circular double-stranded DNA (dsDNA) genome of about 8 kilobases. The HPV genome encodes eight genes, six early (E1, E2, E4, E5, E6 and E7) and two late genes (L1 and L2), the latter encoding the two structural proteins composing the viral capsid (Figure 1.1).

To date, about 200 different HPV genotypes have been identified and characterized, and they are divided into 5 different classes (alpha-, beta-, gamma-, mu-, nu-) depending on evolutionary similarities. HPVs generally infect the basal keratinocytes of a differentiated epithelium and replicate following cell differentiation through all the epithelial layers towards the surface. Depending on the epithelial site of infection, HPVs can replicate both in cutaneous and in mucosal tissues, with particular genotype-specificity. However, despite the big heterogeneity, viruses belonging to different classes may replicate in the same epithelial niche and anatomical site, wherein each viral genotype has evolved to complete its life-cycle.

HPVs are so common among the population that nearly all humans are believed to have been exposed to the virus at least once during their lives [CDC fact sheet].
HPVs can cause distinctive epithelial lesions, usually characterized by the hyper-proliferation of the infected cells wherein the virus is replicating, but unapparent, asymptomatic or malignant lesions can also occur. Nevertheless, most HPV infections are usually cleared by the immune system and do not cause visible pathologies.

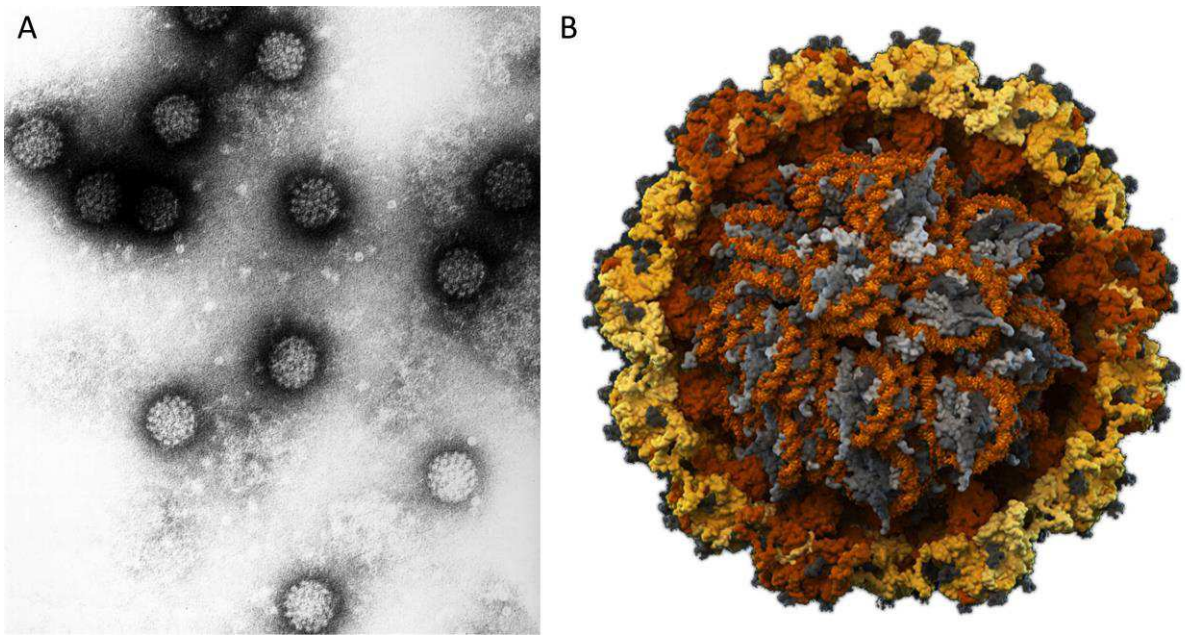

Figure 1.1. Human papillomavirus. (A) Electron microscope image of human papillomaviruses (German Cancer Research Center, DKFZ). **(B)** 3D model of a human papillomavirus (HPV) showing the cross section of a HPV virion. All virus-encoded proteins are shown in yellow shades and host-cell structures (including nucleosomes and surface glycosides) are shown in grey. The way of genome packing is hypothetical. Original image created by the Visual Science Company (www.visualsciencecompany.com/hpv).

1.2 Taxonomic classification.

According to the Papillomavirus Genome Database (PaVE, https://pave.niaid.nih.gov), approximately 220 different HPV genotypes have been classified to date (accessed September 2016). HPV classification relies on genomic homology rather than differences in the anatomical sites of infection or lesion characteristics. The phylogenetic algorithms used to classify new HPV types compare whole genome or subgenomic sequences [De Villiers *et al.*, 2004]. Thus, viruses belonging to different classes may replicate in the same epithelial compartment and share common clinical characteristics.
HPVs are divided into 5 different classes, also referred as *genera*, i.e., Alpha-papillomavirus, Beta-papillomavirus, Gamma-papillomavirus, Mu-papillomavirus and Nu-papillomavirus (Figure 1.2).

The major group of HPVs is the Alpha genus. PVs belonging to this group can infect both mucosal and cutaneous epithelia. They include the supergroup of sexually transmitted PVs, infecting the skin and mucosa of the genital tract, but they can also replicate in oral sites, such as pharynx and tongue. Cutaneous Alpha-PVs induce benign lesions while mucosal

viruses can also induce malignant neoplasias through a process of cellular transformation. Mucosal Alpha-PVs are thus subdivided into 'low-risk' and 'high-risk' genotypes, depending on their ability to induce cancer [Doorbar *et al.*, 2012].

Beta-PVs replicate exclusively in the skin. They usually do not induce visible lesions and persist in a latent state in general population. However, unapparent or latent infections of Beta-PVs can reactivate in immunocompromised patients or in individuals genetically susceptible to these viruses. Sporadically, these patients can develop non-melanoma skin cancer (NMSC) as a result of Beta-PV infections [Howley and Pfister, 2015].

Finally, HPV genotypes classified in the Gamma-, Mu- and Nu- genera all replicate in cutaneous epithelia. They usually induce benign lesions but they can also persist in a latent state. Although not extensively studied as the previous classes, Gamma- and Mu-PV infections are usually characterized by distinguishable intracytoplasmic inclusion bodies [Bolatti *et al.*, 2016]. In addition, along with Beta-PVs, viruses belonging to the Nu genus are also associated to the development of skin cancer [Grimmell *et al.*, 1988].

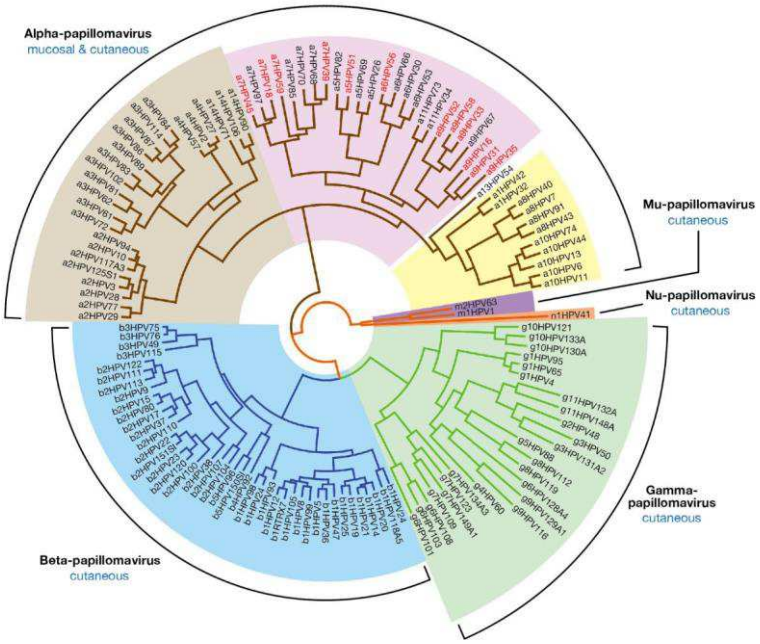

Figure 1.2. Phylogenetic classification of human papillomaviruses based on evolutionary similarities. HPVs are divided into 5 different classes: Alpha-, which comprehends low-risk cutaneous (light-brown), low-risk mucosal (yellow) and high-risk mucosal (pink) PVs; Beta- (blue); Gamma- (green); Mu- (purple); Nu- (orange). High-risk Alphapapillomaviruses highlighted in red are confirmed as "human carcinogens", while the others are considered "probable" or "possible" carcinogens [Egawa *et al.*, 2015].

1.3 Diseases associated with HPV infections.

HPV infections can induce different types of lesions depending on the epithelial area and anatomical site involved, which usually reflect genotype-specificity. Generally, viral life-cycle leads to the development of benign skin tumors as a result of cellular uncontrolled proliferation, but HPV infection by certain viral genotypes can also induce malignant tumors in a subset of anatomical sites [Egawa *et al.*, 2015].

Cutaneous Alpha-PVs, such as HPV2 and HPV10, replicate in the skin and induce common warts (*Verruca vulgaris*). Common warts are small, rough, usually round-shaped excrescences that occur on the skin of hands and feet, but can virtually grow anywhere in the body (Figure 1.3A). Sporadically, some cutaneous Alpha-PV, such as HPV7 and HPV3, can also replicate in mucosal tissues causing papillomas [Doorbar *et al.*, 2015].
Mucosal Alpha-PVs, such as HPV32, HPV6, HPV11 and HPV54, replicate in epithelial mucosal tissues. They can grow both in the genital or respiratory tract, causing anogenital warts (such as condyloma acuminata, venereal warts or anal warts), or oral papillomas, respectively (Figure 1.3B-D) [Doorbar *et al.*, 2015]. Although oral papillomas can induce laryngeal papillomatosis (a rare, potentially fatal medical condition wherein the uncontrolled growth of papillomas can obstruct the airways), lesions caused by these viruses are not considered harmful *per se,* and do not usually correlate with the insurgence of carcinomas, such as anal, cervical or oropharyngeal cancers. Thus, these HPVs are usually classified as 'low-risk' genotypes (LR-HPVs). On the contrary, mucosal Alpha-PVs that strongly correlate with the development of epithelial cancers, such as HPV16, HPV18, HPV31, HPV45 and HPV56, are classified as 'high-risk' genotypes (HR-HPVs). These viruses replicate in mucosal tissues, usually in the genital tract, and are strongly associated with vulvar, anal, penile or cervical cancer [Giuliano *et al.*, 2008]. Recently, increasing association between HR-HPV infections and the development of head-and-neck squamous cell carcinoma (HNSCC) has also emerged [Mallen-St Clair *et al.*, 2016]. At early stages of HR-HPV infection, lesions resemble flat warts (discussed below) and are usually classified as intraepithelial neoplasias type 1. If not efficiently counteracted by the immune system, these lesions often develop into a more severe condition, usually characterized by epigenetic modifications or changes in cell signalling, that lead to a dysregulated viral gene expression [Doorbar, 2005]. At this stage, lesions are classified as intraepithelial neoplasias type 2 and type 3. These are considered precancerous lesions that very easily develop into cancer, where hyper-methylation or integration of viral DNA into host genome is observed, with concomitant loss of productive viral life-cycle [Dutta *et al.*, 2015].

Viral genotypes belonging to the Beta genus, such as HPV5, HPV8 and HPV49, replicate within cutaneous epithelium and can cause different types of warts, such as common warts, plantar warts (*Verruca plantaris*) and flat warts (*Verruca plana*). Phenotypically, plantar warts are very close to common warts with the unique characteristic to have black tiny dots in the center and usually occur on the sole of the feet. Flat warts instead are small, red-coloured, smooth papillomas that tend to accumulate in large numbers on the face, neck,

hands and wrists (Figure 1.3E-F). Infections driven by Beta-PVs tend to remain silent and inapparent, with visible manifestations occurring during condition of stress and reduction of the immune response. Rarely, Beta-PVs can also induce skin cancers acting synergistically with UV radiation and immune suppression to transform keratinocytes [Quint *et al.*, 2015]. In addition, Beta-PV infections correlate with Epidermodysplasia verruciformis (also known as the *tree man illness*), a rare genetic disorder in which patients are highly susceptible to HPV infections, with high risk of developing skin carcinomas.

Gamma-PVs, Mu-PVs and Nu-PVs, such as HPV4, HPV1 and HPV41, respectively, induce benign lesions of the skin, usually common warts or plantar warts. They rarely replicate in mucosal tissues and, apart from HPV41, they have been never linked to the development of skin cancers.

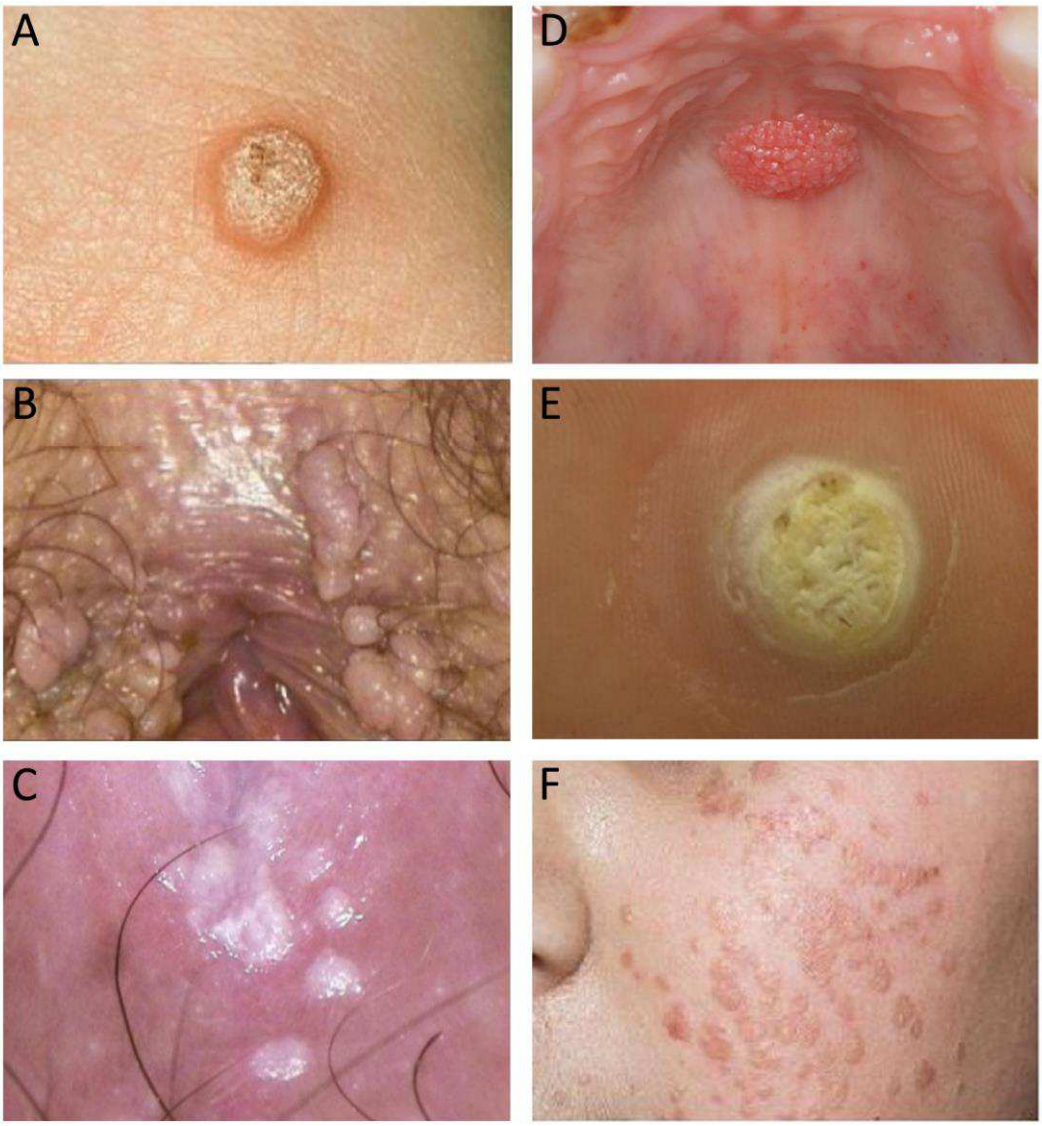

Figure 1.3. Lesions caused by HPV infections. (A) Common wart occurring on a hand. **(B)** Condyloma acuminata on the perineum. **(C)** Genital wart occurring in the vaginal introitus. **(D)** Oral squamous papilloma. **(E)** Plantar wart. **(F)** Flat warts occurring on the face.

1.4 HPV life-cycle.

The molecular mechanisms of HPV life-cycle and the viral genome and protein characteristics known to date usually refer to Alpha-PVs. Alpha genus is the main class of HPVs that has been extensively studied during the last 30 years and thus most knowledge about HPVs derives from some representative genotypes of this class, but general characteristics apply to most, if not all, HPVs.

Papillomaviruses are very simple DNA viruses that encode a restricted small number of viral proteins, and thus, their life-cycle is strictly connected to the transcriptional and replicational machinery of the infected host cell. Indeed, after centuries of evolution, Papillomaviruses have evolved the ability to finely hijack the cellular environment, in order to efficiently replicate within the infected cell [Hebner and Laimins, 2006].

It is commonly accepted that Papillomaviruses require a break in the epithelium to successfully infect the host, such as microwounds or abrasions, in order to reach the basal keratinocytes of the skin (Figure 1.4). These are S-phase-competent cells which express the appropriate cellular machinery required for the initiation of viral replication [Doorbar, 2005]. In addition, these cells express the primary and secondary receptors required for viral attachment and entry, which occur through the interaction with heparin sulphate proteoglycans and alpha-6 integrin, although the involvement of this membrane-associated secondary receptor remains somehow controversial [Giroglou *et al.*, 2001; Yoon *et al.*, 2001].

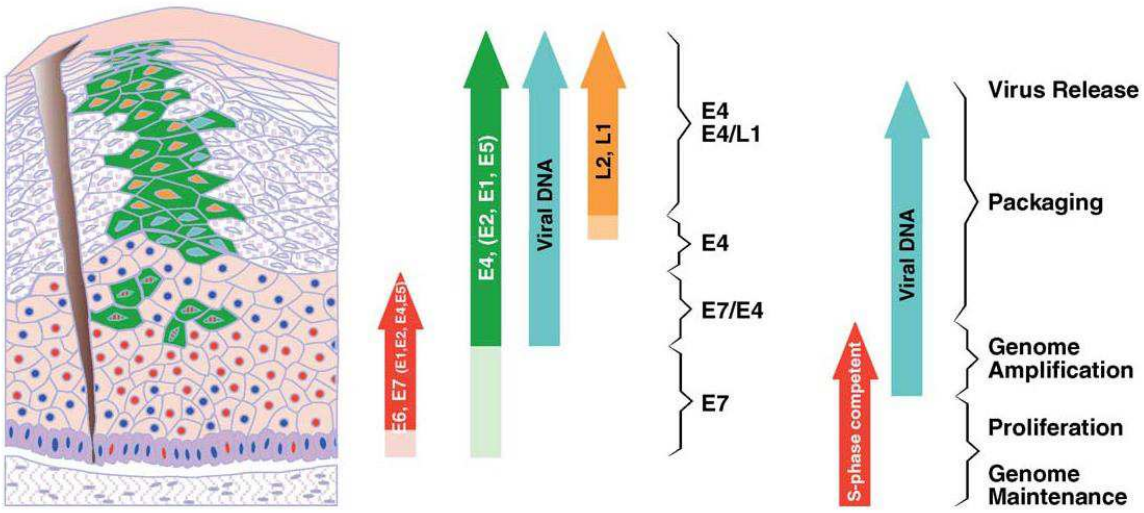

Figure 1.4. Schematic representation of the life-cycle of an Alpha-PV (such as HPV2, HPV11 or HPV16) during a productive infection. The patterns of viral gene expression represented on the right correspond to the different stages of the viral life-cycle as the infected cell migrates towards the epithelial surface [Doorbar, 2005].

Once attached, virions are internalized by endocytosis and undergo endosomal transport and uncoating [Hindmarsh *et al.*, 2007]. After release from the endosome, viral DNA is carried into the nucleus of the cell by L2 protein-DNA complexes [Holmgren *et al.*, 2005].

At the early steps of infection, when the viral DNA enters the nucleus of a basal keratinocyte, viral proteins E1 and E2 are expressed and viral genome is replicated and maintained as a low copy number episome (20-200 copies per cell) [Lambert, 1991]. As soon as the infected cell enters mitosis, two daughter cells will be produced both harbouring episomal viral DNA. This process is a consequence of E1 and E2 protein activities, which allow the virus to synchronally replicate along with the cellular genome and subsequently segregate its DNA by tethering the viral episomes to cellular chromatin [Oliveira *et al.*, 2006]. It has been suggested that persistance of HPV requires the infection of a basal stem cell, rather than a transiently amplifying suprabasal cell [Egawa, 2003]. Thus, as the basal stem cell divides, a differentiating daughter cell will be produced, migrating outwards through the suprabasal layers, while the other will not differentiate, allowing the persistance of viral DNA in the lower lamina of the epithelium.

The fate of a normal cell within stratified squamous epithelia is to leave the basal layers and proceed towards the surface, generating new mature keratinocytes. This event is accompanied by a process of terminal differentiation, and thus the differentiating cell leaves the cell cycle and stops replicating its own DNA. However, HPV requires an active replicational cellular machinery in order to amplify its genome, which will be packed into the capsid of the progeny virions in the upper lamina of the epithelium. Infected keratinocytes that leave the basal layer do not exit the cell cycle as HPV expresses two oncoproteins, E6 and E7, whose function is to keep the infected cell in an S phase-like state. These two proteins modulate the regulation of the cell cycle by impairing the negative regulatory signals that would stop cellular growth. E6 and E7 act on many different cellular proteins important for cell-cycle control, differentiation and apoptosis, for example p53 and pRb, respectively [Howley, 2006]. Thus, the infected cell continuously proliferates while migrating within the parabasal and middle layers, allowing HPV to successfully amplify its DNA.

At this stage of infection, the expression pattern of viral proteins changes and HPV enhances the expression of E1 and E2 and, together with E6 and E7, it starts expressing also E4 and E5. These two proteins modify the cellular environment contributing to viral genome amplification [Davy *et al.*, 2009]. E5 is the third minor oncoprotein, whose function is to contribute to cellular proliferation by cooperating with E6 and E7 [Bouvard *et al.*, 1994]. E4 is highly expressed in the middle-upper layers and blocks the infected cell in the G_2 to M phase transition, creating the optimal environment for viral DNA amplification [Davy *et al.*, 2005].

As the infected cell reaches the granular layer of the epithelium, it exits the cell-cycle, and the virus starts expressing L1 and L2 viral proteins while retaining only high expression levels of E4. L1 and L2 are the major and minor coating proteins of the capsid, respectively, and allow viral genome encapsidation inside the nucleus of the infected cell [Barksdale and Baker, 1993]. L2 binds on the viral genome and induce genome packaging inside L1-rich icosahedral capsid particles. Finally, virus maturation occurs in the most superificial layers,

wherein abundant disulphide bonds occur between L1 molecules, creating highly stable virions. In addition, high levels of E4, organized into amyloid fibres, disrupt keratin structure, contributing to viral release and transmission [McIntosh *et al.*, 2008].
Progeny virions are thus released from the superficial dying keratinocytes and spread in the surrounding tissue.

1.4.1 Genome architecture.

With regard to viral genome architecture, HPVs possess a double-stranded DNA genome that does not usually integrate and exists in the form of episome, with an average length of about 8kb. HPV genome is divided into 3 functional regions: one non-coding regulatory region named Long Control Region (LCR) and two groups of Open Reading Frames (ORF), named early (E) and late (L), respectively.

The LCR contains transcription factor-binding sites and the origin of replication, along with enhancers and silencers. Both viral and cellular proteins can bind on the LCR. E1 and E2 regulate the replication of viral DNA and transcription of early proteins, respectively, and possess highly conserved binding sites on viral LCR [Desaintes and Demeret, 1996]. Cellular transcription factors such as Nuclear Factor 1 (NF1), Activator Protein 1 (AP1) and Specificity protein 1 (Sp1) can also bind, promoting the transcription of viral proteins at the early stage of infection [Chong *et al.*, 1991].

The early ORF includes genes encoding all the early viral proteins (E1, E2, E4, E5, E6 and E7) and occupies most of the viral genome. Transcription of the early proteins occurs through multiple early promoters and stops at different early polyadenilation sites (PE and pAE, respectively), producing polycistronic mRNAs [Zheng and Baker, 2006]. In addition, viral mRNAs undergo abundant alternative splicing events, thus increasing the extent of translated proteins [Rush *et al.*, 2005].

The third region of viral genome is the late ORF which encodes the two structural proteins, L1 and L2. Although the late ORF is located downstream of the early ORF, late promoters (PL) are situated within the early ORF and thus some early proteins are still transcribed during the late phase of infection, such as E5 and E4 [Ozbun and Meyers, 1997]. The activation of PLs follows cell differentiation in the upper epithelial layers [Geisen and Kahn, 1996]. Therefore, viral transcription programs are finely regulated according to the differentiation state of the infected cell, involving host transcription factors that are differentially expressed from the basal layers towards the surface.

1.4.2 E1.

E1 is a replicative protein of about 68 kDa, essential for the replication of viral DNA [Ustav and Stenlund, 1991]. It is the only enzyme encoded by HPV. E1 possesses ATPase and DNA helicase activities, and belongs to the family of ATPases [Yang *et al.*, 1993]. It is composed of three domains: an N-terminal regulatory region, a central DNA-binding domain, and a C-terminal ATPase/helicase domain that can also mediate E1 oligomerization. The C-terminal domain of E1 is the core of its activity, essential to drive viral DNA replication [Amin *et al.*, 2000].

E1 binds with E2, and this interaction facilitates the attachment of E1 to the HPV genome [Frattini and Laimins, 1994]. E1 then binds DNA in the dimeric form on specific E1 binding sites [Auster and Joshua-Tor, 2004]. Following the denaturation of the origin of replication, E1 forms hexamers and this oligomerization is triggered by the interaction of E1 with some cellular chaperone proteins [Liu *et al.*, 1998; Enemark and Joshua-Tor, 2006]. These cellular factors increase E1 affinity for viral DNA and enhance E1 helicase activity, thus facilitating the formation of pre-replication complexes. Once E1 oligomers are formed, the viral protein hydrolyses ATP into ADP and the energy is used to unwind the double helix of viral DNA, which in turns allows the transcription of viral genes [Sanders and Stenlund, 1998].

In order to carry out the complete replication of viral DNA, E1 recruits several cellular proteins involved in eukaryotic genome replication, such as DNA polymerases, topoisomerases and replication factors [Melendy *et al.*, 1995]. E1 possesses nuclear localization and nuclear export sequences (NLS and NES, respectively), but the role of cytoplasmic E1 remains elusive [Fradet-Turcotte *et al.*, 2010]. It can be phosphorylated by cyclin/Cdk complexes, and the interaction with these complexes is driven by a cyclin-binding motif (CBM) in the N-terminal domain of E1 [Ma *et al.*, 1999]. In addition, it was also shown that E1 binds to cellular chromatin and chromatin-remodeling complexes, thus altering the structure of nucleosomes in the proximity of viral DNA [Swindle and Engler, 1998]. This was suggested to serve as a mechanism to enhance the replication of viral genome and to allow viral genes to be efficiently transcribed by the cellular transcriptional machinery.

1.4.3 E2.

The viral regulatory protein E2 is a 40 kDa protein composed of 3 functional regions: an N-terminal transactivating domain, typical of transcription factors, a central hinge region and a C-terminal DNA binding/dimerization domain.

E2 works as a transcription factor during the viral life-cycle and fulfills its functions mainly in the form of dimers [Hedge *et al.*, 1992]. The main function of E2 is to regulate the transcription of viral genes by binding on different E2-binding sites on the LCR [McBride *et al.*, 1991]. Viral gene transcription relies on active cellular transcriptional machinery, and indeed, a complex framework of interactions between E2 and different cellular transcription factors, including p300 and AP1, exists [Krüppel *et al.*, 2008]. E2 is thought to regulate the transcription in a dose-dependent manner, in such a way that at low concentrations it drives the transcription of early genes, while at higher concentrations the transcription is impaired, possibly by hindering the recruitment of cellular transcription factors on viral promoters [Steger and Corbach, 1997]. Additionally, E2 can regulate the transcription of different cellular genes, thus altering their expression depending on the phase of the HPV life-cycle [Lee *et al.*, 2002].

Apart from its crucial role in gene transcription, E2 is also important for the regulation of viral DNA replication and genome partitioning [Sarafi and McBride, 1995]. Indeed, through its N-terminal domain, E2 interacts with the helicase domain of E1 and this interaction serves as an “ignition switch” for viral DNA replication. After the assembly of E1-E2 dimers, E1 can efficiently recognize the origin of replication and E2 is subsequently displaced. In addition, E2 interacts with cellular replication factors that are recruited at the origin of replication.

When an infected basal keratinocyte enters mitosis, E2 can ensure the partitioning of viral episomes to the daughter cells. This is possible through a direct binding between E2 (bound to viral DNA) and mitotic chromosomes, either by binding to chromatin or chromatin-associated proteins, such as Brd4 or ChLR1 [Baxter *et al.*, 2005].

Finally, E2 has also an indirect role for HPV-induced cellular transformation. Indeed, E2 finely regulates the expression of E6 and E7 during the viral life-cycle, but loss of E2, along with a non-productive viral replication, is a common characteristic of HPV-induced carcinomas [Burd, 2003]. This event is usually a result of viral DNA integration into the host genome, an accidental process that results in the disruption of the coding sequence (Cds) of E2, thus abolishing the production of the protein. As a direct consequence, deregulation of *E6* and *E7* genes induces their overexpression, a crucial event for cancer development and progression.

1.4.4 E4.

E4 is an early protein that, during the viral life-cycle, accumulates at high levels within the middle layers of the epithelium. E4 is expressed from a spliced transcript that starts at the E1 ORF, and thus the protein is sometimes referred as E1^E4 [Nasseri *et al.*, 1987]. E4 supports virus maturation and egress in the middle-upper layers of the epithelium. Although the precise molecular mechanisms of this protein remain partly unknown, E4 plays an important role in HPV genome amplification in the upper layers by inhibiting mitotic progression and cellular replication [Knight *et al.*, 2004]. Infected cells harbouring high levels of E4 are thus blocked in the G_2 to M phase transition and this event seems to be required for the final stage of viral DNA amplification, before genome encapsidation [Davy *et al.*, 2005]. In the most superficial layers, where progeny virions are produced, E4 is crucial for viral release as it assembles into amyloid fibres that disrupt cell architecture [McIntosh *et al.*, 2008].

1.4.5 E5.

E5 is a very small, highly hydrophobic protein of about 80 amino acids. It is an accessory protein whose physiologic role is to cooperate with E6 and E7 for efficient hijacking of cellular environment [Moody and Laimins, 2010]. Consequently, like E6 and E7, E5 is considered an oncoprotein for its ability to interfere with some carcinogenic signaling pathways. Due to its extreme hydrophobicity, E5 is hardly detectable and is generally expressed at low levels [Disbrow *et al.*, 2003]. E5 localizes within cellular membranes, particularly within the endoplasmic reticulum (ER), plasma or nuclear membranes, depending on the viral genotype [Conrad *et al.*, 1993]. For example, high-risk E5 proteins preferentially localize within the ER membranes. The main function of E5 is to prevent cell death by inhibiting extrinsic death receptor-mediated and intrinsic ER stress-induced apoptosis [Jiang and Yue, 2013]. E5 can impair the accumulation of Fas receptors and the formation of DISC, induced by TRAIL, on the plasma membrane. Due to its ability to localize within the ER, E5 suppresses also the expression of different cellular proteins of the ER stress pathway, such as IRE1α. This activity prevents pro-apoptotic signals that can activate cell death through intrinsic apoptosis. Although classified as an oncoprotein, E5 is rarely detected in cervical cancers as viral DNA integration results in loss of E5 protein expression [Chang *et al.*, 2001]. For this reason, and also for being the smallest virus-encoded oncoprotein, researchers usually refer to E5 as the third minor HPV oncoprotein.

1.4.6 E6.

E6 is a small, cysteine-rich protein of about 150 amino acids. It is an accessory protein essential for cellular hijacking in order to promote viral replication [Howie *et al.*, 2009]. For its crucial activity and carcinogenic potential, E6 is considered the main HPV oncogene. Structurally, E6 is composed of just two zinc-like finger domains (named $E6_N$ and $E6_C$, respectively), which both contain two highly conserved cysteine motifs (CxxC), connected by a flexible loop of about 35 amino acids. In addition, high-risk E6 proteins possess a C-terminal class I unstructured PDZ-binding motif (PBM) that confers the ability to bind cellular PDZ-containing proteins, such as Scribble (hScrib) and Disc Large (hDlg) (Figure 1.5).

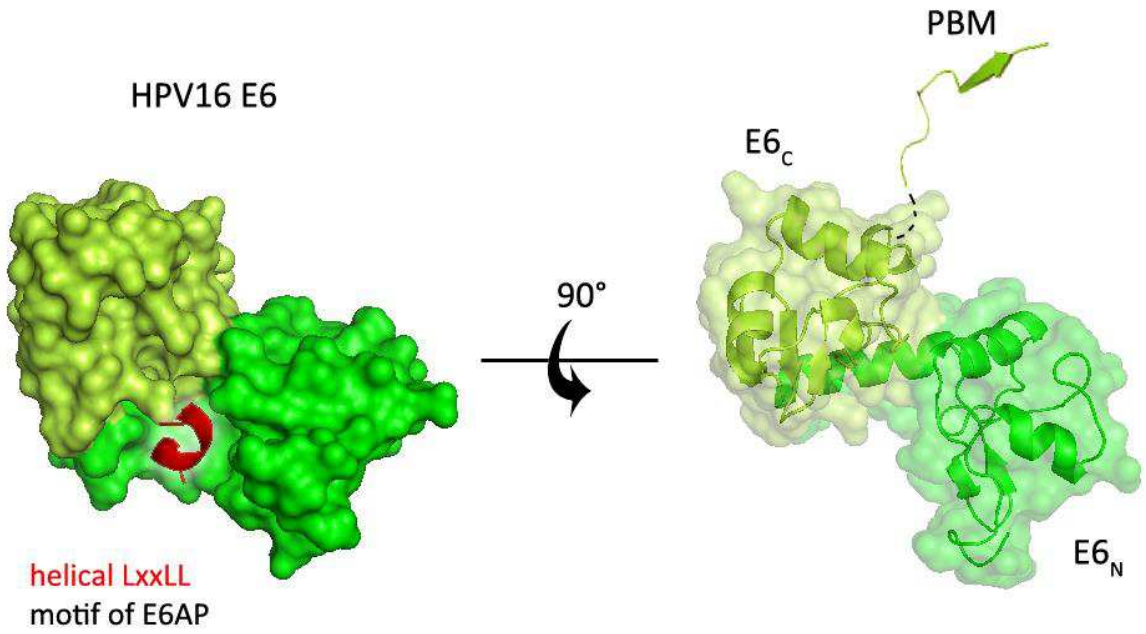

Figure 1.5. Structural model of HPV16 E6 with the LxxLL helical motif of E6AP tightening the conformation of the viral oncoprotein (PDB accession code: 4GIZ). Cartoon representation on the right includes the PBM (PDB accession code: 2KPL). The model was generated in PyMol (DeLano Scientific, California, USA).

The physiological role of E6 is to keep the infected cell in an S-phase-like state, cooperating with E7 for efficient cellular hijacking [Hebner and Laimins, 2006]. In general, E6 is known to block p53-mediated pathways, preventing cellular apoptosis and growth arrest that would result as a consequence of E7 activity [Werness *et al.*, 1990; Kessis *et al.*, 1993]. Although there are differences between the activities of low-risk and high-risk variants, all E6 proteins possess no enzymatic activity and trigger their functions only through protein-protein interactions.

In general, E6 has evolved the ability to bind several cellular proteins and induce their degradation, taking advantage of the cellular proteasome machinery [Scheffner *et al.*, 1990]. High-risk E6 proteins can induce the degradation of its targets by binding to cellular ubiquitin ligases, such as Ubiquitin-protein ligase E3A, also known as E6-associated protein (E6AP) [Huibregtse *et al.*, 1993]. Once bound to E6AP, E6 binds to its cellular targets and stimulates their polyubiquitination. In addition to p53, many other cellular proteins are degraded in a similar manner, such as procaspase 8, Bak, Scribble and MAGI-1 (see also Paragraph 1.6.1) [Thomas and Banks, 1998; Nakagawa and Huibregtse, 2000; Glaunsinger *et al.*, 2000; Filippova *et al.*, 2007].

E6 is a very unstable protein that easily aggregates and precipitates *in vitro* with a high cellular turnover [Kehmeier *et al.*, 2002; Zanier *et al.*, 2007; Zanier *et al.*, 2010]. Within the infected cell, E6 is generally located within the nucleus, and its nuclear import is mediated by its NLSs, but different localizations have been reported depending on the viral genotype involved [Tao *et al.*, 2003; Mesplède *et al.*, 2012].

E6 is translated from a bicistronic pre-mRNA that comprehends coding sequences of both *E6* and *E7* [Schwartz, 2013]. In addition, high-risk E6 proteins undergoe alternative splicing events, which produce a subset of different mRNAs that encode smaller spliced variants, such as E6*I and E6*II [Cornelissen *et al.*, 1990]. These are the two main spliced isoforms whose roles remain so far elusive. Anyway, with regard to E6 oncogenic activities, several reports pointed to a negative regulatory function of E6*I, which seems to modulate the activity of the full-length protein by direct binding [Pim *et al.*, 1997; Pim and Banks, 1999]. However, other reports have reported an intrinsic oncogenic potential of E6*I, which can induce the degradation of different tumor-suppressor proteins in the absence of full-length E6 [Pim *et al.*, 2009]. The expression levels of both spliced isoforms vary depending on the viral genotype, but E6*I is usually expressed at levels comparable to those of the full-length protein, and thus it might substantially contribute to the E6-mediated mechanisms of cellular transformation.

1.4.7 E7.

E7 is an acidic protein of about 100 amino acids which mainly localizes in the nucleus of infected cells [Knapp *et al.*, 2011]. It is composed of 3 conserved regions (CR1, CR2 and CR3, respectively), the first two included within the N-terminal domain, the third in the C-terminal domain. The N-terminus of E7 (CR1/CR2) is unstructured and might fold only upon interactions with cellular targets, while the C-terminal domain is tightly packed into a zinc finger domain.

The main biological function of E7 is to induce cellular proliferation by impairing the exit from the cell cycle, thus inducing cellular immortalization [Hebner and Laimins, 2006]. This is a necessary step to promote viral replication, as it keeps the infected cell in S-phase, thus enhancing the replication of viral DNA. Similarly to other viral oncoproteins, with which it shares sequence similarity (such as polyomavirus early T-antigens), E7 can block the growth arrest of infected cells by impairing the activities of cellular retinoblastoma (Rb) proteins [Münger *et al.*, 1989]. E7 of both low-risk and high-risk PVs can bind pRb and pRb-related proteins, such as p107 and p130, with differential affinities depending on the viral genotype [Hu *et al.*, 1995]. Either pRb degradation or pRb phosphorylation have been reported [McIntyre *et al.*, 1996; Huh *et al.*, 2007]. In any case, E7 binds to pRb through a highly conserved LxCxE motif in its N-terminal domain. The interaction induces pRb inactivation or its proteasome-dependent degradation, and the N-terminal domain of E7 represents the core of its activity [Lee *et al.*, 1998]. However, due to its unfoldedness, structural studies on the N-terminal domain of E7 have been so far hampered [Garcia-Alai *et al.*, 2007(a)].

Similarly to E6, E7 can also interact with many other cellular proteins, such as p21, p600 and c-Myc (see also Paragraph 1.6.1) [Huh *et al.*, 2005; Wang *et al.*, 2007; Shin *et al.*, 2009]. The compact structure of the C-terminal domain of E7 allowed structural studies both through NMR or crystallization [Ohlenschlager *et al.*, 2006; Liu *et al.*, 2006]. This region seems to serve as a platform for different protein interactions as well as for E7 dimerization, whose role seems to be anyhow unrelated to the immortalization activity of the viral protein.

As mentioned in Paragraph 1.4.6, E7 is translated from a bicistronic pre-mRNA that undergoes multiple splicing events. Generally, E7 is translated from a spliced mRNA that also encodes for E6*I [Schwartz, 2013]. Very recently, a spliced E6^E7 isoform has been also reported [Ajiro and Zheng, 2015].

1.4.8 L1 and L2.

L1 and L2 are structural proteins that compose the viral capsid, with an average diameter of 55 nm. The viral capsid has an icosahedral symmetry and is composed of 72 pentamers. A single pentameric unit contains 5 copies of L1, and thus, a total of 360 molecules form the virion.

Due to its preponderance in the structure of viral capsid, L1 is considered the major coating protein. It is highly conserved among PVs and mediates also viral attachment by binding to cell surface receptors of basal keratinocytes. Viral entry is a complex process that involves different protein-protein interactions and relies also on the activity of L2, which is exposed to the surface of the virion upon viral attachment [Sapp and Day, 2009].

L2 is considered the minor coating protein and localizes internally into the virion, since it cannot be detected on the external surface [Richards *et al.*, 2006]. When exposed, it binds to a secondary receptor on the cellular membrane, mediating the entry of the L2-genome complex. Inside the cell, L2 drives the transport of viral genome into the nucleus by binding to syntaxin18 and through its NLS [Bossis *et al.*, 2005]. In addition, L2 is important for genome packaging as it binds to L1 through hydrophobic interactions. The stoichiometry of L1-L2 complexes is 5:1, and thus, one molecule of L2 can bind a single pentameric unit [Finnen *et al.*, 2003].

1.5 Epidemiology and current therapies.

The incidence of HPV infections is so high among general population that approximately all humans are believed to have been infected by a HPV genotype, belonging to any of the five genera, at least once during their lives. This is due to the ubiquitous presence of the virus worldwide, making it one of the most common viral infectious agent, together with herpesviruses and rhinoviruses. However, accurate estimates are practically impossible because most of HPV infections are efficiently cleared by the immune system, usually within 18 months from the initial infection, and cause unapparent or asymptomatic infection diseases [Stanley, 2008].

Classification of HPVs is based on the ability of a viral genotype to induce malignant lesions, and thus reflects the subdivision into low-risk and high-risk genotypes. Epidemiologically, the incidence of HPV infections every year usually refers to the prevalence of mucosal Alpha-PVs among the population suffering from epithelial neoplasias, usually in the anogenital area [Munoz *et al.*, 2003]. Indeed, HPV is the most common sexually transmitted infectious agent, which can infect both males and females, particularly among young persons within the first years after sexual debut [Dunne *et al.*, 2007]. The prevalence of HPV infections in the genital area is about 70 million cases only in the United States of America, with an incidence of 14 new million cases every year. Anyhow, the presence of Alpha-PVs is not solely restricted to the genital area, since HPVs can also replicate in the oropharyngeal tract, and thus the prevalence of HPV infections might be globally underestimated.

In general, the estimated lifetime risk of a HPV infection is very high, but only about 1% of all infections will develop cancer. This process requires the persistence of HPV and the inability of the host immune system to completely remove the infected cells over a prolonged period of time [Siegel *et al.*, 2014]. HPV infections correlate with the development of different mucosal malignancies. They are the aetiological agents of about 99% cases of cervical cancer, 90% cases of cancer of the anus, approximately 70% cases of vaginal and penile cancers and a variable percentage of oropharyngeal cancers (between 30% and 60%) [CDC, Centers for Disease Control and Prevention]. Cervical cancer is the 7th most common type of malignant neoplasia worldwide, and with approximately 500,000 new cases every year, it is the 4th most common cancer in women, with an extremely high mortality rate (50%) [WCRF International]. However, oropharyngeal cancer incidence is expected to surpass cervical cancer by 2020 [Garland *et al.*, 2016].

To date, no specific anti-HPV drugs are commercially available in order to fight pre-existing infections. Prophylactic vaccination has been employed since 2006 as a first line strategy against HPV infections and the spreading of HPV-induced malignancies. Back in 1992, Merck Inc. initiated the HPV Vaccine program. After extensive research on the production of stable and immunogenic virus-like particles (VLP), in the early 2000's Phase II/III clinical trials started using stable L1-based VLPs produced in yeast, as the L1 protein was known to be highly immunogenic. In 2006, the quadrivalent (4vHPV) Gardasil® was licensed by the Food

and Drug Administration (FDA), protecting from genotypes 16, 18, 6 and 11 females between 9 and 26 years old [Villa *et al.*, 2005]. Subsequently, the bivalent (2vHPV) Cervarix® was developed by GlaxoSmithKline and licensed by the FDA, protecting from genotypes 16 and 18. In the years after, the license was extended also for males and in 2014, the nonavalent vaccine (9vHPV) was further developed and licensed for protecting both males and females against genotypes 16, 18, 6, 11, 31, 33, 45, 52 and 58 [Bryan *et al.*, 2016]. Anti-HPV vaccines have been developed in order to limit the spreading of genital warts (mainly caused by HPV6 and 11) and anogenital cancers (induced by the most common high-risk genotypes, i.e., HPV16, 18, 31, 33, 45, 52, and 58). Indeed, data emerging in the last years support the effectiveness of the vaccination program, as the incidence of HPV6, 11, 16 and 18 decreased from 12% to 5% in 2013 in the USA among females 14-19 years old [Markowitz *et al.*, 2013]. In addition, a decline of cervical high-grade lesions prevalence was also observed in Australia in 2011 [Immunize Australian Program]. However, prophylactic vaccines have no effect against pre-existing infections and thus the real effectiveness in the general population is so far limited, as the herd immunity will be effective only after a prolonged period of time and with a sustained worldwide vaccination campaign.

In the absence of specific anti-HPV drugs, current therapies involve the use of classic treatments, such as surgery, radiotherapy and chemotherapy (alone or in combination). *Conization* is one of the common surgery treatments, which is a clinical procedure consisting in the removal of a "suspected" conic piece of tissue from the cervix. However, when the development of a malignant lesion is evident, *total hysterectomy* is usually employed, which consists in the removal of the uterus. In the most severe cases of invasive carcinomas, *radical trachelectomy* or *pelvic exenteration* are employed, with the removal of the uterus and surrounding tissues.
Radiotherapy is a treatment that exploits high-energy wavelengths to kill cancer cells, but with severe collateral effects, since also healthy cells surrounding the tumour are affected. Chemotherapy treatments exploit chemical substances that hamper tumour growth before surgical intervention. The treatment can be systemic or localized, but in both cases collateral effects are often present.

Current drug therapies rely on the use of different drugs proved to be efficacious in the treatment of HPV-induced benign and malignant hyperproliferations. Cidofovir (CDV) is an acyclic nucleoside phosphonate known for its broad-spectrum antiviral activity against DNA viruses, proved to be efficacious in patients suffering from HPV-associated diseases, showing antiproliferative properties [Mertens *et al.*, 2016]. Other drugs used to treat HPV-induced diseases are Imiquimod and Cisplatin [Busch *et al.*, 2016]. However, all these drugs have demonstrated insufficient efficacy if used alone, and Cisplatin, which is a drug commonly used for cancer chemotherapy, has demonstrated high renal cytotoxic effects with only 10-20% of responses. [Suarez-Ibarrola *et al.*, 2016]. In addition, the use of chemotherapeutic agents can result in drug resistance caused by the upregulation of certain signalling pathways in cancer cells.

1.6 Virus-induced human oncogenesis.

The mechanisms of human viral oncogenesis are generally characterized by their intimate addiction to the activity of one or more viral oncoproteins. Oncoviruses are a heterogeneous class of both DNA and RNA viruses that possess the unique ability to transform and immortalize the infected cell through the expression of distinct oncogenes [Mesri *et al.*, 2014]. The role of these viral oncoproteins is strictly connected to the success of viral replication and they generally serve as a "cellular switch", keeping the infected cell on a competent state for productive viral replication (Figure 1.6). Furthermore, centuries of evolutionary pressure have selected viral genotypes able to maximize viral replication and escape the immune system in the infected tissue. This process has in turn selected the most efficient viral protein variants that can potentially induce cancer, a "side effect" of the natural role of these proteins.

As a general rule, the continuous activity of the viral oncoprotein(s), usually associated with persistent infection, is a necessary, but not sufficient, trait for cancer development. The multistep process of viral oncogenesis relies on the intimate need of an "environmental co-factor", which can be either a chronic inflammatory response or a condition of immunosuppression, which drives the infected cell through a slow process of malignant transformation. Viral oncoproteins generally target some selected cellular pathways, which are the central regulators of cell cycle, cell survival and cellular proliferation, in particular p53, NF-kB, Wnt, hTERT, Hippo and pRb-mediated pathways.

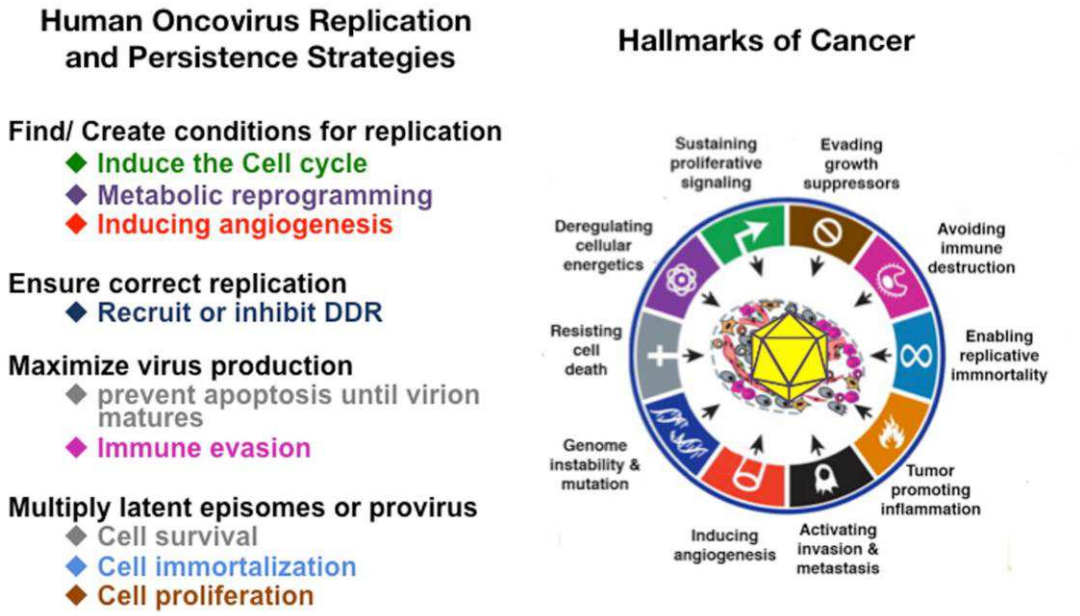

Figure 1.6. General mechanisms of virus-induced oncogenesis. Cancer hallmarks depicted on the right result as a consequence of the activities of the viral oncoproteins, which are needed to maximize viral replication and persistence [Mesri *et al.*, 2014].

1.6.1 Mechanisms of HPV-induced carcinogenesis.

The mechanisms of HPV-induced carcinogenesis rely on the cooperative and continuous activity of E6 and E7. When overexpressed, these two proteins deeply perturb the cellular environment, creating the favourable conditions for cellular transformation. As mentioned in Paragraph 1.4.6 and 1.4.7, the physiological role of these two proteins is to keep the infected cell on a competent state to promote viral replication.

When a HR-HPV genotype (such as HPV16 or HPV18) infects basal keratinocytes, the virus starts replicating within the mucosal epithelium and usually produces a benign lesion (which resembles a flat wart) classified as Low-grade Squamous Intraepithelial Lesion (LSIL) or intraepithelial neoplasia type 1. Generally, also HR-HPV infections are efficiently cleared by the immune system, and thus most infections spontaneously resolve within months. However, if the infection persists, lesions caused by HR-HPVs can easily progress towards malignancy and develop cancer. This process is a direct consequence of viral DNA integration or, alternatively, its hypermethylation, which frequently occur when the infection is driven by a high-risk genotype. This event causes the deregulation of viral genes expression, resulting in the overexpression of E6 and E7, which are the driving forces for cancer development and progression.

However, evidences suggest that the majority of HR-HPV-associated cancers arise from the cervical and anal transformation zones and from the crypts of the oropharynx. In these particular epithelial compartments, cells respond differently to the growth signals from the neighbouring cells and poorly support viral replication [Egawa *et al.*, 2015]. Thus, viral gene expression is poorly controlled and easily results in the development of carcinomas (Figure 1.7).

Accordingly, HPV-induced carcinomas have two distinctive characteristics: the loss of productive viral life-cycle and the complete addiction of malignant cells to the activity of E6 and E7. Indeed, viral DNA persists within the transformed keratinocytes, but its integration in the host genome ultimately leads to the complete inability to produce progeny virions. This event is a result of the progressive loss of all viral proteins, apart from E6 and E7, which are preserved and continuously expressed. Thus, at this stage of the infection, viral load starts decreasing as the virus irreversibly enters a non-productive life-cycle, and the infected cells accumulate higher intracellular levels of E6 and E7 [Doorbar *et al.*, 2012].

The epithelial lesion progressively develops from a Low-grade to a High-grade Squamous Intraepithelial Lesion (HSIL) and secondary genetic changes can accumulate in the host genome (corresponding to intraepithelial neoplasias type 2 and 3). However, the slow process of cancer development is intimately linked to the continuous activity of the viral oncoproteins, since they induce the degradation of several cellular proteins crucial for immune response-related pathways, cell-cycle control and apoptosis, which would induce cell death if rescued [Jiang and Yue, 2013].

In addition, a complex interplay between the two oncoproteins is crucial for cellular transformation because they target different cellular pathways, and thus they depend on each other in order to create the proper environment for cancer development [Chen, 2015; Groves and Coleman, 2015].

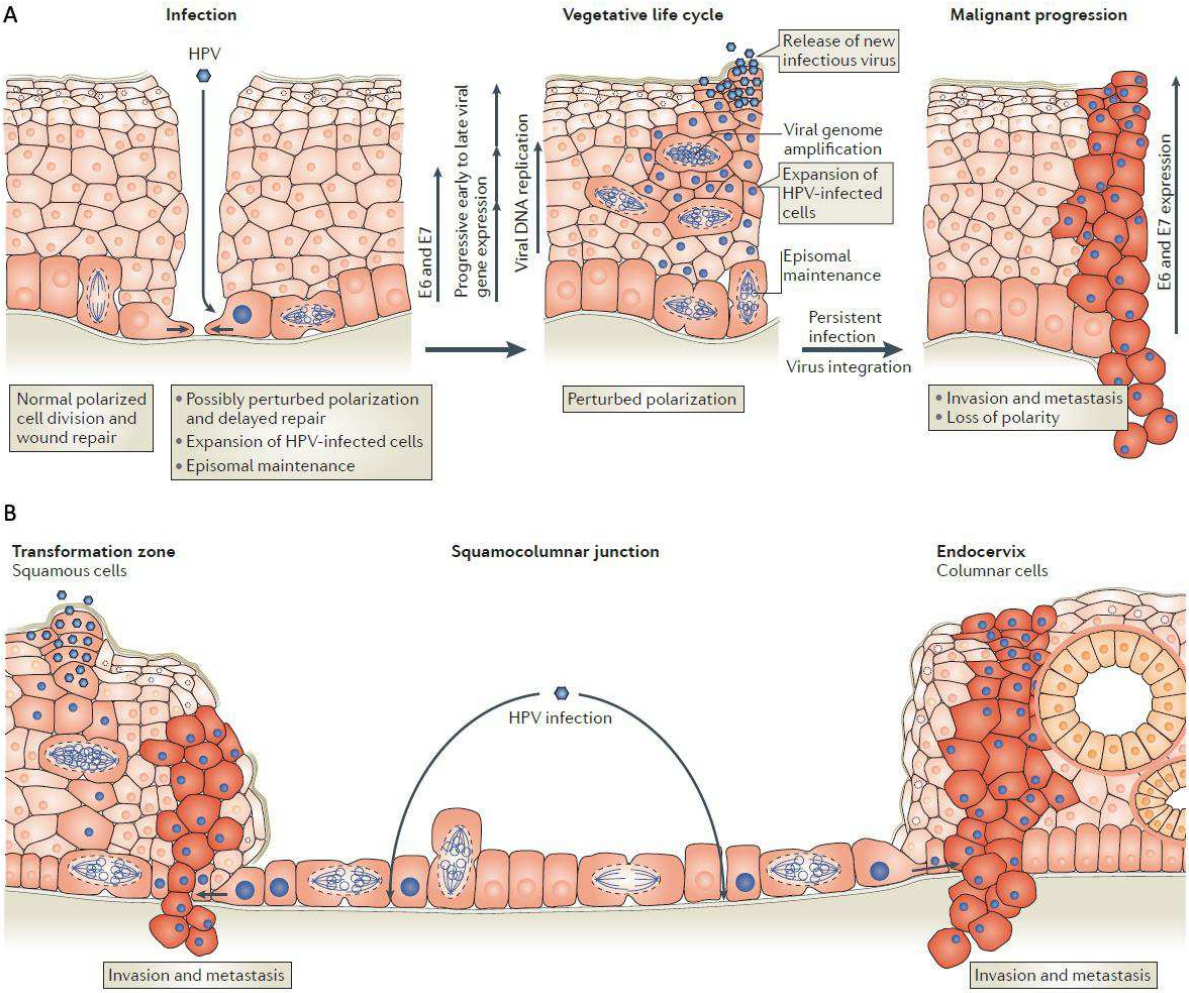

Figure 1.7. Model of how HR-HPV infections progress towards malignancy. (A) Schematic representation of how a productive HR-HPV infection takes place in a stratified epithelium, which requires a microwound in the skin, resulting in the progressive development of a carcinoma. **(B)** Model of how HR-HPV infections at the squamocolumnar junction in the transformation zone result in cancer development. This is considered the preferential site wherein HR-HPV infections easily progress towards cancer, since these cells are not permissive for viral replication. Cells containing viral DNA are shown with blue nuclei [Banks *et al.*, 2012].

E7 mainly affects the cellular proteins of the retinoblastoma family, particularly, pRb, p107 and p130, inducing their proteasome-dependent degradation [Hu *et al.*, 1995]. This event occurs through the direct interaction between E7 and Rb proteins, and the recruitment of cullin 2 ubiquitin ligase in order to drive their degradation [Huh *et al.*, 2007].

The physiological role of the Rb proteins is to inhibit E2F transcription factors, thus blocking the E2F-mediated transcription of cyclins and cyclin-dependent kinases (CDK). When pRb, p107 and p130 are degraded by E7, E2F1-3 can actively transcribe their target genes inducing cellular proliferation (Figure 1.8). However, E7-mediated deregulation of the cell cycle involves different mechanisms, as E7 can also directly bind and stabilize cyclin/CDK complexes, neutralize the activity of CDK inhibitors, such as p21 and p27, and block the activity of E2F6 transcription repressor [McIntyre *et al.*, 1996; Huh *et al.*, 2005; McLaughlin-Drubin *et al.*, 2008; Nguyen and Münger, 2008; Yan *et al.*, 2010].

Downstream of the E7-induced deregulation of Rb proteins is the upregulation of the phosphoinositide 3-kinase (PI3K)/Akt pathway, which is a central signalling pathway that drives cell survival and proliferation. It relies on the phosphorylation-dependent activation of Akt that ultimately activates the mammalian target of rapamycin (mTOR) kinase, which promotes the transcription of several genes involved in protein synthesis, cell growth, motility, metabolism and survival. Indeed, the upregulation of the PI3K/Akt pathway relies on the E7-induced degradation of pRb, but E7 can sustain the activation of Akt also by impairing the activity of Akt inhibitors, such as protein phosphatase 2A (PP2A) [Pim *et al.*, 2005]. Thus, E7 acts by targeting different cellular proteins in order to induce the transcription of S phase genes and sustain cell growth by forcing the cell to continuously divide.

Finally, E7 promotes also cell migration by acting on proteins of the Rho family, which are membrane-bound guanosine triphosphatases (G-proteins) that regulate cytoskeletal dynamics and cellular protrusions. In particular, E7 regulates RhoA by impairing the activity of p190, a known inhibitor of Rho proteins, and thus enhances cell migration and spreading [Todorovic *et al.*, 2014]. Taken together, E7 impairs the functionality of different cell cycle regulators and tends to create a positive feedback loop that pushes the infected cell towards uncontrolled growth and spreading.

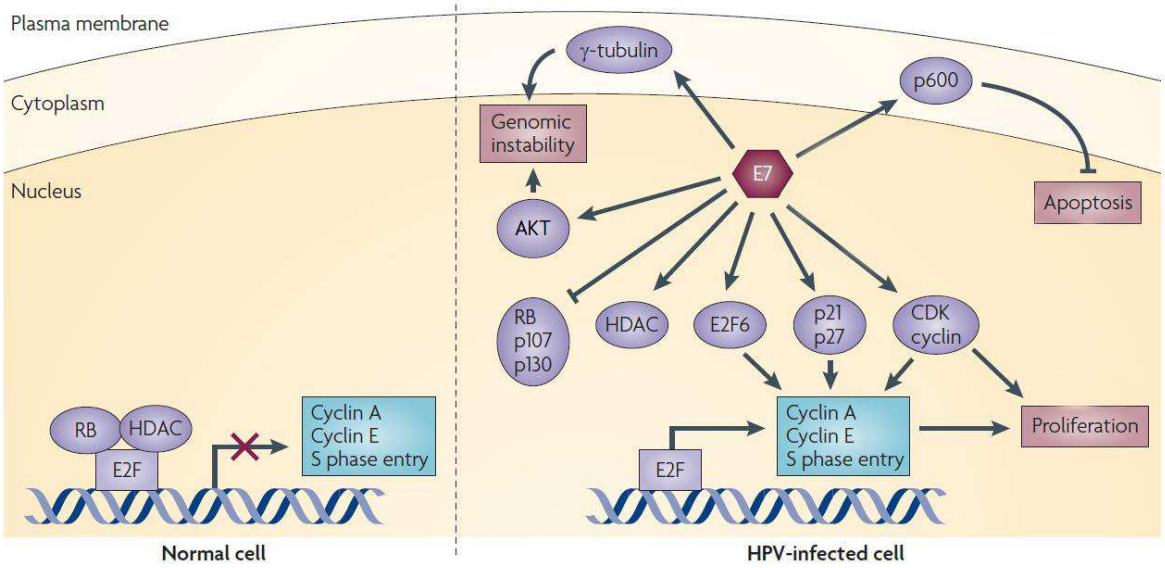

Figure 1.8. Molecular mechanisms of cellular immortalization driven by the E7 oncoprotein of HR-HPV genotypes. E7 can prevent G1-to-S-phase cycle arrest by inducing the degradation of the Rb proteins (pRb, p107 and p130). In addition, E7 can further impair cell cycle control through the deregulation of different inhibitors of the cell cycle, such as p21, p27, and E2F6, and through the stimulation of pro-proliferative factors, such as cyclins, CDKs and the Akt signalling pathway [Moody and Laimins, 2010, modified].

Physiologically, human cells can sense a condition of uncontrolled proliferation, and as a direct consequence, they activate intrinsic apoptotic pathways mainly in a p53-dependent manner. Indeed, the activities of E7 induce the increase of p53 transcription. Although E7 itself can counteract apoptosis by binding to p600 and indirectly inhibiting p53 itself [Huh *et al.*, 2005; Massimi and Banks, 1997], its anti-apoptotic ability is not sufficient to avoid cell death. Thus, HPV has evolved the ability to finely hijack cellular apoptosis mainly through the activities of the second viral oncoprotein, E6.

Similarly to E7, E6 binds to many cellular proteins and induces their proteasome-dependent degradation (Figure 1.9). Historically, the best-known target of E6 is p53, which is a major tumor suppressor protein in eukaryotic cells that induces cell cycle arrest and DNA repair, or alternatively, apoptosis, depending on the extent of cellular damage [Scheffner *et al.*, 1990; Werness *et al.*, 1990]. Normally, p53 is expressed at low levels, usually in an inactive form, but after cytotoxic/genotoxic stress, the expression of p53 increases and the protein is activated by post-translational modifications.

E6 drives the degradation of p53 through the recruitment of the cellular ubiquitin ligase E6AP, which polyubiquitinates p53 [Huibregtse *et al.*, 1993]. Physiologically, E6AP does not regulate the endogenous levels of p53 as it is not able to bind to the tumor suppressor protein, whose levels are instead regulated by the ubiquitin ligase Mdm2 in healthy cells

[Honda and Yasuda, 2000]. However, when E6 binds to E6AP through a direct interaction that involves a leucine-rich (LxxLL) motif of E6AP, the heterodimer E6/E6AP can bind to p53, thus forming the E6/E6AP/p53 trimeric complex [Martinez-Zapien *et al.*, 2016]. As a consequence, p53 is relocated in the cytoplasm where it is efficiently degraded by the proteasome machinery, although the precise molecular mechanisms of the nucleus/cytoplasm shuttling are still unknown [Stewart *et al.*, 2005].

In addition, the ability of E6 to induce the degradation of p53 in an E6AP-independent manner has been reported, suggesting that the viral protein may recruit other cellular ubiquitin ligases [Massimi *et al.*, 2008].

Finally, E6 can impair p53 suppressor activities also by inhibiting its transactivation. In this regard, p300 and ADA3, two cellular proteins that transactivate p53 through post-translational modifications, are targeted by E6, which induces their inhibition and degradation, respectively [Zimmermann *et al.*, 1999; Kumar *et al.*, 2002]. These processes in turns prevent the acetylation-dependent activation of p53.

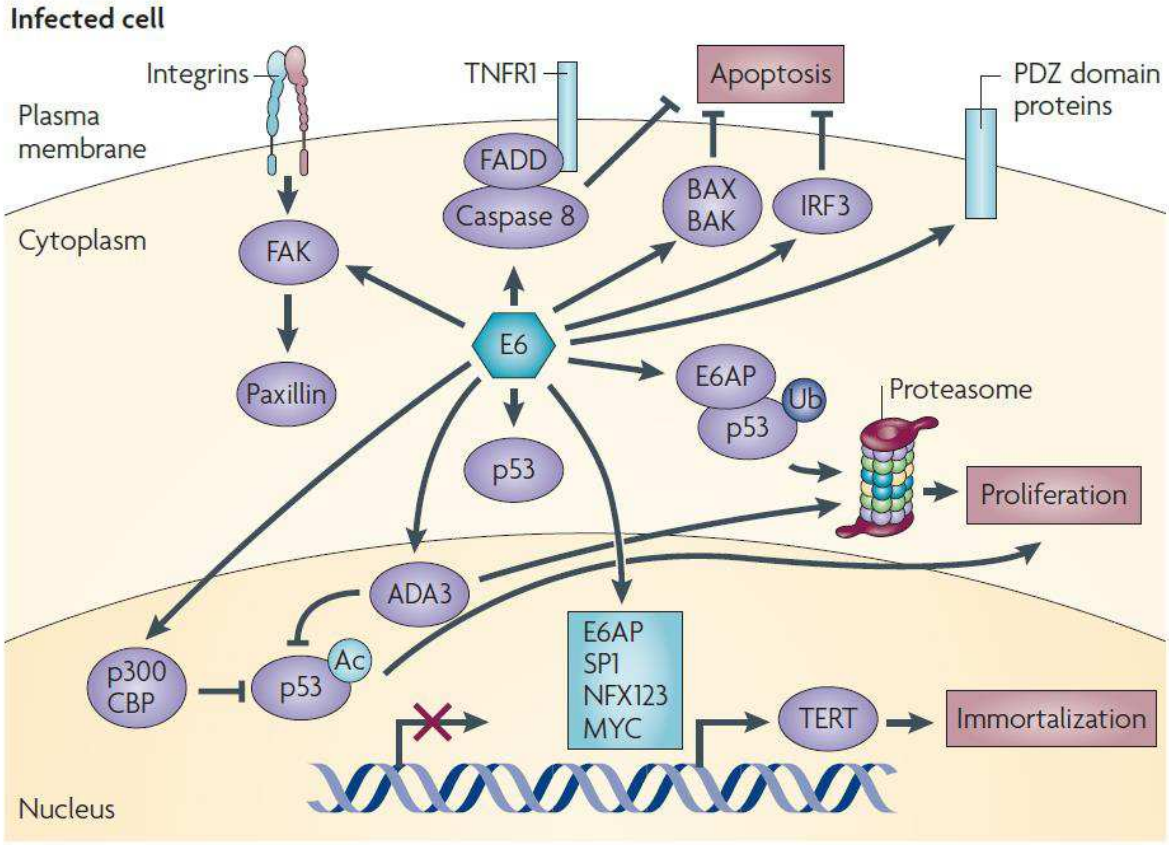

Figure 1.9. Molecular mechanisms of cellular transformation driven by the E6 oncoprotein of HR-HPV genotypes. E6 drives malignant transformation mainly by inducing the proteasome-dependent degradation of several cellular proteins, such as p53, p300, ADA3, PDZ-containing proteins, Bak, and many others. These processes, in turns, sustain cellular immortalization, proliferation and block apoptosis [Moody and Laimins, 2010].

Nevertheless, the anti-apoptotic activity of E6 is not restricted to the sole impairment of p53-dependent pathways. In fact, the viral oncoprotein can prevent cell death by perturbing different cellular proteins important for both intrinsic and extrinsic apoptotic pathways.

With regard to intrinsic apoptosis, the main effectors are the mitochondria, wherein different pro- and anti- apoptotic signalling pathways converge in order to determine whether the cell must die or survive. p53 is a crucial player of intrinsic apoptosis, but it is not the sole protein that can activate the apoptotic signaling cascade, and thus, other signals within the cell can induce apoptosis as a result of E7 activity. In general, when the pro-apoptotic signals are activated following cell stress, pro-apoptotic proteins, such as Bax or Bak, overcome the function of anti-apoptotic mediators and induce the formation of pores within the mitochondrial membrane. This event induces the release of inner mitochondrial proteins, such as cytochrome c, Smac and Diablo, which promote the apoptotic pathway by activating caspase 3 and 7, which will subsequently induce the formation of the apoptosome. Accordingly, E6 has been shown to block Bak by inducing its proteasome-dependent degradation, thus preventing the release of cytochrome c and other pro-apoptotic factors [Thomas and Banks, 1998].

With regard to extrinsic apoptosis, infected cells can be targeted to death through extracellular signals that bind to their relative “death receptor”. Accordingly, three different receptors can activate the extrinsic apoptotic pathway upon activation, i.e., tumor necrosis factor receptor 1 (TNFR-1), Fas receptor and TNF-related apoptosis inducing ligand (TRAIL) receptors. Independently of the specific ligand/receptor involved, these signals induce the activation of caspase 8 and 10 within the death inducing signalling complex (DISC), which subsequently converges on the activation of caspase 3 and 7. Indeed, E6 has been shown to impair all these three signalling pathways by inducing the degradation of several adaptor proteins (such as FADD and TRADD) and, especially, the effector caspase, caspase 8 [Filippova *et al.*, 2002; Filippova *et al.*, 2007].
Finally, also the upregulation of anti-apoptotic proteins, such as c-IAP2 and survivin, has been observed, but this process seems to be a consequence of the E6-mediated activation of cellular proliferative and survival pathways [Yuan *et al.*, 2005; Borbely *et al.*, 2006].

Taken together, it is clear that HPV has evolved the ability to strongly inhibit cellular apoptosis through the multiple activities of the oncoprotein E6. However, E6 does not solely serve as an anti-apoptotic effector, but rather as a promiscuous transforming protein that can affect a large number of cellular targets and signalling pathways. In fact, E6 not only counteract cellular signals that are activated as a consequence of E7 activity, but it also enhances and cooperates with E7 in order to promote cell survival and proliferation.

To exploit these functions, an extremely important characteristic of high-risk E6 oncoproteins is their ability to bind and degrade cytoplasmic PDZ-containing proteins [Massimi *et al.*, 2004]. These are tumor suppressor proteins that orchestrate cytoskeleton dynamics, serving as a scaffold for the regulation of several signalling pathways [Humbert *et al.*, 2008]. In particular, they are also important for the regulation of cell-to-cell and cell-to-extracellular matrix (ECM) contacts, wherein they arrange the architecture of tight junctions,

adherens junctions and focal adhesions. PDZ-containing proteins generally localize in the intracellular side of the plasma membrane, and thus their deregulation involves the cytosolic fraction of E6.

The interaction of high-risk E6 oncoproteins with these cellular tumor suppressor proteins occurs through the C-terminal unstructured PBM, which usually folds into a β-sheet when bound to a PDZ domain [Zhang *et al.*, 2007]. Although there have been controversial results about the effects of E6 on cellular PDZ-containing proteins [Handa *et al.*, 2007; Cavatorta *et al.*, 2004; Choi *et al.*, 2014], it is clear that the inhibition of their function is important for malignant progression, as it contributes to the impairment of several signalling pathways. Whether E6 induces their degradation or their delocalization, loss of PDZ-containing proteins in the proper cellular compartment induces the progressive loss of apico-basal polarity, which is a characteristic trait of differentiated cells. So far, up to 12 different PDZ-containing cellular proteins have been proposed as targets of E6, such as hScrib, hDlg, Multi PDZ protein 1 (MUPP1) and Membrane Associated Guanylate kinase homology proteins with an Inverted domain structure (MAGI) 1-2-3 [Thomas *et al.*, 2016].

High-risk E6 oncoproteins show differential binding capacity towards PDZ-containing proteins, depending on the viral genotype. These cellular targets are usually negative regulators of cell proliferation, and thus their loss correlate with the upregulation of proliferative pathways. Accordingly, the E6-mediated impairment of PDZ-containing proteins has important effects on PI3K/Akt signalling cascade, and thus E6 can support the activity of E7 for the upregulation of the mTOR pathway. The degradation of certain PDZ-containing proteins results in the inhibition of phosphatase and tensin homologue (PTEN), which is a known inhibitor of Akt kinase [Contreras-Paredes *et al.*, 2006]. In addition, E6 can upregulate mTOR and mTOR complexes through other mechanisms of action that do not rely on the degradation of PDZ-containing proteins, such as the sustained activation of the epidermal growth factor receptor (EGFR), which is upstream of the PI3K/Akt cascade, and the degradation of mTOR inhibitors, such as tuberous sclerosis complex 2 (TSC2) [Zheng *et al.*, 2008; Spangle and Münger, 2013]. This process in turns supports the decrease of p16, a known CDK inhibitor, in favour of cyclin D.

The proliferative activity of E6 involves also the upregulation of other survival pathways, particularly Wnt and Hippo.

The Wnt pathway is a highly conserved signalling cascade extremely important for cellular proliferation and differentiation during organ development and tissue homeostasis. When the canonical pathway is activated by the binding of Wnt ligand to its receptor Frizzled, the phosphorylation of the cytoplasmic mediator Dishevelled induces the accumulation of β-catenin in the nucleus, which is the central effector of the Wnt signalling cascade. Nuclear β-catenin can thus promote the transcription of several genes, such as c-jun, c-myc, survivin and cyclin D1. When the pathway is inactive, β-catenin is sequestered in the cytoplasm by the so-called “destruction complex” and is subsequently polyubiquitinated by the β-TrCP ubiquitin ligase, which induces β-catenin degradation.

β-catenin upregulation has been observed in HPV-related cancer samples, and this event relies on the activity of E6 [Pereira-Suàrez *et al.*, 2002]. Although the precise molecular

mechanism remains unclear, it has been suggested that E6 could induce the degradation of a β-catenin inhibitor, i.e., the seven-in-absentia homolog (Siah) protein [Rampias *et al.*, 2010]. However, the Wnt pathway is not the sole signalling cascade responsible for the activation of β-catenin. The activation of PI3K/Akt signalling pathway can induce β-catenin nuclear accumulation through the inhibition of glycogen synthase kinase-3β (GSK3β), which is a component of the destruction complex [Wu and Pan, 2010].

Furthermore, also the Hippo-transducers Yes-associated protein (YAP) and Trascriptional coactivator with PDZ-binding motif (TAZ) are potent regulators of β-catenin. In fact, a fine interplay between Wnt signalling and YAP/TAZ activity exists. YAP/TAZ have been shown to be crucial components of the cytoplasmic destruction complex, instrumental for the recruitment of β-TrCP ubiquitin ligase, in order to promote β-catenin, as well as TAZ, degradation [Azzolin *et al.*, 2014]. Thus, active β-catenin associates to active YAP/TAZ, which all relocate within the nucleus to promote the transcription of target genes, and vice versa, since YAP/TAZ are activated by Wnt growth factors.

YAP and TAZ are two transcriptional coactivators that promote the transcription of genes important for proliferation, survival and stemness, which are transcribed by TEAD and Activator Protein-1 (AP-1) transcription factors. Indeed, active YAP and TAZ accumulate within the nucleus wherein they bind to TEAD and AP-1 proteins [Zanconato *et al.*, 2015]. Phosphorylation of YAP and TAZ induces their inactivation and cytoplasmic retention, with concomitant TAZ and, to a lesser extent, YAP degradation.

In the last years, YAP and TAZ have become central players of regenerative medicine and cancer biology, as they seem to play a crucial role during organ development and regeneration, as well as for cancer progression, metastasis and cancer stem cell reprogramming [Zanconato *et al.*, 2016]. Indeed, their central role accounts for the fine and complex framework of regulatory signals that converge on YAP and TAZ [Piccolo *et al.*, 2014]. Their activity can be stimulated by the Wnt signalling, G protein-coupled receptors (GPCRs), and can be finely regulated by mechanical forces imposed by the environmental extra-cellular matrix, which can either stimulate or repress YAP and TAZ, depending on the stiffness of the ECM. Furthermore, structural complexes of the apico-basal polarity negatively regulate YAP/TAZ activity, recapitulating the mechanisms of anti-proliferative contact inhibition. Similarly, also the Hippo pathway, which is a highly conserved signalling cascade composed of several kinases, such as LATS1-2, MST1-2 and NF2, leads to YAP/TAZ inhibition, following the activation of the phosphorylation cascade.

Intriguingly, E6 can affect these pathways by impairing different regulatory proteins and perturbing the signalling cascades in multiple ways and at different steps. As already mentioned, E6 can induce the upregulation of β-catenin by degrading a β-catenin inhibitor, but β-catenin upregulation can be accomplished also through the E6/E7-mediated induction of the PI3K/Akt signalling [Contreras-Paredes *et al.*, 2006; Rampias *et al.*, 2010]. Furthermore, a recent study reported the E6-mediated induction of YAP in cervical cancer cells as a result of SOCS6 degradation, a known YAP inhibitor [He *et al.*, 2015]. Additionally, this process sustains the upregulation of EGFR and the expression of EGFR ligands, such as TGF-α and AREG.

Thus, the activities of E6 can induce cell survival and proliferation by altering many interconnected signalling pathways.

In addition to the aforementioned roles, E6 has important effects also on human telomerase (hTERT), innate immunity and Notch signalling pathway.
Human telomerase is a ribonucleoprotein that extends the 3' ends of linear chromosomes during eukaryotic DNA replication through the use of an RNA template. Its activity is extremely important to avoid the loss of genetic information and to prevent recombination at the termini. In normal somatic cells, hTERT is quiescient, but it is usually reactivated in cancer cells [Janknecht, 2004].
E6 can induce hTERT activity and this process requires the interaction with E6AP. The E6-mediated induction of hTERT can occur through at least two different mechanisms: the degradation of NFX1-91, which is a transcriptional repressor that prevents hTERT transcription, and the association of E6 with c-myc, which induces the c-myc-mediated transcription of hTERT [Veldman *et al.*, 2003; Gewin *et al.*, 2004]. Both activities thus modulate the transcription of hTERT leading to its upregulation.

E6 can also modulate the transcription of genes involved in the innate immune response-related pathways. The viral oncoprotein can interact with Toll-like receptor-9 (TLR-9) and Interferon regulatory factor-3 (IRF-3), inhibiting their transcription and transactivation ability, respectively [Ronco *et al.*, 1998; Hasan *et al.*, 2007]. As a direct consequence, the induction of interferon-β and the production of cytokines are prevented, thus hiding the cell from the activity of leukocytes of the innate immune system.

With regard to Notch signalling pathway, controversial results have been reported about the activity of E6 towards this signalling cascade.
Notch is another highly conserved cell signalling pathway extremely important during embryonic development. It has multiple functions depending on the tissue involved and can induce either cell differentiation or self-renewal abilities. In the context of adult epidermal cells, Notch is usually activated in order to induce epidermal stem cell proliferation and differentiation. The signalling cascade relies on the activation of Notch receptors following the binding with a Notch protein, such as Jagged and Delta-like ligands, which are transmembrane proteins expressed on the cell surface of neighbouring cells. Following their interaction, the intracellular portion of Notch receptor is cleaved by γ-secretase that releases the Notch intracellular domain (NCID), which is translocated into the nucleus to support gene transcription. This process allows the fine regulation of cell fate in a cell-to-cell contact manner, depending on the pattern of Notch ligands/receptors expressed on the cell surface. Whether E6 upregulates or blunts Notch signalling still remains an open question. Some authors have indeed observed the E6-mediated upregulation of Notch-1 receptor mRNA levels [Daniel *et al.*, 1997], but other studies reported the decrease of Notch-1 in cervical cancer cell lines [Talora *et al.*, 2002]. Nevertheless, to a certain extent, the activity of E6 seems to perturb Notch signalling in a manner that is probably dependent on the interplay among other signalling pathways and the overall malignant genotype of the

transformed cell. Taken together, it is clear how the activities of E6 can deeply perturb the cellular environment and support the proliferative function of E7.

In a more general point of view, E7 can be considered the immortalizing factor of HPV, as it extends the life span of the infected cells. Indeed, E7 can efficiently induce benign epidermal hyperplasias in mice [Song *et al.*, 2000]. However, the transforming potential of E7 is quite weak, and the protein seems to have a crucial role at the promotion stage of cancer development, when cells are induced to grow, rather than at the progression stage. Vice versa, E6 acts weakly at the promotion stage, but has strong transforming potential and efficiently supports cancer progression.

However, as mentioned in Paragraph 1.6, the continuous activity of these viral oncoproteins is necessary but not sufficient for malignant transformation. Accordingly, the ability of the E6/E7-expressing cells to remain invisible to the immune system, while continuously proliferating, allows the accumulation of somatic mutations, which is the essential co-factor that drives cellular transformation. In fact, genomic instability plays a key role in HPV-induced carcinogenesis and actively promotes cellular transformation. This process is in turn a direct consequence of E6/E7 activities, since they increase genomic instability as a result of Akt upregulation, p53 degradation and pRb inhibition, allowing the cell to tolerate the progressive accumulation of genetic mutations and genomic abnormalities. Therefore, the role of HPV oncoproteins is to initiate a complex mechanism of intracellular alterations, perturbing many important signalling pathways. This process results in the progressive instability of the host genome, which accumulates gene mutations following the uncontrolled cellular proliferation, and slowly transforms the infected cell into a cancer cell (Figure 1.10).

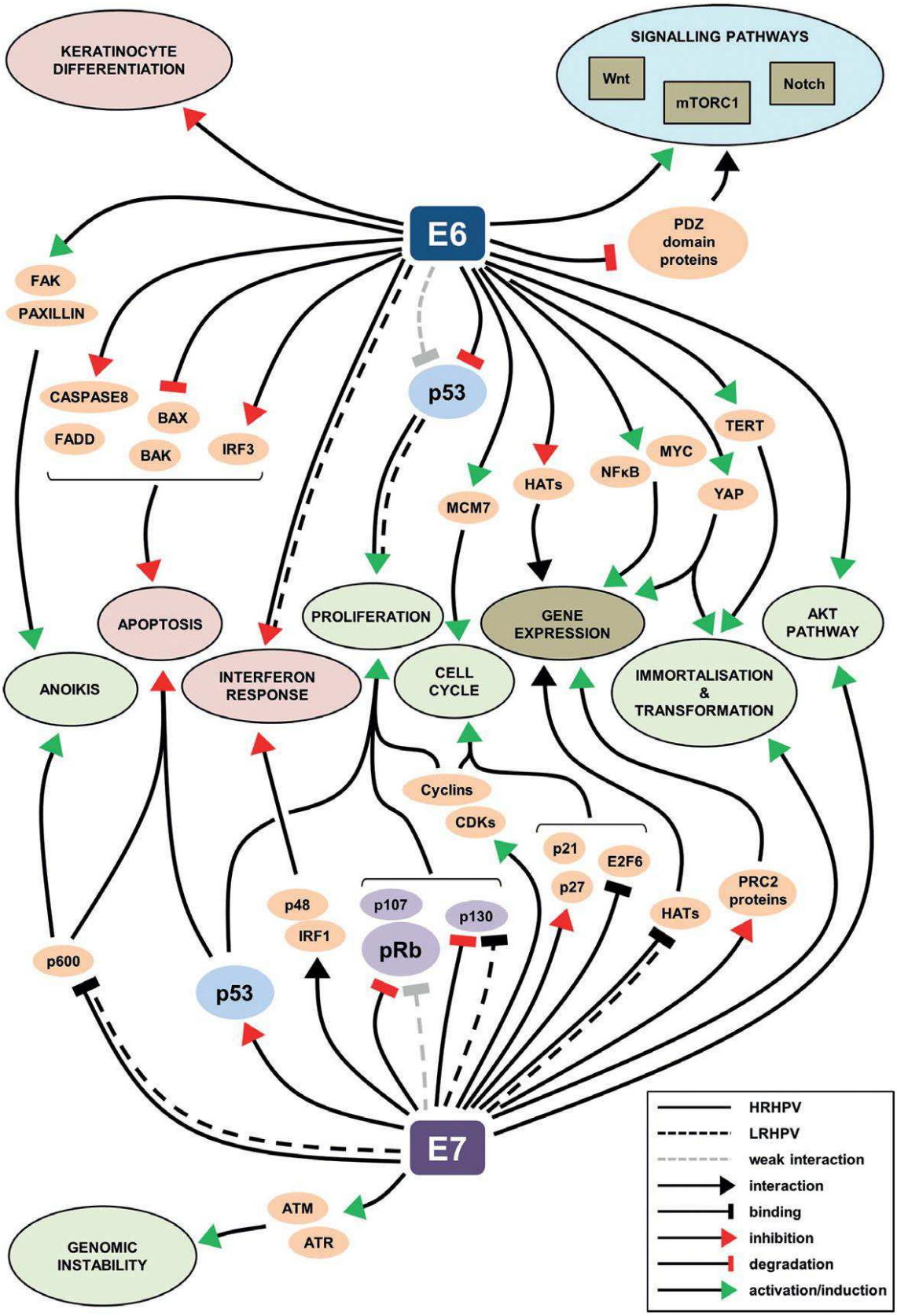

Figure 1.10. Schematic representation of the interplay between the activities of HR-HPV E6 and E7 for the deregulation of cellular signalling pathways. The activities of the two viral oncoproteins have profound effects on cellular proliferation, DNA repair, senescence, apoptosis and gene expression, inducing genomic instability and cellular transformation [Groves and Coleman, 2015, modified].

1.6.2 E6 and E7: molecular targets for therapeutic intervention.

The incontrovertible addiction of cancer cells to the sustained activity of HPV oncogenes is a remarkable characteristic that has intrinsic potential for the treatment of HPV-induced cancers. Indeed, the pivotal role of E6 and E7 for cancer development directly addresses the attention to these two proteins as primary targets for the development of anticancer drugs [D'Abramo and Archambault, 2011].

E6 and E7 possess no enzymatic activity and both proteins trigger their functions exclusively through protein-protein interactions (PPIs). As a direct consequence, a possible strategy to counteract the activity of these two proteins is the development of small molecules that act as PPI inhibitors. The purpose of small-molecule drug discovery is to seek for compounds able to interfere with the pathogenic activity of the targeted protein, with minimal alterations in cellular physiology. With regard to PPIs, this is possible especially when the exogenous protein drives the interactions through accessible pockets or cavities on its surface, where small molecules can be designed to fit with high affinity. However, PPI targets have traditionally been ignored by small-molecule drug developers, despite their therapeutic relevance and untapped abundance, largely because of technological hurdles. Scientific advances recently permitted to overcome these challenges [Mullard, 2012]. Indeed, since few years ago, many big pharmaceutical companies started working on promising drugs such as *navitoclax* (Abboth/Genentech) and *obatoclax* (Teva), both of which are now commercialized as anticancer agents that inhibit the function of the prosurvival BCL-2 family proteins by blocking key PPIs [Mullard, 2012].

So far, despite being attractive molecular targets from a biological point of view, E6 and E7 proved to be refractory to the inhibition by small-molecule compounds, possibly for their small size, but especially because of the lack of detailed structural informations [D'Abramo and Archambault, 2011]. This has forced researchers to look for anti-HPV compounds only through high-throughput screening techniques, by a classical drug discovery approach [Fera *et al.*, 2012; Yuan *et al.*, 2012; Malecka *et al.*, 2014]. However, in recent years, several structural models of E6 and E7 have been published [Ohlenschlager *et al.*, 2006; Liu *et al.*, 2006; Zanier *et al.*, 2013; Martinez-Zapien *et al.*, 2016].
Detailed structural informations allow the rational screening of compounds by *in silico* modeling, through a process known as structure-based drug design. The advantage of this approach is the preliminar selection of candidate molecules that are complementary in shape and charge to the biomolecular target with which they should interact. This process allows the restriction of the number of molecules to be tested and the knowledge-based refinement of the hits.

Accordingly, the availability of high-resolution NMR and crystal structures of E6 and E7 allows the rational design of anti-E6/E7 compounds. However, with regard to the structure of E7, the unfoldedness of its N-terminal domain, through which many crucial PPIs occur, strongly impairs the possibility to develop small-molecule inhibitors directed against those

PPIs and, indeed, structural informations of the N-terminal domain of E7 are so far unavailable [Garcia-Alai *et al.*, 2007(a)]. In addition, E6, rather than E7, has been often depicted as the main oncoprotein to be targeted for cancer treatment because its suppression reactivates p53-mediated pathways [Manzo-Merino *et al.*, 2013]. Indeed, many studies showed that silencing, deregulation or inhibition of E6 lead to apoptosis and malignant cell clearance with a substantial reduction in tumor size in animal models [Gu *et al.*, 2006; Jonson *et al.*, 2008]. Thus, E6 represents a major fascinating target for the development of anti-HPV drugs for therapeutic intervention. Inhibition of E6 oncotic activity could be achieved through the identification of small molecules able to target specific regions on E6 surface involved in PPIs crucial for the degradation of p53 or other onco-suppressor proteins [D'Abramo and Archambault, 2011].

1.6.3 Strategies for the development of anti-E6 compounds.

The physico-chemical and structural characteristics of E6 are key elements in order to understand the mechanisms through which E6 fulfills its functions. Intriguingly, such a small protein can induce the degradation of a multitude of cellular targets. Whether this is possible through structural rearrangements, common interaction surfaces, or through the recruitment of different ubiquitin ligases remains largely unclear.

As mentioned in Paragraph 1.6.2, structural informations are extremely important for structure-based drug design. So far, several NMR and crystal structures of E6 have been published, shedding light on the molecular interactions occurring with E6AP, p53 and PDZ-containing proteins [Charbonnier *et al.*, 2001; Zhang *et al.*, 2007; Liu *et al.*, 2007; Zanier *et al.*, 2013; Martinez-Zapien *et al.*, 2016]. Although E6 has a plethora of interacting partners, E6AP was shown to be crucial for the degradation of many cellular proteins, including p53 [Massimi *et al.*, 2004]. The interaction involves a leucine-rich (LxxLL) α-helix of E6AP that binds within a cavity formed by the two zinc-finger domains of E6, through polar and hydrophobic contacts (Figure 1.11). E6 cannot bind p53 in the absence of E6AP and, vice versa, E6AP cannot bind p53 in the absence of E6 [Ansari *et al.*, 2012]. The formation of the complex thus requires all three elements in such a way that the interaction with E6AP tightens the conformation of E6, keeping the N-terminal and C-terminal domains in close contact, and this event subsequently induces the binding to p53. The three leucine residues of the LxxLL motif of E6AP accommodates within a hydrophobic core formed by N-terminal residues of E6 (mainly Y32, L50, L67, and Y70). However, the interaction is crucially driven by arginine side chains of E6 on the surrounding area that work as keystones for the architecture of the complex, i.e., R10, R55, R102 and R131. In addition, other polar residues of E6 seem to be involved in the interaction, serving as "readers" in order to discriminate differences in the composition of the LxxLL motifs [Zanier *et al.*, 2013].

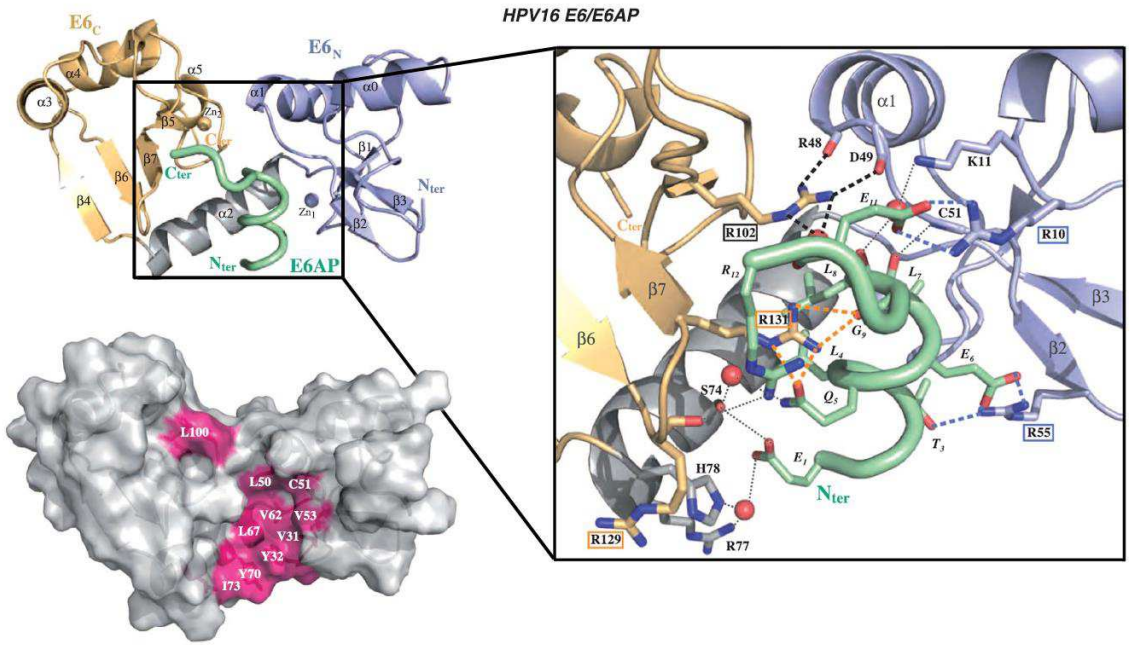

Figure 1.11. Crystal structure of HPV16 E6 bound to the LxxLL peptide of E6AP (green), showing the formation of a deep pocket on E6 protein surface (pink) for the accommodation of the helical-motif of E6AP, which binds to the viral oncoprotein through hydrophobic and polar interactions (insert) [Zanier *et al.*, 2013, modified].

Once formed, the heterodimeric complex E6/E6AP can sequester p53, inducing its polyubiquitination and proteasome-dependent degradation. According to the last published structural model [Martinez-Zapien *et al.*, 2016], p53 binds on a surface that spans both E6 zinc-finger domains, which are tightened by the interaction with E6AP, as previously discussed (Figure 1.12). This event explains the need of the E6/E6AP complex formation prior to the binding to p53. However, the latest crystal structure was solved using only the LxxLL motif of E6AP fused to the maltose-binding protein (MBP), and thus, no structural information about the overall contribution of E6AP to the trimeric complex is available. Anyway, p53 binds to a cleft formed by the $E6_N$ and $E6_C$ domains and the interaction involves the p53 core domain, but at a site different from the DNA-binding region of p53. The binding interface on E6 surface can be divided into three sub-interfaces: I, II and III. The sub-interface I involves polar interactions on the N-terminal part of the $E6_N$ domain, corresponding to the α1-helix, particularly through residues E7 and R8. The sub-interface II mainly involves the α2-helix of the $E6_N$ domain and both hydrophobic and polar contacts occur between E6 and p53, particularly through residues Y43, D44 and F47. The sub-interface III involves only hydrophobic interactions occurring on the $E6_C$ domain, particularly through residues L100 and P112.

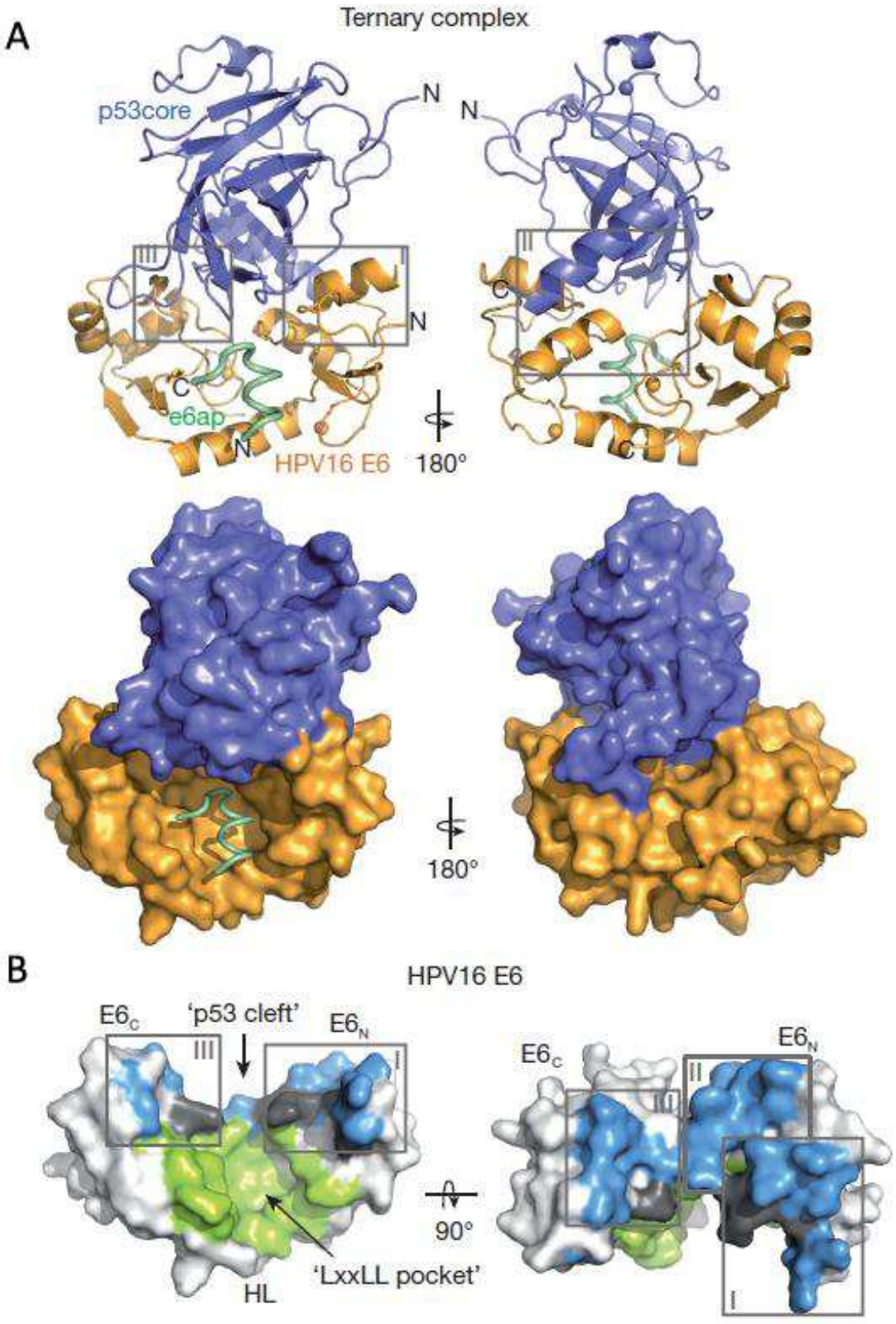

Figure 1.12. Crystal structure of the HPV16 E6/E6AP/p53 ternary complex (orange, green and purple, respectively), showing the formation of the p53 binding interface as a result of the interaction between E6 and E6AP. As shown, p53 binds to E6 on a cleft formed by three sub-interfaces (blue) spanning both the N-terminal and C-terminal domains of E6, which are tightened by the binding of the LxxLL motif of E6AP on a cavity (green) on E6 protein surface (HL: helix linker) [Martinez-Zapien *et al.*, 2016].

Intriguingly, about half of the residues of the sub-interface II involved in the interaction with p53 were observed to be crucial also for E6 self-association [Zanier *et al.*, 2012]. Through NMR studies, Zanier and coworkers published a model in which two E6 monomers interact in a face-to-face manner through their N-terminal domains (Figure 1.13). Noteworthy, the residues that seem to be crucial for the homodimerization reside in a small hydrophobic pocket at the bottom of α2-helix, mainly composed by I23, A24, Y43 and F47, where the side chain of F47, located in the other monomer, fits, and vice versa. Interestingly, these amino acids are highly conserved among high-risk mucosal HPV strains.

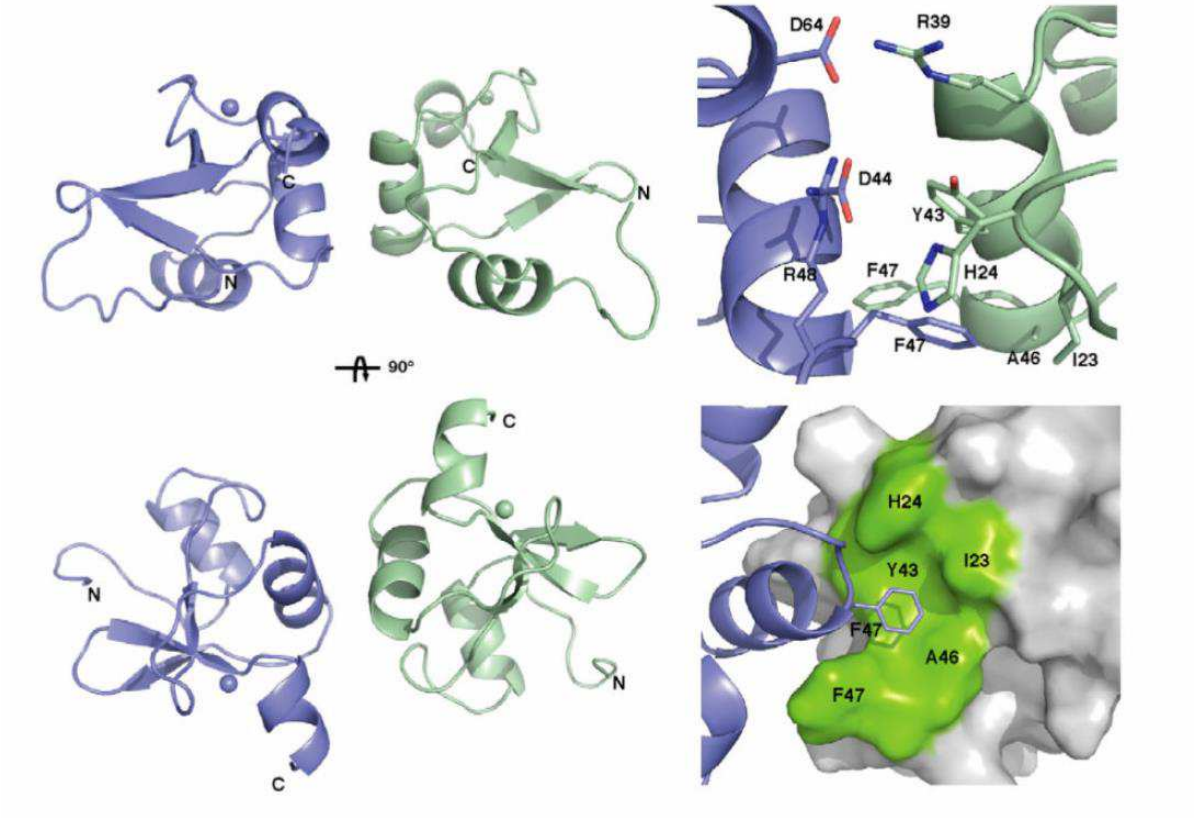

Figure 1.13. Haddock model structure of the HPV16 $E6_N$ homodimer (left) and views of the homodimer interface (right), illustrating the orientation of the hydrophobic residues of an $E6_N$ monomer (purple) relative to the other (green) [Zanier *et al.*, 2012].

Although the role of the dimeric form of E6 remains so far elusive, contrasting results have been published about the involvement of the dimerization for the productive degradation of p53 [Zanier *et al.*, 2012; Martinez-Zapien *et al.*, 2016]. Thus, the question whether the dimerization is needed in order to induce the degradation of p53 remains unanswered. In fact, Zanier and coworkers proposed a model in which the self-association of E6 is a crucial step for the degradation of p53. This hypothesis was mainly supported by their previous observation that the introduction of polar residues in this hydrophobic region (such as a phenylalanine-arginine substitution at position 47) abolished p53 degradation activity while retaining the ability of E6 to interact with both p53 and E6AP in cell-based pull-down assays [Ristriani *et al.*, 2009].

However, in 2016 the same group published contrasting results, as they reported that mutant E6 F47R was not able to bind p53, thus explaining the inability to degrade p53 as a result of its impaired binding capacity [Martinez-Zapien *et al.*, 2016]. Indeed, F47 is one of the key residues of sub-interface II and the introduction of a polar amino acid (i.e., arginine) in this hydrophobic surface might substantially impair the binding between E6 and p53. Accordingly, the authors concluded that E6 dimerization and E6-p53 interaction are likely two distinct processes that occur on partly overlapping surfaces.

In addition to the aforementioned NMR and crystal structures, detailed structural informations about the PBM-PDZ domain interaction are also available [Liu *et al.*, 2007; Zhang *et al.*, 2007]. Binding of E6 to PDZ-containing proteins relies on the positioning of the C-terminal 7-amino-acid peptide R-R/T-E-T-Q/E-V/L-L of high-risk E6 oncoproteins on a shallow cavity on the surface of PDZ domains (Figure 1.14). It has been observed that the interaction directly involves six of the seven residues of the PBM [Zhang *et al.*, 2007]. Furthermore, differences in the amino acid composition of the PBMs among different viral genotypes, together with the variability of the three residues upstream of the PBM, modulate target specificity [Thomas *et al.*, 2016].

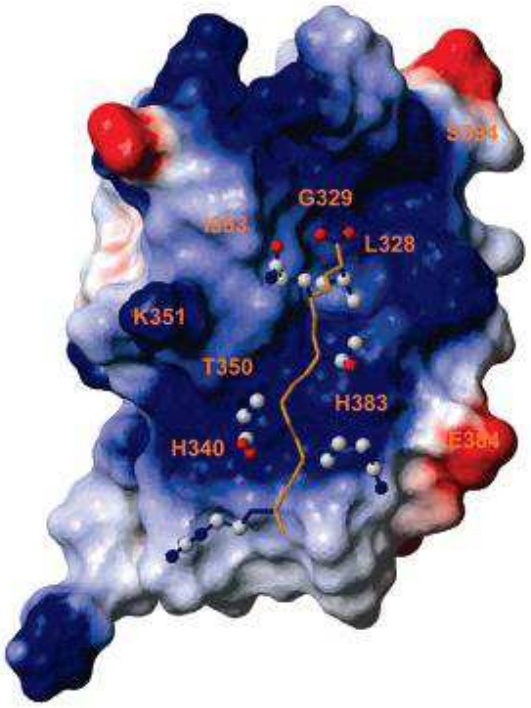

Figure 1.14. Ribbon representation of the C-terminal PBM of HPV18 E6 bound to the PDZ domain of human Disc Large, coloured according to the electrostatic potential. Residues highlighted in orange are directly involved in the binding with the PBM of E6. Positive potential is shown in blue, negative potential in red [Liu *et al.*, 2007].

According to the published structural models, different strategies can be envisaged to design effective inhibitors of E6.

The first and so far most popular strategy is the targeting of E6/E6AP binding interface. Indeed, disrupting this interaction has the intrinsic advantage of targeting a cavity on E6 protein surface, which ideally enables the development of potent and specific E6 inhibitors. Although this approach has been pursued by several groups, with overall good results [Baleja *et al.*, 2006; Cherry *et al.*, 2013], it has been questioned that this could not be an exhaustive strategy because some functions of E6 with respect to p53 inhibition seem to be performed in the absence of E6AP binding [Camus *et al.*, 2007; Massimi *et al.*, 2008]. In addition, it has been suggested that while drugs designed to interact with the E6AP (LxxLL peptide)-binding pocket of E6 could prevent the E6AP-dependent degradation of p53, they could also stabilize E6 expression, with difficult-to-predict consequences [Ansari *et al.*, 2002].

Another possible strategy is the targeting of PBM-PDZ domain interactions. Although this approach has intrinsic potential with regard to the inhibition of E6 transforming activities, only one report has been published about the successful inhibition of this interaction [Ramirez *et al.*, 2015]. However, the possibility to impair PBM-PDZ recognition was possible only through the use of a chimeric inhibitor protein, wherein a recombinant PDZ domain was expressed in HPV-positive cell lines, functioning as a competitor against the natural interactions between E6 and cellular PDZ-containing proteins. As a matter of fact, no reports involving small-molecule inhibitors have been successfully published, most likely due to the difficulty in the identification of compounds that could specifically block E6-PDZ domain binding without affecting normal cellular PDZ domain-dependent interactions.

A third strategy is the targeting of E6-p53 binding interface. Indeed, this represents a fascinating target for the development of anti-E6 compounds. Anyhow, this strategy has been so far hampered by the lack of a crystal structure of the E6/E6AP/p53 trimeric complex, which has become available only very recently [Martinez-Zapien *et al.*, 2016]. Intriguingly, the p53-binding cleft on E6 protein surface represents a potential binding site for small-molecule inhibitors. In addition, key residues on the p53-binding cleft appear to be highly conserved among high-risk genotypes, particularly the α2-helix corresponding to the sub-interface II, which drives also E6 self-association. Although this latter interaction remains poorly characterized, targeting this binding interface could represent a novel strategy for the development of anti-E6 compounds.

2. Aim

HR-HPVs are still a major cause of epithelial cancers worldwide, being the aetiological agents of cervical, oropharyngeal and anogenital cancers. Although a vaccination program has been started to prevent virus infection, there is still a need of specific treatments for patients already infected and at a high risk for developing HPV-associated malignant tumors. Furthermore, the vaccination program, if globally implemented, would still take up to 20 years to have a significant impact on the incidence of HPV-related cancers, and the accessibility in many developing countries, in terms of cost and logistic, will remain an issue. Finally, no specific anti-HPV drugs are commercially available yet.

The viral oncoprotein E6 is the major player responsible for cellular transformation during HR-HPV-induced cancer progression, and thus represents a fascinating target for the development of anti-HPV drugs. Although deeply studied since the early Nineties, the oncoprotein E6 possesses intriguing transforming abilities, particularly because of its very small dimensions (being composed of 151 amino acids), and still represents an eclectic and versatile protein able to impair several signalling pathways.
Since the initial discovery of the ability of E6 to degrade p53 [Scheffner *et al.*, 1990], the viral oncoprotein was always thought to act as a monomer in the infected cell in order to induce the degradation of its cellular targets. However, recent studies on E6 demonstrated that it can also self-associate in homo-dimers *in vitro* through a highly conserved interaction surface (corresponding to the N-terminal α2-helix) [Zanier *et al.*, 2012], which was later observed to be important also for the binding of E6 to p53 [Martinez-Zapien *et al.*, 2016]. Although the homodimerization of E6 remains an event poorly characterized, targeting the PPIs driven by this highly conserved surface on the viral oncoprotein may represent a novel strategy for the development of anti-HPV drugs.

Thus, the goals of this PhD project were the investigation of the existence of HPV16 E6 as a homodimer in a cellular context, the characterization of its biological importance relative to E6 transforming activities and the identification of compounds able to target the α2-helix of the N-terminal domain of the viral oncoprotein.

With regard to the study of E6 dimerization, different protein-protein interaction assays have been employed:
- Bioluminescence Resonance Energy Transfer (BRET) assay, in which either YFP or *Renilla* Luciferase (RLuc) are fused to the viral protein. When coelenterazine is added, RLuc-tagged E6 emits a blue luminescent light. If a second E6 molecule, carrying YFP, interacts (through the dimerization of E6), the energy is transferred producing a yellow signal.

- ELISA-based *in vitro* assay, in which recombinant purified E6 molecules have been used to study the site-specific self-association of the viral oncoprotein. We coated the surface of wells of microtiter plates with recombinant $E6_N$ proteins and, by incubating a second recombinant $E6_N$ protein, we measured the direct interaction between the N-terminal domains of E6.

With regard to the functional characterization of the dimeric form of E6, different cell-based assays have been developed, transfecting HPV-negative cells with either wild-type or dimerization-defective E6 mutants and monitoring the changes in the endogenous levels of different cellular proteins, such as p53, Scribble, and TAZ.

Finally, two different *in silico* screenings of small-molecule libraries have been performed to find compounds able to target the α2-helix of the N-terminal domain of HPV16 E6. The hits emerged from the screenings were tested, first in the ELISA-based $E6_N$ homodimerization assay to assess their ability to impair E6 self-association, and subsequently in cell-based assays to evaluate their ability to block the E6-mediated degradation of p53 and their ability to specifically target HPV-positive cells in cell viability and cell proliferation assays.

3. Materials and Methods

3.1 Materials.

3.1.1 Compounds.

Anti-E6 compounds selected from the virtual screenings were purchased from Specs chemistry database (Zoetermeer, The Netherlands, www.specs.net).
Compound powders were kept at 4°C in the dark. Upon resuspension in DMSO (Sigma-Aldrich), 50 mM stocks solutions were stored at -20°C, protected from light.

3.1.2 Proteins.

Glutathione S-Transferase (GST), 6 histidine-tagged (6his)-$PA_{239-716}$ (representing the C-terminal domain of Polymerase Acidic protein from influenza A virus) and UL44 (DNA polymerase processivity factor from human cytomegalovirus) were expressed in *E. coli* BL21(DE3)/pLysS strain and purified through affinity chromatography as previously described [Loregian *et al.*, 2004; Massari *et al.*, 2013].
GST-$E6_N$, 6his-$E6_N$ and untagged $E6_N$ proteins were expressed and purified as described in Paragraph 3.2.13

3.1.3 Oligonucleotides.

Synthetic oligonucleotides for gene cloning, mutagenesis and DNA sequencing were purchased from Promega and are listed in Tables 3.1, 3.2, 3.3 and 3.4.
siRNA oligos for gene silencing, which are dsRNA oligos with overhanging dTdT, and control (scrambled) siRNA were purchased from Thermo Fisher Scientific and Qiagen, respectively, and are listed in Table 3.5.

Table 3.1 Oligonucleotides for ligase-dependent cloning

Oligonucleotide	Sequence 5’ to 3’
E6 pET28 FOR	TTTATGAATTCATGTTTCAGGACCCACAGG
E6 pET28 REV	TAAAGCGGCCGCTTACAGCTGGGTTTCTCTACG
E6N pET28 REV	TAAAGCGGCCGCTTAGCTGTAATGTCTATACTC
E6 pD15 FOR	AAAAAACTCGAGATGTTTCAGGACCCACAGG
E6 pD15 REV	TAAAAAACGCGTTTACAGCTGGGTTTCTCTACG
E6N pD15 REV	TAAAAAACGCGTTTAGCTGTAATGTCTATACTC

Table 3.2 Oligonucleotides for Gateway® cloning

Oligonucleotide	Sequence 5’ to 3’
E6 attB1	GGGGACAAGTTTGTACAAAAAAGCAGGCTCGATGTTTCAGGACCCACAGGAGCG
E6 attB2 STOP	GGGGACCACTTTGTACAAGAAAGCTGGGTCTTACAGCTGGGTTTCTCTACGTG
E6 attB2 noSTOP	GGGGACCACTTTGTACAAGAAAGCTGGGTCCAGCTGGGTTTCTCTACGTGTTC
E6 NT attB2 STOP	GGGGACCACTTTGTACAAGAAAGCTGGGTCTTAGCTGTAATGTCTATACTCACTAA TTTTAG
E6 NT attB2 noSTOP	GGGGACCACTTTGTACAAGAAAGCTGGGTCGCTGTAATGTCTATACTCACTAATTTT AG
p53 attB1	GGGGACAAGTTTGTACAAAAAAGCAGGCTCGATGGAGGAGCCGCAGTCAGATCC
p53 attB2 STOP	GGGGACCACTTTGTACAAGAAAGCTGGGTCTTAGTCTGAGTCAGGCCCTTCTG

Table 3.3 Oligonucleotides for site directed mutagenesis

Oligonucleotide	Sequence 5’ to 3’
E6 S16C FOR	CCAGAAAGTTACCACAGTTATGCACAGAGCTGCAAACAAC
E6 S16C REV	GTTGTTTGCAGCTCTGTGCATAACTGTGGTAACTTTCTGG
E6 S51C FOR	GACTTTGCTTTTCGGGATTTATGCATAGTATATAGAGATGGG
E6 S51C REV	CCCATCTCTATATACTATGCATAAATCCCGAAAAGCAAAGTC
E6 F47R FOR	CGTGAGGTATATGACTTTGCTCGTCGGGATTTATGCATAGTATATAGAG

E6 F47R REV	CTCTATATACTATGCATAAATCCCGACGAGCAAAGTCATATACCTCACG
E6 mut donor FOR	CAACAGTTACTGCGACGTGAAGTATATGACTTTGCTTTTCGG
E6 mut donor REV	CCGAAAAGCAAAGTCATATACTTCACGTCGCAGTAACTGTTG
E6 F47R mut donor FOR	CAACAGTTACTGCGACGTGAAGTATATGACTTTGCTCGTCGG
E6 F47R mut donor REV	CCGACGAGCAAAGTCATATACTTCACGTCGCAGTAACTGTTG
E6 F47R mut donor Y43E FOR	GTTACTGCGACGTGAAGTAGAAGACTTTGCTCGTCGGG
E6 F47R mut donor Y43E REV	CCCGACGAGCAAAGTCTTCTACTTCACGTCGCAGTAAC

Table 3.4 Oligonucleotides for DNA sequencing

Oligonucleotide	Sequence 5’ to 3’
pD15 seq FOR	TGGCGACCATCCTCCAAA
pD15 seq REV	TATGCTAGTTATTGCTCA
pET28 seq FOR	AATACGACTCACTATAGG
pET28 seq REV	CTAGTTATTGCTCAGCGGTGG
HCMV seq FOR	CGCAAATGGGCG
pDONR seq FOR	TAACGCTAGCATGGATCTC
pDONR seq REV	GCAATGTAACATCAGAGAT
pDEST seq	TAATACGACTCACTATAGGG
pcDNA seq	TAGAAGGCACAGTCGAGG
pT-REX seq	CGCAAATGGGCGGTAGGCGTG

Table 3.5 Oligonucleotides for gene silencing

siRNA	Target gene	Sequence 5’ to 3’	Reference
16E6-191	HPV16 E6	UGUGUGUACUGCAAGCAAC	Koivusalo *et al.*, 2005
18E6/E7-755	HPV18 E6/E7	CCACAACGUCACACAAUGU	Kuner *et al.*, 2007

3.1.4 Plasmids.

p513 plasmid is a pSG5-derived vector for protein expression in eukaryotic cells, containing: Simian Virus 40 (SV40) promoter/enhancer and polyadenylation site for efficient recombinant protein production in transfected cells, ColE1 origin of replication for high-copy number replication in *E. coli* strains, ampicillin resistance gene for selection of transformed bacteria and a Multi Cloning Site (MCS) for gene cloning.

pcDNA3 plasmid is used to express recombinant proteins in eukaryotic cells and contains: human cytomegalovirus (HCMV) promoter/enhancer and polyadenylation site for high expression levels in transfected cells, ColE1 origin of replication for high-copy number replication in *E. coli* strains, ampicillin resistance gene for selection of transformed bacteria and an MCS for gene cloning.

pcDNA3-derived plasmid for Gateway® cloning is an engineered destination vector that lacks any MCS but allows gene cloning through the bacteriophage lambda site-specific recombination system (see also Paragraph 3.2.1.5). It contains a *ccd*B gene that allows the selection of *E. coli* following recombination and transformation. Recombinant proteins are expressed with N-terminally tagged *Renilla* Luciferase (RLuc).

pDEST destination plasmids are used to express Yellow Fluorescent Protein (YFP)- or FLAG-tagged proteins in eukaryotic cells and contain: HCMV promoter/enhancer and polyadenylation site, ColE1 origin of replication, ampicillin resistance gene, *ccd*B gene and site-specific recombination sequences for Gateway® Technology. Recombinant proteins are expressed in transfected cells with YFP or FLAG® epitope tag fused either at the N-terminus or at the C-terminus of cloned gene, depending on the specific pDEST vector used for gene cloning.

pT-REX plasmid is a pcDNA4-derived destination vector for Gateway® Technology containing: HCMV promoter/enhancer and polyadenylation site, ColE1 origin of replication, ampicillin resistance gene, *ccd*B gene and site-specific recombination sequences for Gateway® cloning technique. Recombinant proteins are expressed with RLuc fused at the C-terminus of cloned gene.

pDONR207 plasmid is an entry vector used to transfer any gene of interest into the previously described destination vectors (pcDNA3, pDEST and pT-REX) through Gateway® site-specific recombination system. It contains: pMB1 origin of replication, gentamicin resistance gene and *ccd*B gene for double selection of *E. coli* following recombination and transformation.

pET28a+ plasmid is a vector used for protein expression in prokaryotic cells. It allows the expression of recombinant proteins with an N-terminal 6 histidine-tag (6his) for protein purification. It contains: T7 RNA polymerase promoter, kanamycin resistance gene for *E. coli* selection and a MCS for gene cloning.

pDEST15 plasmid allows the expression of recombinant proteins in *E.coli* strains tagged with GST at the N-terminus of cloned gene for purification purposes. It contains a T7 RNA polymerase promoter, an ampicillin resistance gene and a MCS for gene cloning.

pCS2+ plasmid is a pBluescript II-derived vector for protein expression in eukaryotic cells, containing: simian CMV promoter, two MCSs for gene cloning, one upstream and one downstream the SV40 polyadenylation site, and an ampicillin resistance gene.

3.1.5 Cell Lines.

HEK 293T: HPV-negative human embryonic kidney epithelial cell line derived from a fetus, in which the SV40 T-antigen was inserted. These cells were used for their easy transfectability and abundant exogenous protein production.

C33A: HPV-negative human epithelial cancer cell line, derived from cervical cancer of a 66-year old Caucasian female. These cells are defective for both p53 and pRb function.

H1299: HPV-negative human epithelial cancer cell line, derived from non-small cell lung cancer of a 43-year old male. These cells are $p53^{-/-}$ due to a homozygous partial deletion of the *TP53* gene.

Hela: HPV-positive human epithelial cancer cell line, derived from a cervical adenocarcinoma of a 31-year old female. These cells contain an integrated copy of HPV18 genome.

CaSki: HPV-positive human epithelial cancer cell line, derived from a metastatic site of a cervical carcinoma belonging to a 40-year old female. These cells contain integrated copies of HPV16 genome (up to 600 copies per cell) as well as sequences related to HPV18.

SiHa: HPV-positive human epithelial cancer cell line, derived from a grade II cervical squamous cell carcinoma of a 55-year old female. These cells contain an integrated copy of HPV16 genome (1-2 copies per cell).

HFF: Human Foreskin Fibroblasts from the America Type Culture Collection (ATCC).

3.1.6 Bacterial strains.

***E. coli* DH5α**: strain of *Escherichia coli* containing multiple mutations that enable high-efficiency transformations. This strain was used for the replication and purification of the aforementioned plasmids.

***E. coli* BL21(DE3)/pLysS**: strain of *Escherichia coli* containing an IPTG-inducible gene for T7 RNA polymerase and a pLysS plasmid, which encodes T7 lysozyme. T7 lysozyme reduces the basal expression of exogenous proteins by inhibiting the T7 RNA polymerase. This strain was used for the *in vitro* expression and purification of the aforementioned recombinant proteins.

Transformed bacteria were grown in liquid Luria Bertani (LB) medium (1% tryptone, 1% NaCl, 0.5% yeast extract) or, alternatively, on solid LB plates (supplemented with 1.5% agar), with the appropriate antibiotic.

3.1.7 Antibodies.

3.1.7.1 Primary antibodies.

Santa Cruz Biotechnology

Goat polyclonal anti-HPV16 E6 (N-17) [catalog number sc-1584]

Goat polyclonal anti-HPV16 E6 (C-19) [catalog number sc-1583]

Goat polyclonal anti-Scribble (C-20) [catalog number sc-11049]

Sigma Aldrich

Rabbit polyclonal anti-WWTR1 (TAZ) [catalog number HPA007415]

Mouse monoclonal anti-FLAG M2 [catalog number F3165]

Mouse monoclonal anti-β-actin [catalog number A5441]

Mouse monoclonal anti-6his [catalog number H1029]

Active Motif

Rabbit polyclonal anti-p53 [catalog number 61657]

GenScript

Mouse monoclonal anti-GST HRP-conjugated [catalog number A00866]

QED Bioscience

Rabbit polyclonal anti-6his HRP-conjugated [catalog number 18814P]

3.1.7.2 Secondary antibodies.

Santa Cruz Biotechnology

Goat anti-mouse HRP-conjugated [catalog number sc-2055]

Goat anti-rabbit HRP-conjugated [catalog number sc-2054]

Millipore

Rabbit anti-goat HRP-conjugated [catalog number AP106P]

3.2 Methods.

3.2.1 Molecular Biology techniques.

3.2.1.1 PCR amplification.

For cloning purposes, genes on interest were amplified with the appropriate primers listed in Tables 3.1 and 3.2 through a standard PCR technique. Genes were amplified using Taq Gold DNA polymerase (Perkin Elmer).

3.2.1.2 Enzymatic restriction.

For ligase-dependent cloning, PCR products and relative plasmids were digested with the appropriate restriction enzymes (NE BioLabs) for 4-6 hours at 37°C.

3.2.1.3 DNA purification.

Digested DNA products were subjected to electrophoresis on 0.8-1.5% agarose gels. Bands of interest were cut and purified either using Wizard® SV Gel and PCR Clean-Up System (Promega) or through a standard phenol-chloroform protocol for DNA purification, and subsequently concentrated using ethanol precipitation.

3.2.1.4 Ligase-dependent cloning.

Complementary DNA products were ligated after DNA purification using T4 DNA Ligase (NE BioLabs) overnight at 16°C. Competent *E. coli* DH5α were then transformed with ligation products and plated on LB-plates with the appropriate antibiotic. Colonies were screened and ligated plasmids were subjected to DNA sequencing.

3.2.1.5 Gateway® Technology.

The Gateway® cloning system allows the highly efficient introduction of DNA sequences into appropriate vectors through site-specific recombination in a ligase-independent manner. The technology takes advantage of the recombination properties of the bacteriophage lambda. Genes of interest were amplified using appropriate primers listed in Table 3.2, bearing attB recombination sites on the flanking regions. DNA products were then purified as previously described and inserted within entry vectors using BP Clonase (Invitrogen) overnight at 25°C, according to manufacturer's protocol. Competent *E. coli* DH5α were then transformed with recombination products and plated on LB plates with the appropriate antibiotic. Colonies were screened and plasmids were subjected to DNA sequencing. Genes of interest were then moved from entry vectors to destination vectors using LR Clonase (Invitrogen) overnight at 25°C, according to manufacturer protocol. Successive steps were the same as previously described.

3.2.1.6 Site-directed mutagenesis.

The site-directed point mutagenesis was performed taking advantage of the QuikChange® Site-Directed mutagenesis system (Stratagene). Point mutations were introduced with specific primers listed in Table 3.3 and mutated plasmids were generated using Pfu Turbo DNA polymerase (Agilent Technologies), according to manufacturer's protocol. PCR products were then digested with DpnI restriction enzyme for 2 hours at 37°C in order to remove parental DNA. Competent *E. coli* DH5α were then transformed with amplification products and plated on LB-plates with the appropriate antibiotic. Colonies were then screened and mutated plasmids were subjected to DNA sequencing.

3.2.1.7 DNA sequencing.

Recombinant and mutated plasmids were analysed with Sanger sequencing using BigDye Terminator v3.1 Cycle Sequencing kit (Applied Biosystems) containing fluorescent labelled dideoxynucleotide terminators (ddNTPs). Reactions and PCR conditions were set according to the manufacturer's protocol, and performed using sequencing primers listed in Table 3.4. Amplification products were purified by a standard ethanol precipitation procedure and examined by capillary electrophoresis on an ABI Prism 3130xl (Applied Biosystems).

3.2.2 Recombinant plasmid construction.

Plasmid pcDNA-Xpress-His-USP15 was purchased from Addgene Inc. (Cambridge, MA, USA). Plasmids p513-HPV16 E6, E6 F47R, E6 6C/6S and plasmid pcDNA3-E6AP were a kind gift of Prof. Lawrence Banks (ICGEB, Trieste, Italy).
Plasmid pCS2+ HA-p53, containing wild-type human *TP53* gene with an N-terminal nine-residue tag of hemagglutinin (HA), was a kind gift of Prof. Michelangelo Cordenonsi (Department of Molecular Medicine, Padua, Italy).
Plasmids pcDNA3-RLuc and pcDNA3-RLuc-UL44 were a kind gift of Dr. Gualtiero Alvisi (Department of Molecular Medicine, Padua, Italy).

For Bioluminescence Resonance Energy Transfer assays, plasmid p513-HPV16 E6 6C/6S was preliminarily reverted into the non-aggregating wild-type-like mutant E6 4C/4S as previously described [Zanier *et al.*, 2012] using the QuikChange® Site-Directed mutagenesis system (Stratagene). HPV16 E6 DNA sequences (E6 wild-type, E6 4C/4S and E6 N-terminal domain, $E6_N$ amino acids 1-80) were then PCR amplified from the respective p513 plasmid using specific primers for Gateway® cloning system. Forward primers contained the attB1 recombinant site while complementary reverse primers contained the attB2 recombinant site with or without a TAA stop codon. Purified PCR products were cloned into a Gateway® entry vector (pDONR207) using BP Clonase (Invitrogen). Sequence-verified clones were used to transfer E6 sequences into Gateway® destination vectors (pDEST, pcDNA3, and pT-REX) using LR Clonase (Invitrogen). Final constructs consisted of E6, E6 4C/4S and $E6_N$ with either N-terminal or C-terminal YFP, and with either N-terminal or C-terminal RLuc. Additionally, plasmid expressing FLAG-$E6_N$ was also constructed for BRET competition assays. Recombinant plasmids were then mutagenized to create splicing-defective mutants as previously described [Pim *et al.*, 2009] and to create dimerization-defective mutants (F47R and F47R/Y43E) using the QuikChange® Site-Directed mutagenesis system (Stratagene) as described in Paragraph 3.2.1.6.

For the production of recombinant p53 constructs, wild-type human p53 was PCR amplified from pCS2+ HA-p53 plasmid using specific primers for Gateway® cloning system. Cloning strategy was the same as described above. Final constructs consisted of wild-type p53 with either N-terminal or C-terminal RLuc.

For *in vitro* protein expression and purification, E6 4C/4S and $E6_N$ sequences were PCR amplified from the respective p513 plasmid and cloned into pET28a+ and pDEST15 vectors in order to produce 6his-tagged and GST-tagged proteins, respectively. E6 sequences were ligated downstream of the 6his and GST sequences, between EcoRI and NotI sites of pET28a+ plasmid, and between XhoI and MluI sites of pDEST15 plasmid, respectively.

3.2.3 Cell culture and transient transfection techniques.

All cells were grown at 37°C, 5% CO_2, in Dulbecco's modified Eagle's medium (DMEM, Life Technologies, Thermo Fisher Scientific) supplemented with 10% fetal bovine serum (FBS) and 1% penicillin/streptomycin (pen/strep), except for CaSki cells, that were cultivated in Roswell Park Memorial Institute medium (RPMI, Life Technologies, Thermo Fisher Scientific) supplemented as described above.

In order to optimize recombinant protein expression through transient transfections, HEK 293T, C33A and H1299 cells were preliminarily subjected to test experiments using different transfection reagents, as a mean to determine the best transfection reagent to be used for further experiments. Cells were plated on 24-well plates and transfected with 2.5 µg of pDEST-YFP-E6 vector using Lipofectamine2000® (Thermo Fisher Scientific), ExGen500® (Biomol GmbH), Arrest-In™ (Open Biosystems) or $CaPO_4$ as follows:

- **Lipofectamine2000®**: transfections were carried out in DMEM with a Lipofectamine-DNA ratio of 2:1 (µl/µg), according to manufacturer's protocol. Transfection mixtures were then distributed dropwise over the culture medium and then replaced with complete DMEM after 6 hours.

- **ExGen500®**: transfections were carried out in 150 mM NaCl with an ExGen-DNA ratio of 3.3:1 (µl/µg), according to manufacturer's protocol. Transfection mixtures represented 1/10 of the total volume of the culture medium and were distributed dropwise over the cells, then replaced with complete medium after 6 hours.

- **Arrest-In™**: transfections were carried out in DMEM with an Arrest-In:DNA ratio of 5:1 (µl/µg), according to manufacturer's protocol. Culture medium was removed and the transfection mixtures were gently added to the cells. After 6 hours, transfection medium was replaced with complete DMEM.

- **$CaPO_4$**: transfections were carried out in ddH_2O containing HEPES Buffered Saline 1x (HBS, 25 mM HEPES, 140 mM NaCl, 750 µM Na_2HPO_4) and 125 mM $CaCl_2$ for the production of $CaPO_4$-DNA crystals. Transfection mixtures were then distributed dropwise over the culture medium and then replaced with complete DMEM after 6 hours.

At 24 hours post-transfection, cells were collected, washed twice with Phosphate Buffered Saline 1x (PBS), resuspended in 100 µl PBS and transferred into a black 96-well OptiPlates (Costar) for fluorimetric analysis. Cells were exposed at an excitation wavelength of 485 ± 15 nm, measuring YFP emission at 535 ± 25 nm, integrated over 1 s, using a VICTOR X2 Multilabel Plate Reader (PerkinElmer).

For silencing of E6/E7 protein expression in HPV-positive cell lines, SiHa, CaSki and Hela cells were plated at 30% confluence and transfected with anti-E6/E7 siRNAs with Lipofectamine RNAiMax (Thermo Fisher Scientific) according to manufacturer's protocol. Cells were then harvested and plated for proliferation assays described in Paragraph 3.2.12.

3.2.4 Bioluminescence Resonance Energy Transfer (BRET) assays.

In order to detect the homodimerization of HPV16 E6 in living cells, 10^5 or $2x10^5$ HEK 293T cells were seeded on 24-well plates and transfected with 500 ng of YFP-tagged constructs to test localization and expression levels, by detecting the fluorescent signal as described below. To maximize protein expression levels, subsequent experiments were carried out cotransfecting 500 ng of USP15. Appropriate amounts of each RLuc-tagged construct were selected to yield a luminometric signal of about 2000 ± 500 luminescence units (LU) at 5 minutes after substrate addition as described below. RLuc-tagged constructs were then transfected alone or in combination with YFP-tagged fusion proteins to calculate BRET values as described below. Transfections of recombinant full-length E6 4C/4S proteins were normalized using p513-E6 plasmid instead of empty vector, and transfected cells were treated with proteasome inhibitor MG-132 (Z-Leu-Leu-Leu-al, Sigma-Aldrich) at a final concentration of 40 µM for 3 hours before harvesting. As a negative control, RLuc-UL44 was cotransfected with YFP-E6 4C/4S in the presence of 500 ng of USP15. Data were collected at 24 hours post-transfection as described below.

For BRET saturation assays, 10^5 HEK 293T cells were seeded on 24-well plates and fixed amounts of RLuc-$E6_N$, RLuc-$E6_N$ F47R and RLuc-$E6_N$ F47R/Y43E were cotransfected with 500 ng of USP15 in the presence of increasing quantities of the relative YFP-tagged protein or empty vector. As a negative control, plasmid pcDNA-RLuc was cotransfected with 500 ng of USP15 in the presence of increasing quantities of YFP-$E6_N$ or empty vector. Data were collected at 48 hours post-transfection as described below.

For BRET competition assays, $2x10^5$ HEK 293T cells were seeded on 24-well plates and transfected with RLuc-E6 4C/4S and YFP-E6 4C/4S as previously described, in the presence of exogenous p53 and E6AP or empty vector. As a positive control, recombinant full-length E6 4C/4S constructs were cotransfected with FLAG-$E6_N$. Data were collected at 24 hours post-transfection after treatment with proteasome inhibitor MG-132 as previously described. Cells were then harvested and stored at -80°C for western blot analysis.

To determine the interaction between HPV16 E6 and p53 in living cells, 10^5 HEK 293T cells were seeded on 24-well plates and transfected with RLuc-p53 in the presence of YFP-E6 4C/4S, YFP-E6 4C/4S F47R, YFP-E6 4C/4S F47R/Y43E or empty vector. All transfections were performed including 500 ng of USP15. As a negative control, RLuc-p53 was cotransfected with YFP-$E6_N$. At 3 hours before harvesting, cells were treated with MG-132. At 24 hours post-transfection data were collected as described below.

All transfections were performed using Lipofectamine2000® (Thermo Fisher Scientific) as described in Paragraph 3.2.3.

3.2.5 BRET data analysis.

At 24 or 48 hours post-transfection, HEK 293T cells were washed and resuspended in 290 µl PBS. Cells were transferred in triplicate (90 µl per well) into black 96-well OptiPlates (Costar) for fluorimetric/luminometric analysis. Fluorimetric analysis was performed exposing cells at an excitation wavelength of 485 ± 15 nm, measuring YFP-tagged proteins emission at 535 ± 25 nm ($Em_{fluo}535$), integrated over 1 s, using a VICTOR X2 Multilabel Plate Reader (PerkinElmer). Luminometric analysis was performed adding 10 µl/well of benzyl-coelenterazine 50 µM (P.j.k. GmbH) measuring the emission signals at 535 ± 25 nm ($Em_{lum}535$) and 460 ± 25 nm ($Em_{lum}460$), integrated over 1 s, at 5 and 15 minutes after substrate addition. BRET values (BV) were calculated for each well, after blank substraction, as $Em_{lum}535/Em_{lum}460$. BRET ratios (mBR) were calculated for cells cotransfected with YFP- and RLuc- tagged constructs as $(BV_{sample} - BV_{background})x1000$ at 15 minutes after substrate addition, where $BV_{background}$ represents the $Em_{lum}460$ of cells transfected with the relative RLuc-tagged construct alone. For BRET saturation experiments, mBRs were plotted against Y/R values, expressed as $Em_{fluo}535/Em_{lum}460$ calculated at 5 minutes after substrate addition.

3.2.6 Microscopy.

At 24 hours post-transfection, HEK 293T cells transfected with YFP-tagged constructs were observed with an inverted Leica DM IL LED microscope, with a 40X objective, at an excitation wavelength of 488 nm.

3.2.7 Cell-based p53 degradation assay.

To monitor the E6-mediated degradation of p53 in HPV-negative cell lines, $6x10^5$ C33A cells/well or $3x10^5$ HEK 293T cells/well were seeded on 6-well plates and transfected with 5 µg of splicing-defective p513-E6, p513-E6 F47R, p513-E6 F47R/Y43E or empty vector using $CaPO_4$ and Lipofectamine2000® (Thermo Fisher Scientific), respectively. Cells were grown in complete medium at 37°C for 48 hours before harvesting.

For small molecule testing, selected compounds were diluted in complete medium and added to C33A cells after the 6 hour-incubation time of the transfection protocol (see also Paragraph 3.2.3). Cells were then treated for 48 hours before harvesting.

To monitor the compound 12-induced proteasome-dependent degradation of E6, C33A cells were transfected and treated as previously described. At 3 hours before harvesting, proteasome inhibitor MG-132 (Sigma Aldrich) was added at a final concentration of 40 µM in the presence of fresh compound 12.

3.2.8 Cell-based assay for TAZ induction.

To monitor the E6-mediated induction of TAZ in HPV-negative cell lines, $6x10^5$ C33A cells/well were seeded on 6-well plates and transfected with 1 µg of splicing-defective p513-E6, p513-E6 F47R, p513-E6 F47R/Y43E or empty vector using $CaPO_4$. Similarly, $2.5x10^5$ H1299 cells were transfected with 0.5 µg of p513-E6, p513-E6 F47R, p513-E6 F47R/Y43E or empty vector using Arrest-In™ (Open Biosystems). Cells were grown at 37°C in serum-reduced medium (DMEM, 1% FBS, 1% pen/strep) in order to enhance Hippo downregulation as previously described [He *et al.*, 2015]. Cells were harvested when they reached confluence at 48 and 24 hours post-transfection, respectively.

3.2.9 Western Blot.

3.2.9.1 Protein extraction and quantification.

Adherent HEK 293T and H1299 cells were trypsinized and harvested, whereas floating C33A cells were also collected before trypsinization of adherent cells. Cells were pelleted at 100 x g for 5 minutes at 4°C and frozen at -80°C. Pellets were then thawed, resuspended in RIPA buffer (50 mM Tris, 150 mM NaCl, 1% NP-40, 0.1% SDS) with Halt Protease Inhibitor Cocktail 1x (Thermo Fisher Scientific) and incubated on ice for 30 minutes to let the lysis occur. Samples were then centrifuged at 15000 rpm for 15 minutes at 4°C to remove cellular debris. Protein supernatants were collected and quantified using Pierce™ BCA Protein Assay Kit (Thermo Fisher Scientific) on 96-well plates, according to manufacturer's protocol. In this way, protein concentrations are determined through the reduction of Cu^{2+} to Cu^{+} by proteins in an alkaline medium, with the selective colorimetric detection of the Cu^{+} cations through the use of the bicinchoninic acid (BCA) contained in the working reagent. Absorbance values were read at 620 nm on a spectrophotometer microplate reader (Tecan Sunrise).

3.2.9.2 SDS-PAGE and protein transfer.

Cellular proteins were separated according to their molecular weight through sodium dodecyl sulphate-polyacrylamide gel electrophoresis (SDS-PAGE) by loading 50 µg of cellular lysates on 8-12% SDS-PAGE gels, depending on the size of the protein to be visualized. Samples were mixed with Loading buffer 5x (312.5 mM Tris-HCl , 50% glycerol, 10% SDS, 5% β-mercaptoethanol, 0.5% bromophenol blue, pH 6.8) and boiled for 5 minutes prior to loading. Electrophoretic runs were performed at 80 V for about 3 hours in Running buffer (25 mM Tris, 192 mM glycin, 0.1% SDS) with Prestained Protein Sharpmass V marker (Euroclone). Proteins were then transferred to polyvinylidene difluoride (PVDF) membranes, previously activated in 100% methanol for 30 seconds, in a wet transfer apparatus (BioRad) at 350 mA, for 1 hour on ice, in Transfer buffer (25 mM Tris, 192 mM glycin, 20% methanol, 0.03% SDS). Gels and membranes were equilibrated in Transfer buffer before the electrophoretic run. For transferring high molecular weight proteins (approximately >150 KDa), cellular lysates were loaded on 7.5% SDS-PAGE gels and proteins were separated as previously described. Proteins were then transferred on PVDF membranes overnight at 30 V in cold room. Following transfer, PVDF membranes were incubated in blocking solution, TBST-5% milk (Tris Buffered Saline 1x, TBS, 0.1% Tween20, 5% milk) for 2 hours at room temperature (RT) and subsequently incubated overnight with the primary antibodies on a platform shaker. Membranes were then washed 4 times on agitation with TBST (15 minutes per wash), incubated with the relative horseradish peroxidase (HRP)-conjugated secondary antibodies for 1 hour at RT on agitation, and washed 4 times with TBST as before.

3.2.9.3 Detection of blotted proteins.

Protein bands were detected through the HRP-dependent activation of a chemoluminescent substrate, using either a VersaDoc imager (BioRad) or BioMax X-ray films (Kodak) with LiteAblot EXTEND (Euroclone) and ECL (GE Healthcare) substrates, respectively. For the detection of blotted proteins, primary antibodies were used as follows: anti-p53 1:5000 in TBST-5% milk; anti-β-actin 1:8000 in TBST-5% milk; anti-WWTR1 (TAZ) 1:1000 in TBST-0.5% milk; anti-Scribble 1:500 in TBST-0.5% milk; anti-FLAG 1:2000 in TBST-5% milk. Wild-type E6 was detected using anti-HPV16 E6 (N-17) 1:500 in TBST-0.1% milk. However, for the simultaneous detection of wild-type and mutant E6, anti-HPV16 E6 (C-19) was used, 1:200 in TBST-0.1% milk. For GST pull-down assays, monoclonal anti-6his was used 1:10000 in TBST-5% milk. Secondary antibodies were all used 1:2000 in TBST-5% milk. For a detailed list, see also Paragraph 3.1.7.

3.2.9.4 Stripping and reprobing.

For the reprobing of blotted membranes, stripping was performed by immersing the membranes into Stripping buffer (62.5 mM Tris-HCl, 2% SDS, 0.8% β-mercaptoethanol, pH 6.8), with a 30-minute incubation at 50°C. Membranes were then extensively washed with TBS, re-blocked with TBST-5% milk and incubated overnight with the primary antibody as previously described.

3.2.10 Cell growth curves.

In order to determine the proper number of cells to be plated on 96-well plates for compound testing, cell growth curves were determined by plating different amounts of SiHa, CaSki, Hela, C33A and HFF cells on 96-well plates, ranging from 10^3 to 10^5 cells/well. Following cell adhesion, compound treatment was simulated simply by growing cells at 37°C for 24 or 48 hours. Cell confluence was determined by means of the relative cell viability through the 3-(4,5-dimethylthiazol-2-yl)-2,5-diphenyl tetrazolium bromide (MTT) method. Cells were incubated with 10 µl/well of MTT substrate (Sigma Aldrich), previously dissolved in PBS (5 mg/ml), for 4 hours at 37°C to allow the incorporation and the reduction of the tetrazolium salt. Cells were then lysed with 100 µl/well of Solubilizing solution (10% SDS, 0.01 N HCl) overnight at 37°C. Absorbances were read at 620 nm on a spectrophotometer microplate reader (Tecan Sunrise).

3.2.11 Cytotoxicity assays.

$2x10^4$ SiHa, $1.5x10^4$ CaSki, $5x10^3$ Hela, $5x10^4$ C33A and 10^4 HFF cells were seeded on 96-well plates 24 hours prior to drug addition. Increasing concentrations of test compounds were added on cells in complete fresh medium (DMEM, 10% FBS, 1% pen/strep) for 48 hours. The cytotoxicities were assayed by the 3-(4,5-dimethylthiazol-2-yl)-2,5-diphenyl tetrazolium bromide (MTT) method as described in Chapter 3.2.10.

3.2.12 Proliferation assays.

3.2.12.1 Colony formation assay.

To evaluate cell proliferation on plastic surface after compound treatment, SiHa, CaSki, Hela and C33A cells were seeded in duplicate on 6-well plates 24 hours prior to drug addition at a density of $5x10^2$, $2.5x10^2$, 10^2 and $1.5x10^2$ cells/well, respectively. Cells were then treated twice a week with compounds 3 and 6 at 50 and 100 μM and with compound 12 at 20 and 50 μM, respectively, in complete fresh medium for two weeks, until colonies have formed in the control samples, where the cells were treated with 0.1% DMSO in complete fresh medium. Cells were then fixed and stained with crystal violet using a Fixing/Staining solution (0.05% crystal violet, 1% formaldehyde, 1% methanol in PBS) for 20 minutes at RT, then washed with water and air dried. Colonies were counted by visual inspection and aggregates with > 50 cells were scored as colonies.

3.2.12.2 Soft agar colony formation assay.

To evaluate the anchorage-independent growth of cells after compound treatment, 10^4 SiHa, CaSki and Hela cells were plated in duplicate on 6-well plates 24 hours prior to drug addition in complete growth medium containing 0.3% low melting agarose (Invitrogen), over a 0.6% low melting agarose layer without cells. SiHa and CaSki cells were treated for 8 weeks while Hela cells were treated for 3 weeks as described in Paragraph 3.2.12.1 until colonies have formed in the control samples. Cells were then fixed in 4% paraformaldehyde (PFA) in PBS for 20 minutes at RT and observed under phase-contrast microscopy. Aggregates with > 50 cells were scored as colonies and counted.

3.2.13 Protein expression and purification.

3.2.13.1 Test expression experiments.

Before large-scale protein expressions, the expression level and solubility of 6his-E6 4C/4S, GST-E6 4C/4S, 6his-$E6_N$ and GST-$E6_N$ proteins were determined by the visual estimation of the intensity of the corresponding band on SDS-PAGE gels after small scale test expressions.

To test the yield of recombinant protein production, competent *Escherichia coli* strain BL21(DE3)pLysS was transformed with plasmids pDEST15-$E6_N$, pDEST15-E6 4C/4S, pET28a-$E6_N$ or pET28a-E6 4C/4S and grown at 37°C in 100 ml LB medium containing the appropriate antibiotic until the OD_{600} was 0.8. Protein expressions were induced either for 4 hours at 37°C or overnight at 16°C, by the addition of 0.5 mM isopropyl-β-D-thiogalactopyranoside (IPTG). Expression results were checked on 8-15% SDS-PAGE gels stained with Coomassie solution (40% methanol, 10% acetic acid, 0.05% (wt/vol) Coomassie Brilliant Blue) for 1 hour at RT and destained with Destaining solution (40% methanol, 10% acetic acid) until the background returned clear.

To test the solubility of the recombinant proteins, expressions were induced both at 37°C or at 16°C as described above. Cells were then pelleted, resuspended in PBS with 1 mg/ml lysozyme and complete protease inhibitors (Roche Molecular Biochemicals) and lysed by two freeze/thaw cycles. Bacterial lysates were then centrifuged at 13000 x g for 3 minutes, supernatants were collected while pellets were resuspended in PBS. Expression results were checked on 8-15% SDS-PAGE gels as described above.

3.2.13.2 Protein expression and purification.

Competent *Escherichia coli* strain BL21(DE3)pLysS was transformed with plasmids pDEST15-$E6_N$ or pET28a-$E6_N$ to express recombinant GST-$E6_N$ or 6his-$E6_N$ proteins, respectively. Cells were grown at 37°C in LB medium containing the appropriate antibiotic until the OD_{600} was 0.8 and protein expressions were induced by the addition of 0.5 mM IPTG overnight at 16°C.

For GST-$E6_N$ protein purification, cells were pelleted, resuspended on ice in Resuspension buffer (20 mM Tris-HCl, 100 mM NaCl, 10 mM DTT, 0.2 mM EDTA, pH 7.5) with 1 mg/ml lysozyme and complete protease inhibitors (Roche Molecular Biochemicals) and lysed by two freeze/thaw cycles and by sonication. Bacterial lysate was centrifuged at 16000 x g for 30 minutes at 4°C, supernatant was collected, centrifuged again at 16000 x g for 10 minutes at 4°C and applied to Glutathione Sepharose 4Fast Flow resin (GE Healthcare) packed on a Glass Econo-Column (BioRad) equilibrated in Resuspension buffer.

Bound protein was extensively washed with Resuspension buffer and eluted with Elution buffer (20 mM Tris-HCl, 100 mM NaCl, 10 mM DTT, 20 mM glutathione, pH 8).

For untagged $E6_N$ protein purification, GST-$E6_N$ protein bound to GSH-resin was extensively washed with Resuspension buffer, equilibrated in Cleavage buffer (50 mM Tris-HCl, 150 mM NaCl, 1 mM DTT, 1 mM EDTA, pH 7.5) and incubated with 1 ml of PreScission Protease (GE Healthcare) 1:10 in cleavage buffer for 4 hours at 4°C. The untagged $E6_N$ protein was then eluted with Cleavage buffer.

For 6his-$E6_N$ protein purification, cells were pelleted, resuspended on ice in Resuspension buffer (20 mM Tris-HCl, 500 mM NaCl, 10 mM β-mercaptoethanol, 25 mM imidazole, pH 7.5) with 1 mg/ml lysozyme and protease inhibitors, lysed and pelleted as described above. Lysate was applied to a 1 ml HisTrap FF column (GE Healthcare) equilibrated with Resuspension buffer using an Äkta Purifier apparatus (GE Healthcare). Bound protein was extensively washed with Resuspension buffer and then eluted with Elution buffer (20 mM Tris-HCl, 500 mM NaCl, 10 mM β-mercaptoethanol, 250 mM imidazole, pH 7.5).

Purified proteins (GST-$E6_N$, 6his-$E6_N$ and untagged $E6_N$) were dialyzed at 4°C against Storage buffer (20 mM Tris-HCl, 150 mM NaCl, 5 mM DTT, 30% (vol/vol) glycerol, pH 7) in slow agitation using either Dialysis tubing cellulose membranes (Sigma Aldrich) or Slide-A-Lyzer dialysis cassettes (Thermo Fisher Scientific) and then stored at -80°C. Purification results were checked onto 12-15% SDS-PAGE gels as previously described.

3.2.13.3 Protein quantification.

Purified proteins were quantified using the Bio-Rad Protein Assay kit (BioRad) on 96-well plates, according to manufacturer's protocol. Quantification is based on the method of Bradford, through which the concentration of soluble proteins is determined by means of the color change of the Coomassie Brilliant Blue dye. Absorbance values were read at 620 nm on a spectrophotometer microplate reader (Tecan Sunrise).

3.2.14 GST pull-down assay.

$E6_N$ self-association was preliminary assayed through a GST pull-down. Purified recombinant GST or GST-$E6_N$ were incubated with Glutathione Sepharose 4Fast Flow agarose beads (GE Healthcare) in Binding buffer (2.5 mM HEPES, 12.5 mM $MgCl_2$, 20% glycerol, 0.1% NP-40, 150 mM KCl, 0.015% (wt/vol) BSA, 1 mM DTT, pH 7.5) in the presence of 6his-$E6_N$. Binding reactions were performed either at 4°C or RT for 2 hours in slow agitation with a 6his-$E6_N$:GST-$E6_N$ ratio of 4:1 (nmol/nmol). Samples were then loaded and packed on Poly-Prep columns (BioRad), washed 5 times with TNEN buffer (20 mM Tris-HCl, 100 mM NaCl, 0.5 mM EDTA, 0.25% NP-40, pH 8) and bound proteins were eluted with Elution buffer (20 mM Tris-HCl, 100 mM NaCl, 0.5 mM EDTA, 0.25% NP-40, 20 mM glutathione, pH 8). Samples were then loaded on a 15% SDS-PAGE gel and analyzed through western blotting as described in Paragraph 3.2.9.

3.2.15 ELISA $E6_N$ homodimerization assay.

In preliminary experiments, 96-well microtiter plates (Nuova Aptaca) were coated with 400 ng of GST-$E6_N$ or 6his-$E6_N$ in PBS for 3 hours at 37°C and blocked with 2% (wt/vol) BSA (Sigma Aldrich) in PBS for 2 hours at 37°C. Wells were washed with PBST (PBS, 0.3% Tween20) and those coated with GST-$E6_N$ were incubated overnight with increasing quantities of 6his-$E6_N$ or 6his-$PA_{239\text{-}716}$, while wells coated with 6his-$E6_N$ were incubated with increasing quantities of GST-$E6_N$ or GST, in PBS at RT. Wells were then washed with PBST and incubated for 1 hour at RT with HRP-conjugated anti-6his antibody (QED Bioscience, 1:10000 in PBS with 2% (vol/vol) FBS) and HRP-conjugated anti-GST antibody (GenScript, 1:5000 in PBS with 2% (vol/vol) FBS), respectively. Wells were washed again with PBST, incubated with the chromogenic substrate 3,3',5,5'tetramethylbenzidine (TMB, KPL Inc.) and acidified with HCl 3.6%. Absorbances were read at 450 nm on a spectrophotometer microplate reader (Tecan Sunrise).

For preliminary competition assays, wells were coated with 400 ng of 6his-$E6_N$ as described before, and incubated overnight with 400 ng of GST-$E6_N$ in the absence or presence of increasing amounts of purified 6his-$E6_N$. Samples were washed, incubated with the HRP-conjugated anti-GST antibody (GenScript) and processed as previously described.

To evaluate the aspecific interaction between $E6_N$ and GST, 96-well microtiter plates (Nuova Aptaca) were coated with 400 ng of GST as described above and incubated overnight with increasing amounts of 6his-$E6_N$ in the absence or presence of increasing amounts of GST-$E6_N$. Interaction signals were detected using the HRP-conjugated anti-6his antibody (QED Bioscience) as previously described.

For the detection of $E6_N$ homodimerization and to subsequently test the ability of candidate compounds to inhibit $E6_N$ self-association, 96-well microtiter plates (Nuova Aptaca) were coated with 400 ng of untagged $E6_N$ in PBS for 3 hours at 37°C and blocked as previously described. Coated wells were washed with PBST and, for interaction assays, incubated overnight with increasing quantities of 6his-$E6_N$ or 6his-$PA_{239-716}$ in DMEM at 30°C while, for inhibition assays, incubated overnight with 400 ng of 6his-$E6_N$ in the absence or presence of increasing quantities of $E6_N$, UL44 or test compounds in DMEM at 30°C. After washing with PBST, samples were incubated with HRP-conjugated anti-6his antibody (QED Bioscience) and processed as described above.

3.2.16 Statistical analyses.

Data were analyzed with unpaired Student *t* test or one-way analysis of variance (ANOVA) using GraphPad Prism 6 (GraphPad Software Inc.). Values were presented as Mean ± SD of at least two independent experiments. Statistical significance was calculated with a p value < 0.05. Binding curves were calculated by non-linear regression of the data.

4. Results

4.1 Biological studies on the homodimerization of HPV16 E6.

4.1.1 HPV16 E6 can self-associate in living cells.

To study the site-specific homodimerization of HPV16 E6 in living cells, the N-terminal domain of E6 ($E6_N$) and full-length E6, bearing a substitution in the splicing donor site (G226A) which prevents the expression of the spliced isoforms, were preliminarily chosen for BRET assay. A panel of recombinant proteins bearing either YFP or *Renilla* Luciferase (RLuc) at the N-terminal or at the C-terminal end of each E6 sequence was produced. Recombinant constructs were transfected into HEK 293T cells, which are easily transfectable and allow high levels of exogenous protein production. Transfections were performed with Lipofectamine2000®, which was chosen because of the higher reproducibility observed in preliminary experiments, as compared to other transfection reagents (data not shown). Expression levels of YFP-tagged proteins were preliminarily evaluated by the means of the fluorescent emission signals at 535 nm. Notably, the constructs with the N-terminal YFP tag resulted to be more stable than the counterparts with the C-terminal YFP tag (data not shown). The latter were then excluded from the successive experiments, as BRET assays require high amounts of YFP-tagged proteins to saturate the interacting molecule carrying *Renilla* Luciferase. Subsequently, the localization of YFP recombinant proteins was detected in HEK 293T cells. The recombinant N-terminal domain was ubiquitously localized into the cell, while wild-type E6 localized predominantly into the nucleus as expected, thanks to the presence of all its three NLS sequences (Figure 4.1). However, overexpression of YFP-E6 induced the formation of distinctive nuclear foci that resembled nuclear aggresomes, which were recently reported to occur as a result of E6 protein aggregation following its overexpression in transfected cells [Stutz *et al.*, 2015]. Thus, to circumvent the possible drawbacks due to the E6-mediated aggregation of YFP-E6, we also constructed recombinant constructs using a splicing-defective, non-aggregating mutant isoform (E6 4C/4S), where four non-conserved cysteines on the protein surface are mutated into serines, without affecting protein functionality [Zanier *et al.*, 2012]. Notably, recombinant E6 4C/4S localized mainly into the nucleus as expected but generally with no formation of the nuclear foci previously observed with the wild-type protein (Figure 4.1).

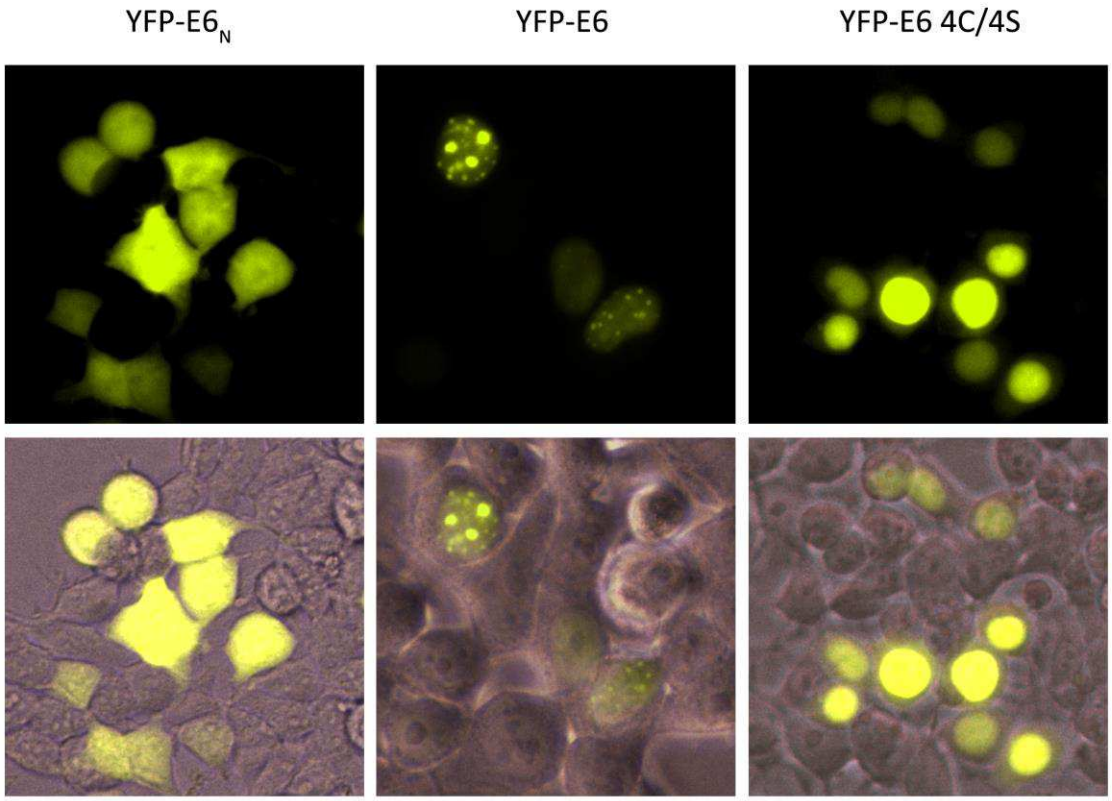

Figure 4.1. Cellular localization of YFP-tagged recombinant proteins. HEK 293T cells were transfected with YFP-$E6_N$, YFP-E6 or YFP-E6 4C/4S and localization of recombinant constructs was visualized at 24 hours post-transfection. Fluorescent signals (upper panels) were merged with cell images visualized under phase-contrast microscopy (lower panels).

To further increase the expression levels of YFP-tagged proteins, recombinant constructs were then cotransfected with the ubiquitin carboxyl-terminal hydrolase 15 (USP15), which was previously shown to stabilize E6 protein levels in cells [Vos *et al.*, 2009]. In addition, in experiments with full-length E6, cells were also treated with the proteasome inhibitor MG-132, in order to further enhance E6 protein stability. HEK 293T cells were then transfected with RLuc-tagged constructs in the presence of the relative YFP-tagged partner or empty vector, in order to detect the RLuc-dependent emission of YFP as a consequence of E6 self-association. Notably, in preliminary experiments we observed different emissions of both RLuc-E6 and RLuc-E6 4C/4S in the absence or the presence of YFP-E6 and YFP-E6 4C/4S, respectively. Thus, we tested whether the global intracellular production of full-length E6 may have an effect on the intracellular levels of E6 itself. Indeed, emission signals of RLuc-E6 and RLuc-E6 4C/4S were drastically increased when the transfections were performed in the presence of untagged E6, instead of empty vector (Figure 4.2). This result agrees with previous data according to which HPV16 E6, and high-risk variants in general, are RNA-binding proteins which can bind their own pre-mRNA, possibly enhancing their own translation [Bodaghi *et al.*, 2009].

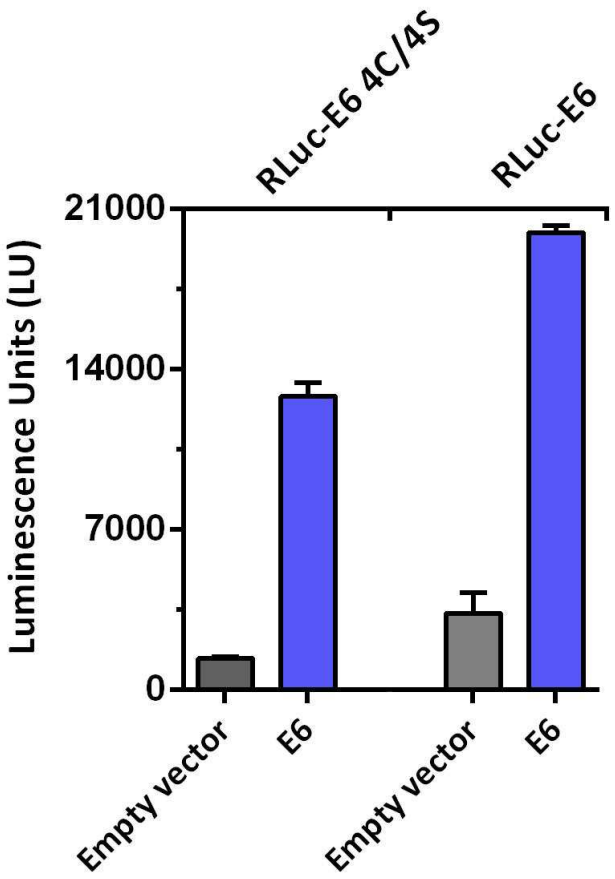

Figure 4.2. Different emission signals of RLuc-E6 and RLuc-E6 4C/4S. HEK 293T cells were transfected with either RLuc-E6 or RLuc-E6 4C/4S in the presence of empty vector or untagged full-length E6. Emission signals were detected at 5 minutes after substrate addition and significantly increased luminescence signals were detected when recombinant full-length proteins were transfected in the presence of untagged E6 instead of empty vector.

Thus, in order to detect the homodimerization of full-length E6, HEK 293T cells were transfected with RLuc-E6 or RLuc-E6 4C/4S in the presence of the relative YFP-tagged partner or untagged full-length E6. In these conditions, we could successfully detect the dimerization of both $E6_N$ and E6 4C/4S, with self-association signals of 155 ± 16 mBR and 103 ± 10 mBR, respectively. Interaction signals were significantly above the relative background of non-specificity, where YFP-$E6_N$ and YFP E6 4C/4S were cotransfected with RLuc and RLuc-UL44, respectively (Figure 4.3). Unfortunately, we could not detect the homodimerization of wild-type E6 in these experimental conditions, possibly because of the propensity of the wild-type protein to aggregate upon ectopic overexpression.

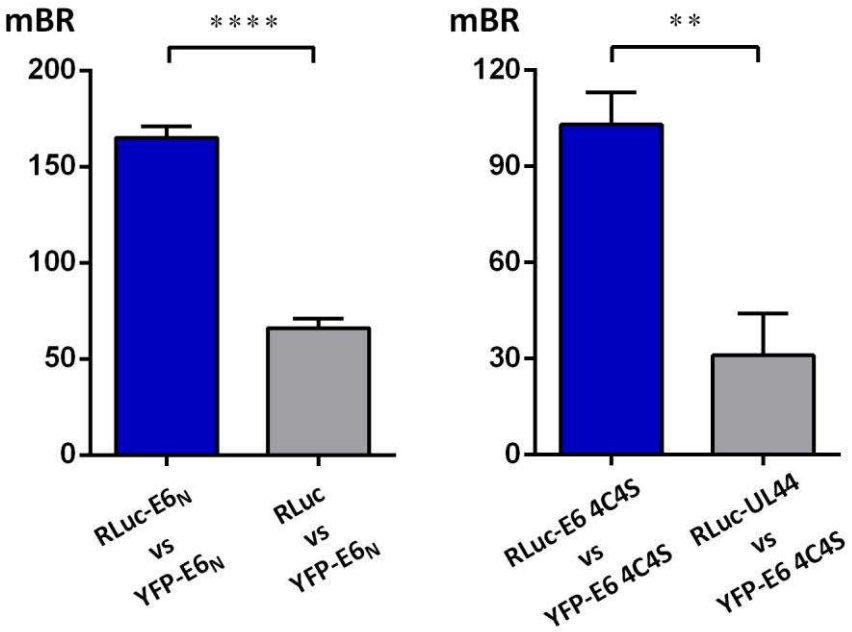

Figure 4.3. Self-association signals of $E6_N$ and E6 4C/4S detected by BRET assay. HEK 293T cells were transfected with RLuc-$E6_N$ and RLuc-E6 4C/4S in the presence of YFP-$E6_N$ and YFP-E6 4C/4S, respectively. Controls of non-specific interaction were obtained by transfecting HEK 293T cells with YFP-$E6_N$ and YFP-E6 4C/4S in the presence of an unfused or an unrelated protein, i.e., RLuc or RLuc-UL44, respectively.

Strikingly, the introduction of point mutations in the predicted dimeric interface (F47R and F47R/Y43E) significantly reduced the self-association signals of both $E6_N$ and E6 4C/4S, confirming that E6 homodimerization is driven specifically by the α2-helix of the N-terminal domain (Figure 4.4). Subsequently, $E6_N$, $E6_N$ F47R and $E6_N$ F47R/Y43E recombinant proteins were used to further study their self-association capacities in a BRET saturation assay, being the only constructs suitable for this kind of experiment. HEK 293T cells were transfected with increasing amounts of either wild-type or mutant YFP-tagged $E6_N$ in the presence of the relative RLuc-tagged protein, and binding curves were obtained. Indeed, mutant constructs exhibited a significative reduction of self-association, close to the background of non-specificity, suggesting the effectiveness of these point mutations in disrupting the interaction (Figure 4.5).

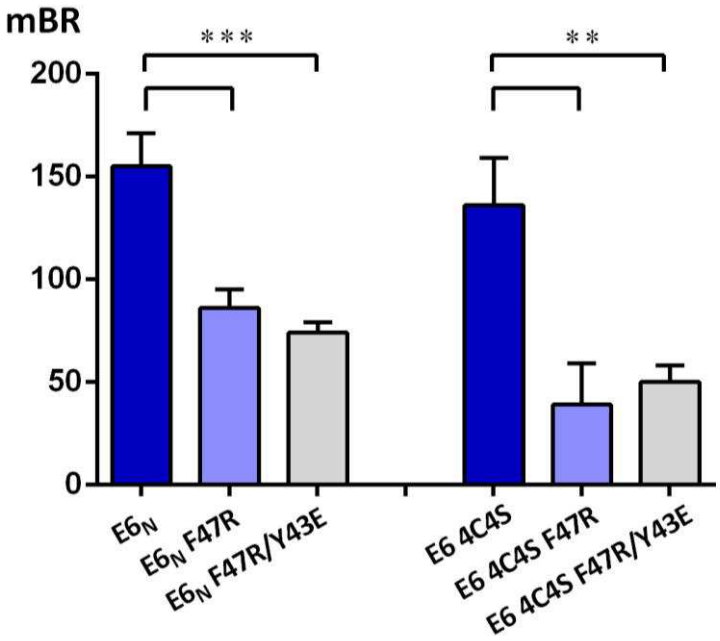

Figure 4.4. Self-association signals of wild-type and dimerization-defective $E6_N$ and E6 4C/4S mutants detected by BRET assay. HEK 293T cells were transfected with RLuc-tagged wild-type or dimerization-defective $E6_N$ and E6 4C/4S in the presence of the relative YFP-tagged construct. Dimerization-defective mutants were obtained through a single or double point mutation (resulting in the amino acid substitutions F47R and F47R/Y43E, respectively) in the *$E6_N$* and *E6 4C/4S* sequences.

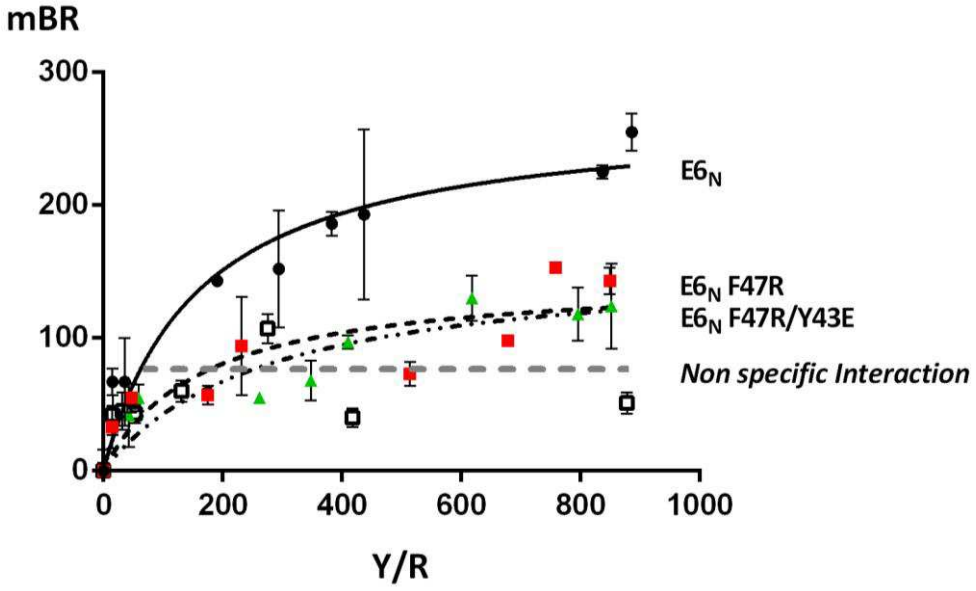

Figure 4.5. Binding curves of HPV16 $E6_N$, $E6_N$ F47R and $E6_N$ F47R/Y43E obtained by BRET saturation assay. HEK 293T cells were transfected with RLuc-tagged $E6_N$, $E6_N$ F47R and $E6_N$ F47R/Y43E in the presence of increasing amounts of the relative YFP-tagged protein. Dimerization-defective mutants showed a significantly reduced ability to self-associate, close to the background of non-specificity obtained by cotransfecting HEK 293T cells with RLuc and YFP-$E6_N$.

4.1.2 HPV16 E6 directly dimerizes through its N-terminal domain.

The detection of E6 self-association in living cells strongly suggested the occurrence of the homodimerization as a result of the direct interaction between two E6 monomers, as confirmed by the inability of the mutants to dimerize. However, the possibility that a third cellular binding partner may have induced the close contact of two E6 molecules in the BRET assay could not be ruled out. Thus, we sought to investigate the homodimerization of HPV16 E6 also *in vitro*, as a way to determine the dependency of E6 self-association on the presence of other cellular proteins. We constructed recombinant vectors expressing both $E6_N$ and full-length E6 4C/4S with N-terminal 6his or GST tags for purification purposes. Notably, we did not choose to express recombinant wild-type full-length E6 due to its known tendency to strongly aggregate and precipitate *in vitro* [Nominé *et al.*, 2001; Zanier *et al.*, 2007; Zanier *et al.*, 2010]. Preliminarily, recombinant proteins were expressed in *E. coli* either at 37°C for 4 hours or at 16°C overnight, in order to determine the culture conditions that could enhance recombinant protein production. Nevertheless, no significative differences were preliminarily observed between the two culture conditions (Figure 4.6).

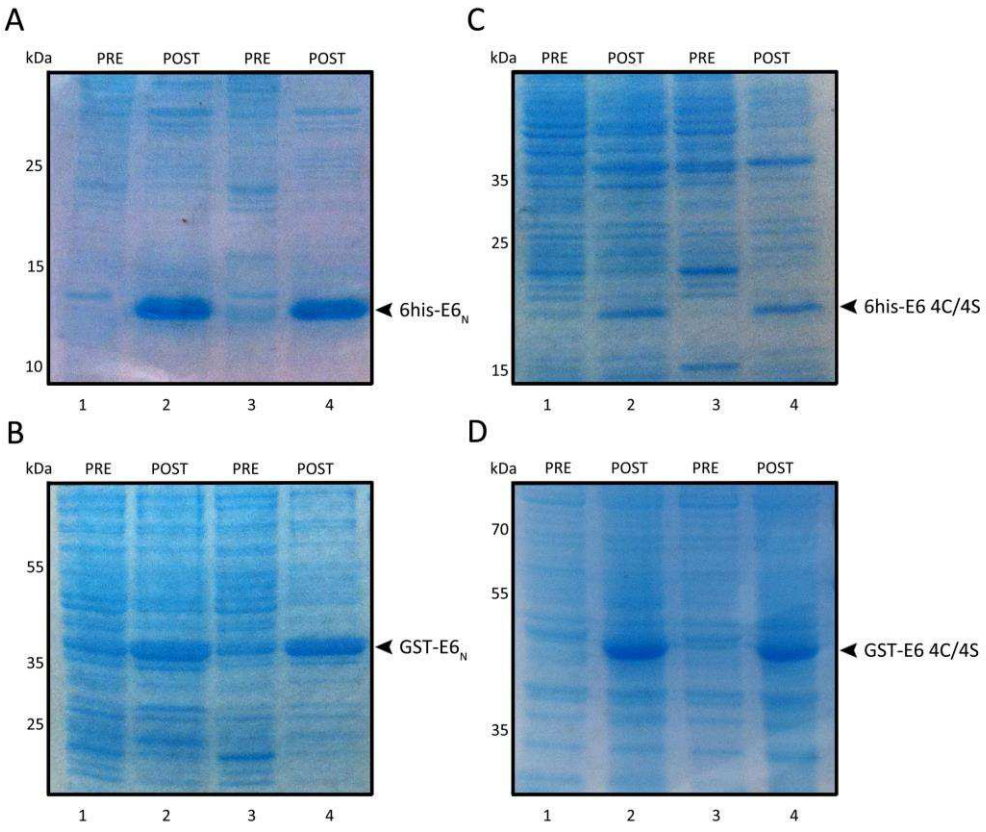

Figure 4.6. ***In vitro*** **expression levels of recombinant (A)** 6his-$E6_N$, **(B)** GST-$E6_N$, **(C)** 6his-E6 4C/4S and **(D)** GST-E6 4C/4S. Protein expressions were induced either for 4 hours at 37°C (lanes 2) or overnight at 16°C (lanes 4). Expression levels were determined by means of the intensity of the relative band on SDS-PAGE gels.

Following these test expression studies, the intracellular solubility of the recombinant proteins was investigated by analyzing their presence in the insoluble or soluble cellular fraction. Notably, GST-E6$_N$ and 6his-E6$_N$ were found in both fractions while both GST-E6 4C/4S and 6his-E6 4C/4S were found only in the insoluble fraction after cell lysis (Figure 4.7). Thus, recombinant full-length proteins were excluded from following purifications due to the difficulty in retrieving the proteins in the supernatant of cell lysates. Furthermore, we chose to perform subsequent expressions overnight at 16°C in order to minimize the possible temperature-dependent aggregation of the exogenous proteins expressed in *E. coli*. Recombinant GST-E6$_N$ and 6his-E6$_N$ proteins were then expressed and successfully purified from *E. coli* with one-step affinity purification on glutathione or nickel-charged resin, respectively.

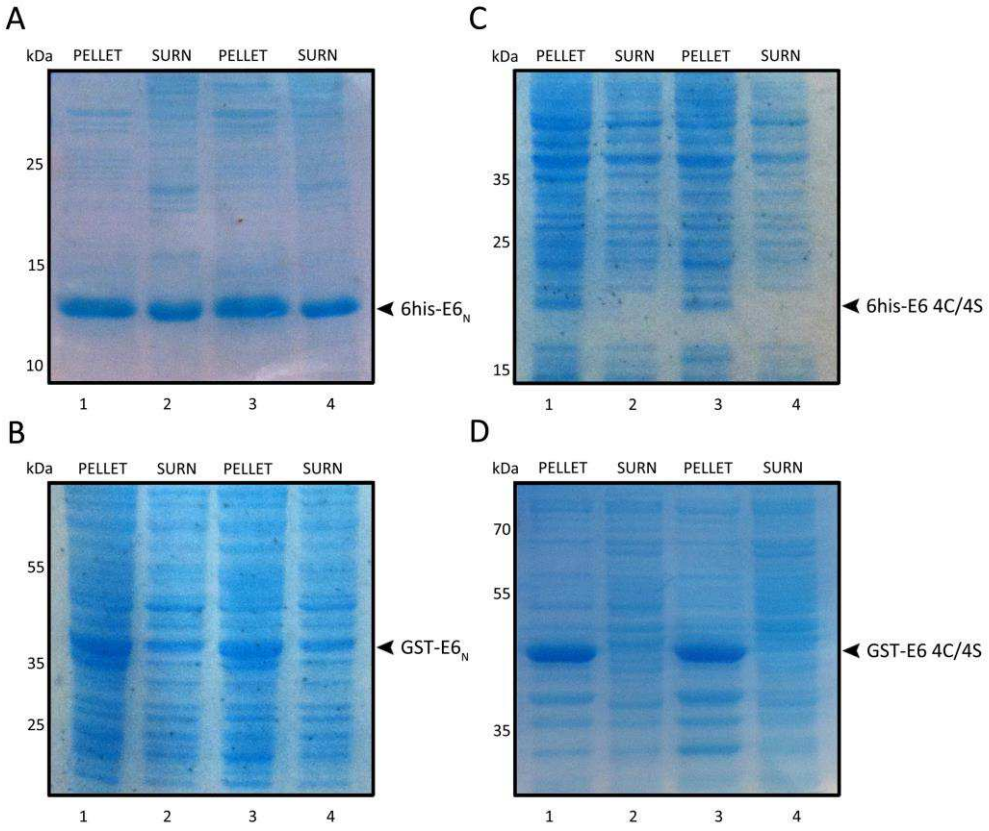

Figure 4.7. Solubility of recombinant proteins: (A) 6his-E6$_N$, **(B)** GST-E6$_N$, **(C)** 6his-E6 4C/4S and **(D)** GST-E6 4C/4S. Protein expressions were induced either for 4 hours at 37°C (lanes 1 and 2) or overnight at 16°C (lanes 3 and 4). Supernatant and pellet samples were obtained through the separation of the soluble fraction from the insoluble fraction by centrifugation after cell lysis. The intracellular solubility of the recombinant proteins was determined by observing the presence of the relative band in the pellets (lanes 1 and 3) or supernatants (lanes 2 and 4) on SDS-PAGE gels.

To preliminarily assess the ability of GST-E6$_N$ and 6his-E6$_N$ to dimerize *in vitro*, we set-up a GST pull-down assay. Recombinant 6his-E6$_N$ was incubated with GST-E6$_N$, or GST alone as a control, in the presence of glutathione resin. We then assessed the ability of GST-E6$_N$ to pull-down the 6his-tagged protein after the elution step. Unfortunately, 6his-E6$_N$ was found only in the input fraction and was never detected in the elution samples, suggesting its inability to bind to GST-E6$_N$ in these experimental conditions (Figure 4.8).

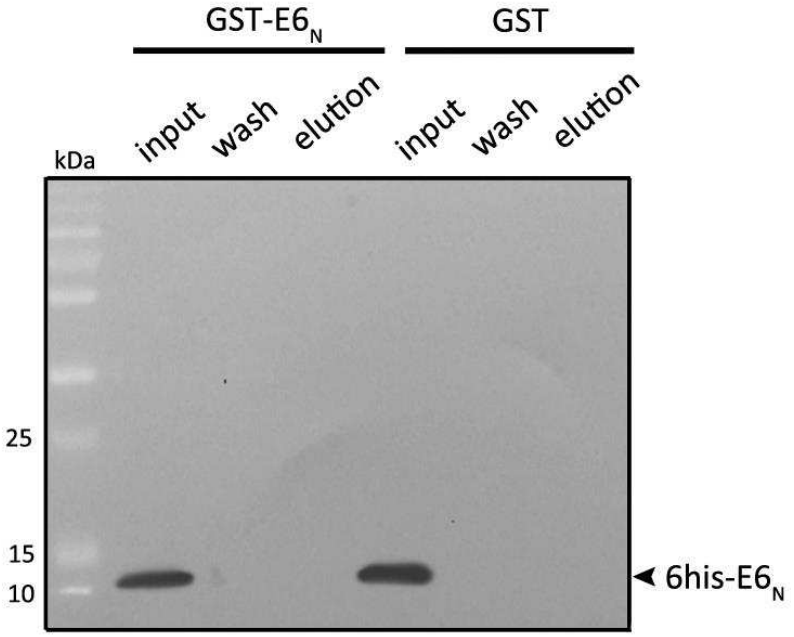

Figure 4.8. GST pull-down assay between 6his-E6$_N$ and GST-E6$_N$ shows the inability of the recombinant proteins to associate in these experimental conditions. Recombinant E6$_N$ proteins were incubated with glutathione agarose beads (input), loaded on columns, washed (wash) and eluted (elution). The binding between 6his-E6$_N$ and GST-E6$_N$ was determined by the presence of 6his-E6$_N$ in the elution samples, detected using a HRP-conjugated anti-6his antibody.

Thus, we analyzed the self-association of E6$_N$ proteins through an ELISA-based *in vitro* assay by coating the wells of microtiter plates with either GST-E6$_N$ or 6his-E6$_N$ and then incubating with the relative partner of the coated protein. Preliminary experiments were conducted by coating microplate wells with 6his-E6$_N$ and then, after washes and blocking, incubating with increasing amounts of GST-E6$_N$ or GST as a control. Notably, we could detect a binding curve as a result of the association between the two recombinant E6$_N$ proteins, but unfortunately the background signal obtained with the GST control was considerably high (Figure 4.9). To test whether the detected association between 6his-E6$_N$ and GST-E6$_N$ was a result of a specific interaction, we performed an ELISA competition assay, by coating wells with 6his-E6$_N$ and then incubating with GST-E6$_N$ in the presence of increasing amounts of the competitor 6his-E6$_N$. Unexpectedly, the interaction signal increased instead of decreasing (Figure 4.10).

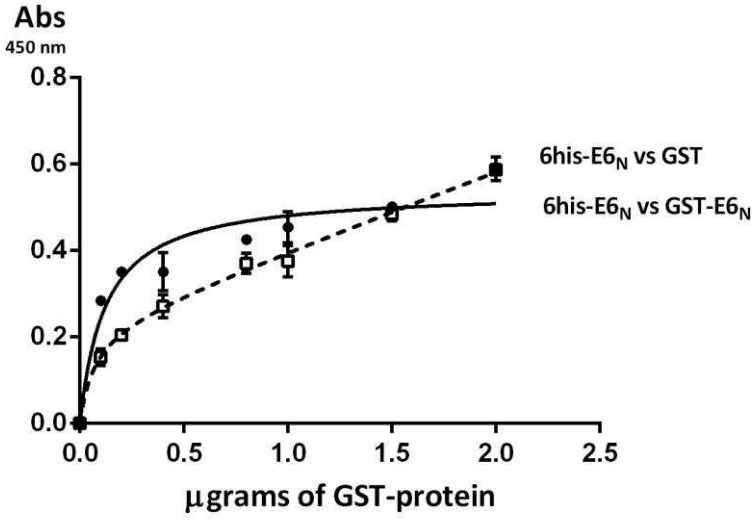

Figure 4.9. Preliminary ELISA-based assay for the detection of $E6_N$ self-association. Microtiter plates were coated with 6his-$E6_N$ and incubated with increasing amounts of GST-$E6_N$ or GST as control. Bound proteins were detected by the use of a HRP-conjugated anti-GST antibody.

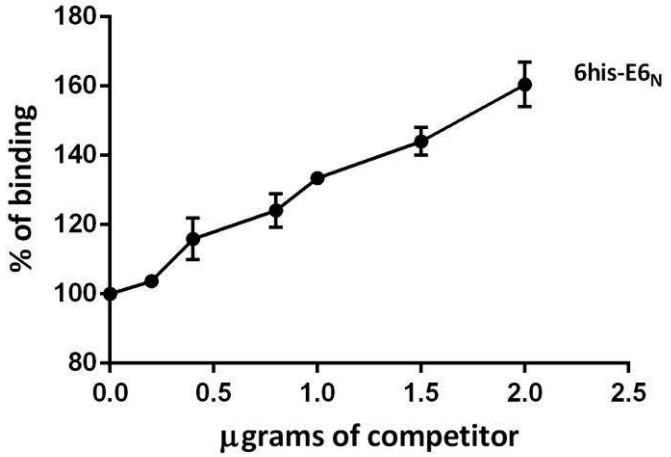

Figure 4.10. Preliminary ELISA-based competition assay. Microtiter plates were coated with 6his-$E6_N$ and incubated with an equivalent amount of GST-$E6_N$ in the presence of increasing quantities of competitor 6his-$E6_N$. GST-$E6_N$ bound to the coated 6his-$E6_N$ was detected by the use of a HRP-conjugated anti-GST antibody. Interaction signal increased instead of decreasing.

Thus, in light of these preliminary results, we tried to detect the interaction between the $E6_N$ proteins in the other way around, coating the wells with GST-$E6_N$ and then incubating with increasing quantities of 6his-$E6_N$. Unexpectedly, the binding curve obtained by incubating GST-$E6_N$ with 6his-$E6_N$ did not represent a site-specific interaction (Figure 4.11).

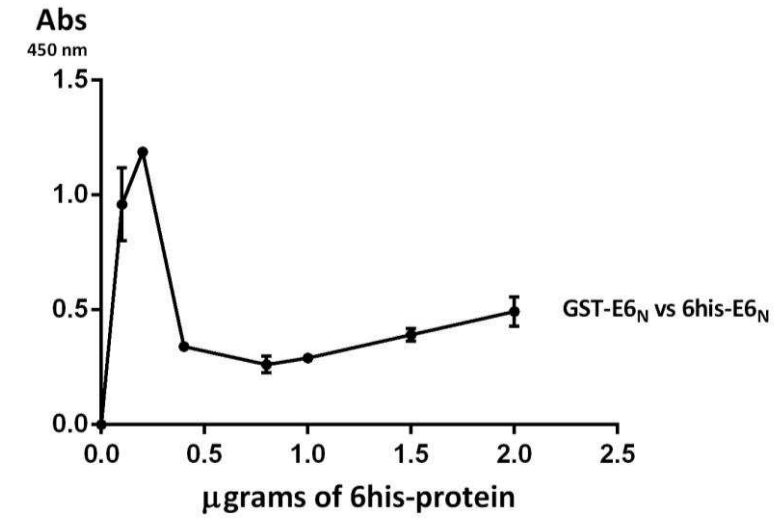

Figure 4.11. Alternative ELISA-based assay for the detection of $E6_N$ self-association. Microtiter plates were coated with GST-$E6_N$ and incubated with increasing amounts of 6his-$E6_N$. 6his-$E6_N$ bound to the coated GST-$E6_N$ was detected by the use of a HRP-conjugated anti-6his antibody.

Thus, we wished to investigate a possible non-specific interaction between $E6_N$ and GST, an event that could possibly explain both the high association signal observed between 6his-$E6_N$ and GST, and the inability of 6his-$E6_N$ to compete in the presence of GST-$E6_N$. Indeed, when we coated wells of microtiter plates with only GST and then incubated with 6his-$E6_N$, we could detect a considerable signal of interaction. Furthermore, the association signal decreased following the incubation with higher amounts of 6his-$E6_N$, suggesting a shift in the binding equilibrium from the interaction of $E6_N$ with GST in favour of $E6_N$ self-association (Figure 4.12).

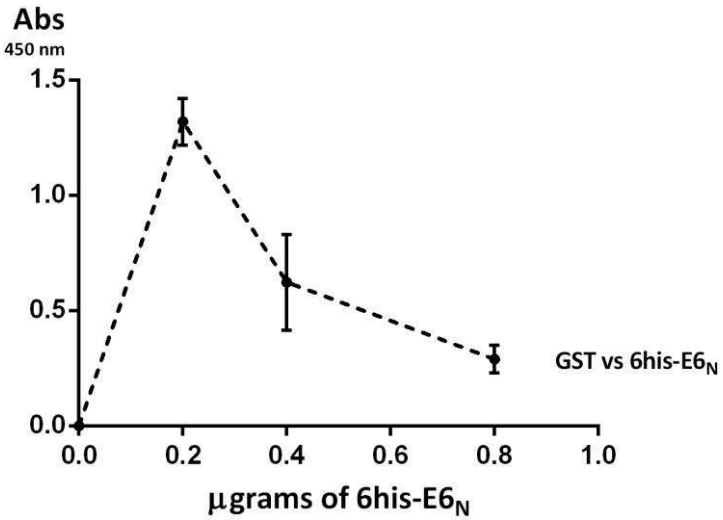

Figure 4.12. An ELISA-based assay demonstrates the aspecific binding of $E6_N$ to the GST tag. Microtiter plates were coated with GST and incubated with an equivalent amount of 6his-$E6_N$ in the presence of increasing quantities of GST-$E6_N$. 6his-$E6_N$ bound to the coated GST was detected by the use of a HRP-conjugated anti-6his antibody.

Thus, the observation of non-specific binding between GST and $E6_N$ protein prompted us to cleave the GST tag during subsequent purifications, whereas the 6his tag was maintained. Indeed, when we coated wells with untagged $E6_N$, we obtained a binding curve following the incubation with increasing amounts of 6his-$E6_N$, with negligible absorbances upon incubation with an unrelated 6his-tagged protein (6his-$PA_{239-716}$; Figure 4.13). The specificity of the interaction was then confirmed with a competition assay, where increasing amounts of untagged $E6_N$ protein effectively reduced the interaction of 6his-$E6_N$ with the coated $E6_N$. In contrast, addition of increasing amounts of an unrelated protein, i.e., untagged UL44 protein from human cytomegalovirus, did not block the interaction between 6his-$E6_N$ and $E6_N$, as expected (Figure 4.14), thus demonstrating that E6 can physically self-associate through the direct interaction between two N-terminal domains.

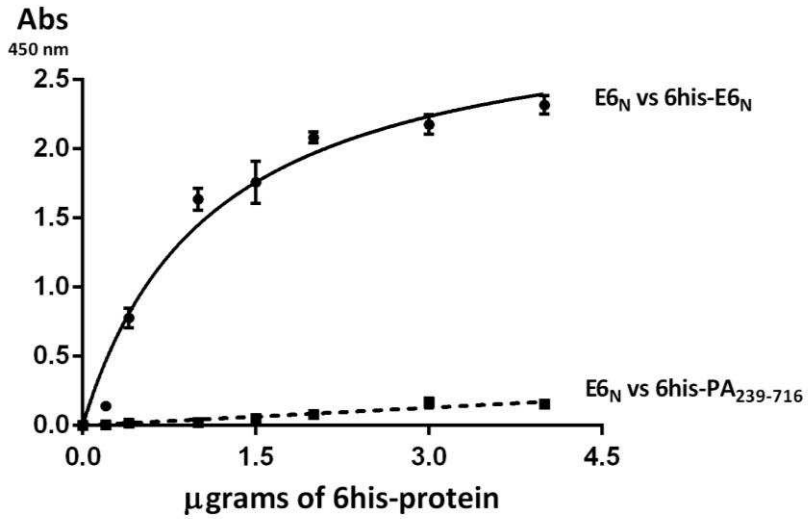

Figure 4.13. ELISA-based $E6_N$ homodimerization assay. Microtiter plates were coated with untagged $E6_N$ and incubated with increasing amounts of 6his-$E6_N$ or 6his-$PA_{239-716}$ as a control. Bound proteins were detected by the use of a HRP-conjugated anti-6his antibody.

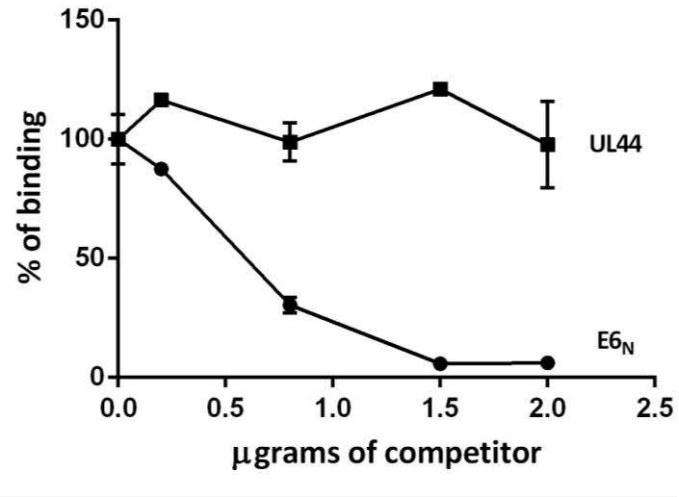

Figure 4.14. An ELISA-based $E6_N$ competition assay confirms the specificity of $E6_N$ dimerization. Microtiter plates were coated with untagged $E6_N$ and incubated with an equivalent amount of 6his-$E6_N$ in the presence of increasing amounts of competitors untagged $E6_N$ or UL44 as a control. Interaction signal decreased only in the presence of the competitor $E6_N$ as expected.

4.1.3 The α2-helix of HPV16 E6 is important for the degradation of p53.

The results presented so far demonstrate the existence of a dimeric form of HPV16 E6 in a cellular context. Taking into account the data published in the literature, according to which substitutions in the α2-helix of E6 were reported to significantly impair the degradation of p53 mediated by the viral oncoprotein [Ristriani *et al.*, 2009], we then wished to confirm the importance of the hydrophobic residues of the α2-helix of HPV16 E6 for the productive degradation of p53. Thus, we developed a cell-based p53 degradation assay by transfecting HPV-negative C33A and HEK 293T cells with plasmids encoding wild-type E6 or dimerization-defective E6 mutants. Preliminarily, cells were subjected to test transfections by transfecting YFP-E6 with different transfection reagents and detecting the relative emission signals in order to determine the experimental conditions that allow efficient E6 overexpression (data not shown). HEK 293T and C33A cells were then transfected with E6, E6 F47R or E6 F47R/Y43E and analyzed through western blotting. Indeed, while wild-type E6 triggered the degradation of p53, as expected, dimerization-defective E6 mutants were unable to induce the degradation of the endogenous p53 in both cell lines (Figure 4.15), in agreement with previous reports [Zanier *et al.*, 2012]. Noteworthy, the inability of the E6 F47R and E6 F47R/Y43E mutants to degrade p53 was observed even though these mutants had the propensity to accumulate at higher levels when compared to wild-type E6. This result is in line with previous studies reporting that the introduction of polar residues in the hydrophobic core of the α2-helix of HPV16 E6 increases the overall stability of the viral oncoprotein [Ristriani *et al.*, 2009].

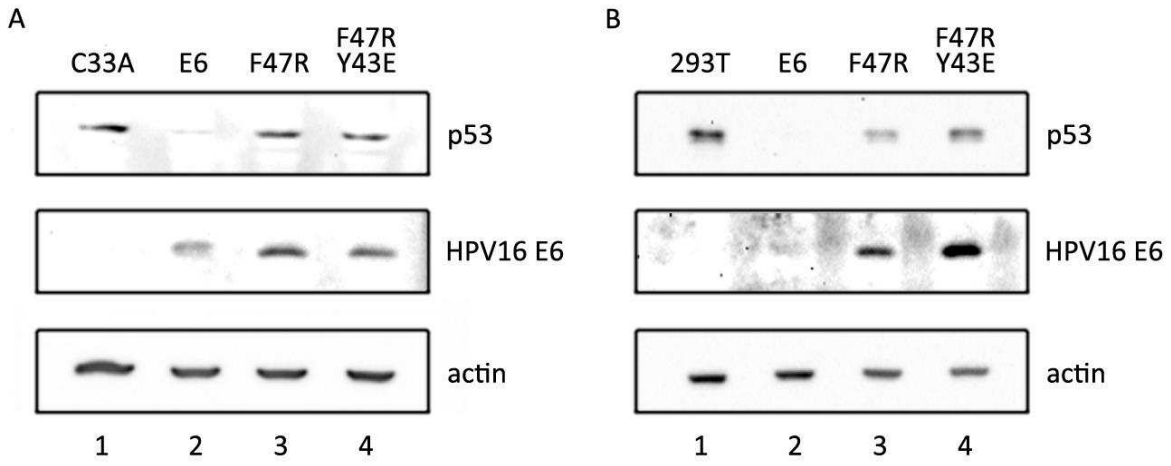

Figure 4.15. Cell-based p53 degradation assay. (A) C33A and **(B)** HEK 293T cells were transfected with empty vector (1) or with plasmids encoding splicing-defective E6 (2), splicing-defective E6 F47R (3), or splicing-defective E6 F47R/Y43E (4). Cells were harvested and cellular lysates were analyzed by western blotting using anti-p53, anti-HPV16 E6 (C-19), and anti-actin antibodies at 48 and 24 hours post-transfection for C33A and HEK 293T cells, respectively.

4.1.4 The α2-helix of HPV16 E6 mediates the interaction with p53.

To study whether dimerization-defective E6 mutants are unable to induce the degradation of p53 as a result of their inability to bind p53, rather than due to an impaired ability to self-associate, we wished to investigate their relative capacity to bind p53 compared to the wild-type oncoprotein. To this aim, we developed an E6-p53 BRET assay in HEK 293T cells. For determining the proper experimental conditions to detect the interaction between E6 and p53 in transfected cells, we decided to use p53 as the donor RLuc-tagged partner, rather than the acceptor YFP-tagged protein. Indeed, using p53 as the acceptor partner would have resulted in the overexpression of a tumor suppressor protein in immortalized cells, with possible negative consequences on the proliferation and survival of transfected cells. Additionally, using E6 as the donor partner would have resulted in expressing low levels of RLuc-tagged E6 proteins. This, in turns, could have potentially resulted in the undetectable binding of E6 to the endogenous p53, rather than binding to the exogenous YFP-tagged p53.

Taking into account these preliminary considerations, we chose to use p53 as the donor recombinant protein and E6 as the acceptor partner, and thus we constructed recombinant vectors expressing wild-type p53 tagged with *Renilla* Luciferase both at the N-terminal and at the C-terminal end of the tumor suppressor protein. Furthermore, according to the latest structural model of the E6/E6AP/p53 trimeric complex [Martinez-Zapien *et al.*, 2016], only full-length E6 proteins can be used to study the interaction of E6 with p53, because both domains of E6, i.e., the N-terminal and C-terminal domain, are required to bind E6AP and, subsequently, to bind p53. HEK 293T cells were then cotransfected with either N-terminally or C-terminally RLuc-tagged p53 constructs in the presence of YFP-E6 4C/4S, YFP-E6 4C/4S F47R, YFP-E6 4C/4S F47R/Y43E or empty vector. Possible non-specific interaction was evaluated by cotransfecting RLuc-tagged p53 proteins with YFP-$E6_N$, since the formation of the trimeric complex E6/E6AP/p53 cannot occur in the absence of the C-terminal domain of E6. In preliminary experiments we observed the ability of YFP-E6 4C/4S to induce the degradation of RLuc-tagged p53 proteins, since decreased emission signals of both RLuc-p53 and p53-RLuc were detected when coexpressed with YFP-E6 4C/4S (data not shown). These data suggested that the YFP and RLuc tags did not significantly impair the ability of E6 4C/4S to bind, and in turn degrade, p53. Subsequent experiments were then performed cotransfecting USP15 and treating cells with proteasome inhibitor MG-132, in order to increase the expression levels of recombinant full-length E6 constructs and block the E6-mediated degradation of p53, respectively. In this way, we could successfully detect the interaction between RLuc-p53 and YFP-E6 4C/4S, with an association signal of 167 ± 21 mBR, significantly above the background of non-specificity (Figure 4.16). Strikingly, in the same experimental setting, mutant recombinant constructs YFP-E6 4C/4S F47R and YFP-E6 4C/4S F47R/Y43E had a significantly decreased ability to bind RLuc-p53 with association signals of 110 ± 2 mBR and 64 ± 3 mBR, respectively (Figure 4.16).

In addition, the same results could be obtained using the p53-RLuc construct (data not shown). Thus, these results suggest that the introduction of the same point mutations that disrupt E6 homodimerization are also impairing the binding between E6 and p53, in agreement with the recently published results [Martinez-Zapien *et al.*, 2016].

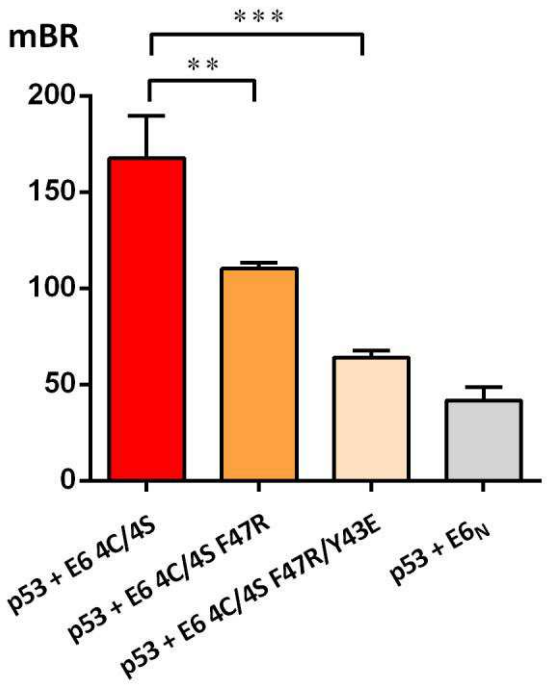

Figure 4.16. BRET assay monitoring the interaction between p53 and wild-type or mutant E6 proteins. HEK 293T cells were transfected with RLuc-p53 in the presence of YFP-E6 4C/4S, YFP-E6 4C/4S F47R or YFP-E6 4C/4S F47R/Y43E. Mutant E6 4C/4S proteins showed a significant reduced ability to bind p53 when compared to wild-type E6. Control of non-specificity was obtained by cotransfecting HEK 293T cells with RLuc-p53 and YFP-$E6_N$.

4.1.5 HPV16 E6 homodimerization and E6-p53 interaction are two independent processes.

The results presented so far demonstrate that the homodimerization of HPV16 E6 and the binding of HPV16 E6 to p53 are two protein-protein interactions (PPIs) that involve the same key residues of the hydrophobic core of the α2-helix. Accordingly, these PPIs appear to be likely two distinct processes occurring on the same surface of the viral oncoprotein. Thus, to test whether indeed p53 can bind E6 independently of the homodimerization of the viral oncoprotein, we sought to investigate whether these interacting partners could compete with each other for the binding on the same interaction surface on E6. To this aim, we developed a BRET competition assay in HEK 293T cells.

In theory, the physical competition between p53 and E6 could be studied by detecting E6-p53 interaction in the absence or presence of a competitor E6, or *vice versa*, by detecting the homodimerization of E6 in the absence or presence of p53. However, considering the low steady-state levels of E6 in transfected cells, we chose to perform the BRET competition assay through the second strategy, wherein the self-association of E6 is detected in the presence of the competitor p53. This is justified also by the impossibility to express high levels of E6 through transient transfection techniques, particularly when employing an untagged protein. In addition, the use of small tags or untagged competitors should be preferred in competition assays, since the steric hindrance induced by the addition of large tags could possibly prevent an efficient competition.

Thus, HEK 293T cells were cotransfected with RLuc-E6 4C/4S and YFP-E6 4C/4S in the absence or the presence of exogenous HA-tagged p53. As previously described, transfections were performed in the presence of USP15 and cells were treated with proteasome inhibitor MG-132 prior to data collection. Although this experimental setting was originally required to enhance the expression levels of recombinant full-length E6 proteins, treatment with proteasome inhibitor MG-132 in the presence of USP15 also results in the downregulation of the E6-mediated degradation of p53, an event that could have induced the degradation of the competitor. As a positive control, RLuc-E6 4C/4S and YFP-E6 4C/4S were cotransfected with FLAG-$E6_N$ in the same experimental conditions. Strikingly, in repeated experiments we never observed the ability of exogenous p53 to compete with E6 self-association, nor to stabilize the formation of the dimeric form of E6, while FLAG-$E6_N$ successfully impaired the binding of YFP-E6 4C/4S to RLuc-E6 4C/4S (Figure 4.17). Taken together, these results indicate that E6-p53 interaction and E6 homodimerization are likely two separated processes which occur independently of each other, as suggested by the inability of p53 to compete with E6 self-association.

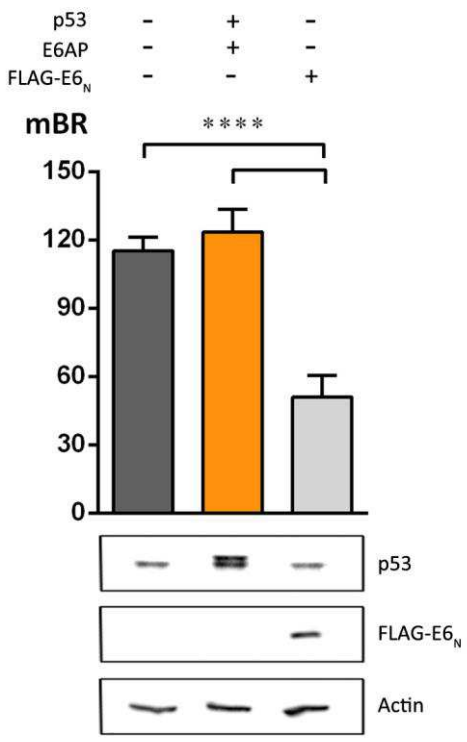

Figure 4.17. BRET competition assay in HEK 293T cells shows the inability of exogenous p53 to compete with E6 self-association. HEK 293T cells were transfected with recombinant E6 4C/4S proteins in the absence or the presence of competitor proteins HA-p53 and E6AP. As a positive control, RLuc- and YFP- tagged E6 4C/4S constructs were cotransfected with FLAG-$E6_N$. Cells were then harvested and cellular lysates were analyzed by western blotting using anti-p53, anti-FLAG, and anti-actin antibodies.

4.1.6 Effects of HPV16 E6 on Scribble protein levels.

The previous observation that the homodimerization of E6 occurs independently of the binding of E6 to p53 disagrees with the original model in which E6 self-association was proposed as a necessary step for the degradation of p53 [Zanier *et al.*, 2012]. However, our results strongly agree with the structural model of the E6/E6AP/p53 trimeric complex and support the idea that E6 homodimerization is an independent process that likely is not involved in the degradation of p53 [Martinez-Zapien *et al.*, 2016].

Thus, in an attempt to determine the role of the dimeric form of E6 in the context of its transforming activities, we sought to investigate the possible correlation between E6 self-association and the degradation of other proteins known to be targeted by the viral oncoprotein, for example, the cytoplasmic PDZ-containing cellular proteins.

Particularly, we studied the effect of wild-type E6 and dimerization defective mutants on the levels of the PDZ-containing protein Scribble, which is known to be a favourite target of HPV16 E6 [Thomas *et al.*, 2016]. Thus, we transfected HPV-negative C33A and HEK 293T cells with either wild-type E6 or dimerization-defective E6 mutants, and analyzed the endogenous levels of Scribble by western blotting. We chose to use both C33A and HEK 293T cells because of their different cellular morphology. Although both are epithelial cell lines, round-shaped C33A cells might possess altered or mislocalized levels of Scribble due to the known tendency of malignant cells to loose focal adhesions and adherence in general. On the contrary, HEK 293T cells still retain an epithelial-like morphology characterized by distinctive membrane protrusions, ECM-cell and cell-cell junctions that correlate with the proper expression and localization of Scribble and cytoskeletal proteins in general.

Unfortunately, we failed to find a correlation between E6 homodimerization and the E6-mediated degradation of Scribble in both cell lines, since no difference in the levels of Scribble was detected upon overexpression of dimerization-defective E6 mutants (F47R and F47R/Y43E) as compared to the wild-type E6 protein (Figure 4.18). However, Scribble degradation was not observed even in cells transfected with wild-type E6, a result that contrasts with previous studies reporting the E6-mediated degradation of Scribble and other cellular PDZ-containing proteins [Nakagawa and Huibregtse, 2000; Massimi *et al.*, 2004]. A possible explanation for these discrepancies is discussed in the “Discussion and Conclusions” chapter.

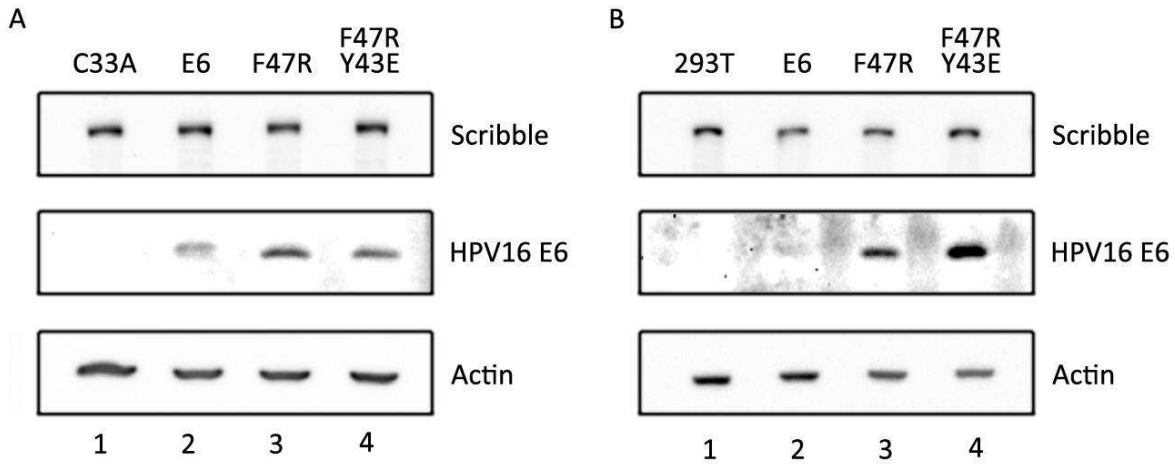

Figure 4.18. Effect of wild-type E6 or dimerization-defective E6 mutants on the endogenous levels of Scribble. (A) C33A and **(B)** HEK 293T cells were transfected with empty vector (1) or with plasmids encoding splicing-defective E6 (2), splicing-defective E6 F47R (3), or splicing-defective E6 F47R/Y43E (4). Cells were harvested and cellular lysates were analyzed by western blotting using anti-Scribble, anti-HPV16 E6 (C-19), and anti-actin antibodies at 48 and 24 hours post-transfection for C33A and HEK 293T cells, respectively.

4.1.7. The dimerization of HPV16 E6 is required for the upregulation of TAZ.

Recently, the interplay between the activity of high-risk E6 proteins and Hippo signaling pathway has been reported [He *et al.*, 2015]. In fact, it was shown that high-risk E6 oncoproteins are capable of upregulating YAP as a result of the E6-mediated degradation of SOCS6, a known YAP inhibitor. Thus, we sought to investigate whether E6 self-association might correlate with YAP, and/or possibly TAZ, upregulation, the two main transducers of the Hippo signaling cascade.

Preliminarily, we wished to confirm the E6-mediated upregulation of YAP in our experimental setting, and thus C33A cells were transfected with wild-type E6 or dimerization-defective E6 mutants and transfected cells were harvested at high density for western blot analysis. Strikingly, in an attempt to detect the accumulation of the endogenous levels of YAP following the expression of wild-type or mutant E6 proteins, we observed that wild-type HPV16 E6 was able to upregulate TAZ and, most importantly, this effect was abolished by the introduction of polar residues in the hydrophobic core of the α2-helix (Figure 4.19). However, dimerization-defective mutants that were not able to upregulate TAZ were still able to upregulate YAP, suggesting the possible involvement of E6 self-association only in the stabilization of TAZ, rather than YAP, protein levels (data not shown).

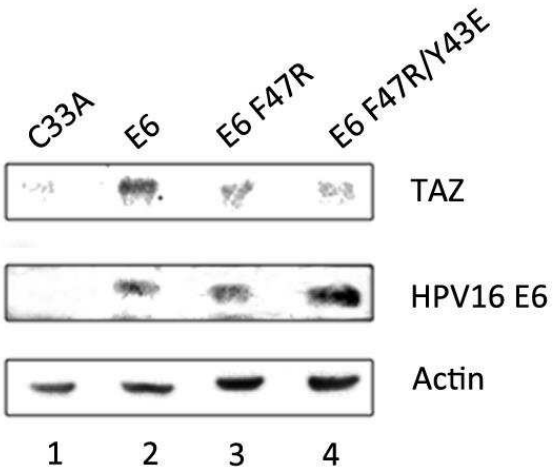

Figure 4.19. Effect of wild-type E6 or dimerization-defective E6 mutants on the endogenous levels of TAZ. C33A cells were transfected with empty vector (1) or with plasmids encoding splicing-defective E6 (2), splicing-defective E6 F47R (3), or splicing-defective E6 F47R/Y43E (4). Cells were grown in serum-reduced conditions (1% FBS), harvested at high density and cellular lysates were analyzed by western blotting using anti-TAZ, anti-HPV16 E6 (C-19), and anti-actin antibodies at 48 hours post-transfection.

Indeed, in repeated experiments we confirmed that TAZ upregulation possibly depends on the self-association of E6, since dimerization-defective E6 mutants were constantly incapable of stabilizing TAZ in transfected cells (Figure 4.20A). Nevertheless, we wished to further support the idea that the homodimerization of E6 might be a key interaction necessary for the upregulation of TAZ. To this aim, we wanted to study TAZ upregulation mediated by E6 in the absence of p53, in order to exclude the involvement of the interaction between E6 and p53, which occurs through the same protein surface on the viral oncoprotein. Thus, we transfected H1299 cells, a p53-null epithelial cancer cell line, with the same constructs and analyzed the endogenous levels of TAZ by western blotting when the cells reached confluence. Strikingly, we observed the upregulation of TAZ only upon overexpression of wild-type E6 also in this cell line (Figure 4.20B), in agreement with the previous result obtained in C33A cells.

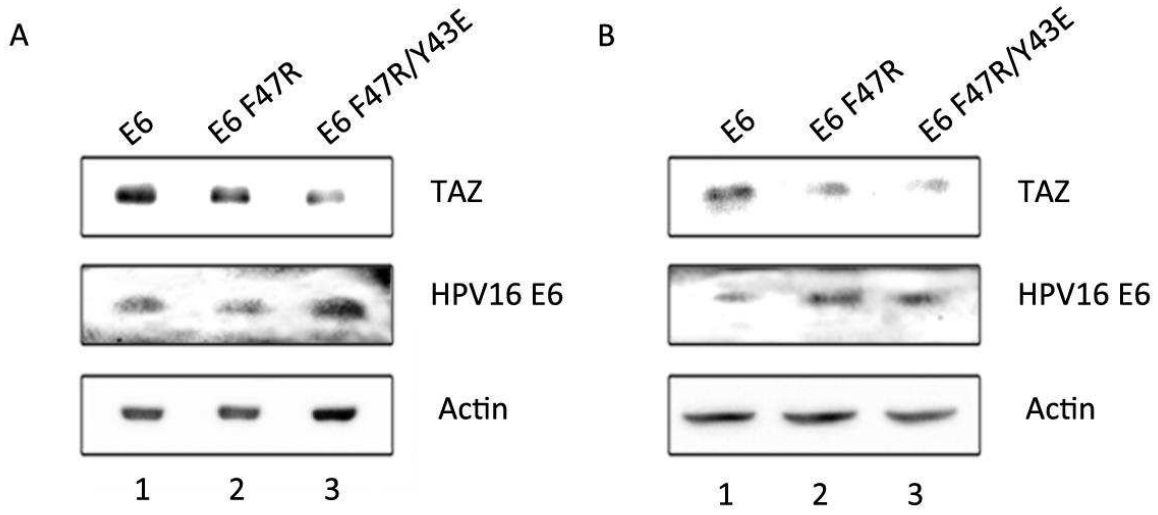

Figure 4.20. E6 homodimerization-dependent upregulation of TAZ. (A) C33A and **(B)** H1299 cells were transfected with plasmids encoding splicing-defective E6 (1), splicing-defective E6 F47R (2), or splicing-defective E6 F47R/Y43E (3). Cells were grown in serum-reduced conditions (1% FBS), harvested at high density and cellular lysates were analyzed by western blotting using anti-TAZ, anti-HPV16 E6 (C-19), and anti-actin antibodies at 48 and 24 hours post-transfection for C33A and H1299 cells, respectively.

4.2 Studies on the development of anti-E6 compounds targeting the α2-helix of HPV16 E6.

4.2.1 *In silico* screenings.

In parallel to the biological studies investigating the role of the dimeric form of E6 in the context of the E6-mediated mechanisms of cellular transformation, we performed, in collaboration with the group of prof. Gabriele Cruciani (University of Perugia, Italy), *in silico* drug screenings in order to search for small molecules able to target the α2-helix of HPV16 E6.

The first *in silico* screening was aimed at identifying compounds able to impair E6 self-association. The N-terminal domain of E6 from the NMR dimer structure (pdb: 2LJY) was used as a template [Zanier *et al.*, 2012]. The screening was conducted against a druggable pseudo-cavity that we identified around Phe47 of E6 and the Specs database was screened with FLAP (Fingerprints for Ligands And Proteins) software [Baroni *et al.*, 2007]. A prefiltering run was performed, fixing the interaction with Phe47 of the chain A of the dimer structure as a constraint. Prefiltering results were ranked by the GlobSum descriptor, and the 100 top-

ranked compounds were used to generate a GRID Molecular Interaction Fields (MIFs)-based database in FLAP. Thus, the screening was refined according to the calculated MIFs and the results were ranked by GlobProd descriptor in order to obtain a ranking of potentially active compounds (data not shown).

Subsequently, a second *in silico* screening was performed taking advantage of the crystal structure of the trimeric complex E6/E6AP/p53, and using the chain of E6 as the target structure. The strategy was the same as described before but the screening was performed also against two larger virtual databases, i.e., the ChemDiv and Vitas-M databases. Noteworthy, the druggable cavity identified with this screening partly but significantly overlapped the pseudo-cavity previously identified using the NMR dimeric structure of HPV16 E6 (Figure 4.21). Indeed, E6 self-association and the interaction of E6 with p53 involve the same key residues in the hydrophobic core of the α2-helix.

Fourteen compounds, among the 50 top-ranked which resulted positive hits in both screenings, were then selected for testing, based on chemical diversity and availability criteria.

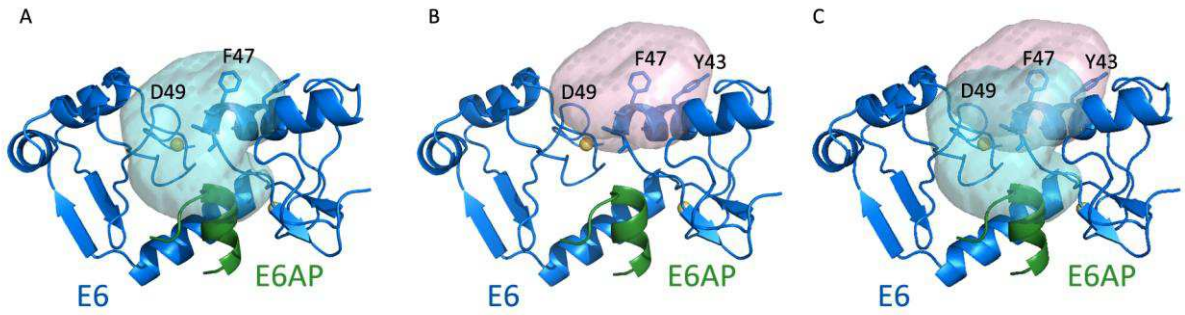

Figure 4.21. Druggable pockets at the E6/E6AP-p53 and E6 dimerization binding interfaces. **(A)** Druggable cavity at the E6/E6AP-p53 binding interface calculated on the E6/E6AP/p53 crystal structure (PDB accession code: 4XR8); **(B)** Druggable cavity at the E6 dimerization interface calculated on the NMR E6 dimeric structure (PDB accession code: 2LJY); **(C)** Overlap between the two detected cavities. For clarity, virtual cavities were superimposed on the model of full-length HPV16 E6 of the E6/E6AP/p53 crystal structure.

4.2.2 Ability of the compounds to impair HPV16 E6 self-association.

To test the ability of selected compounds to inhibit E6 self-association, we used the ELISA-based $E6_N$ homodimerization assay to perform a dose-response analysis of the 14 hit compounds. Dose-response analyses of the inhibition of E6 dimerization were performed by assaying four concentrations (10-50-100-200 µM) of each compound and IC_{50} values (compound concentration that reduces $E6_N$ dimerization by 50%) were estimated. Among the hits, two compounds – 6 and 12 – exhibited the strongest inhibitory activity (IC_{50} values of 40 ± 12 and 20 ± 5 µM, respectively). Two other compounds – 11 and 14 – caused a reproducible dose-dependent reduction, but with higher IC_{50} values. The remaining compounds did not exhibit any inhibitory activity at the tested concentrations (data not shown). Importantly, an unrelated small molecule, FLU-1, previously shown to inhibit the influenza A virus PA-PB1 interaction [Muratore *et al.*, 2012], did not interfere with $E6_N$ dimerization (Figure 4.22).

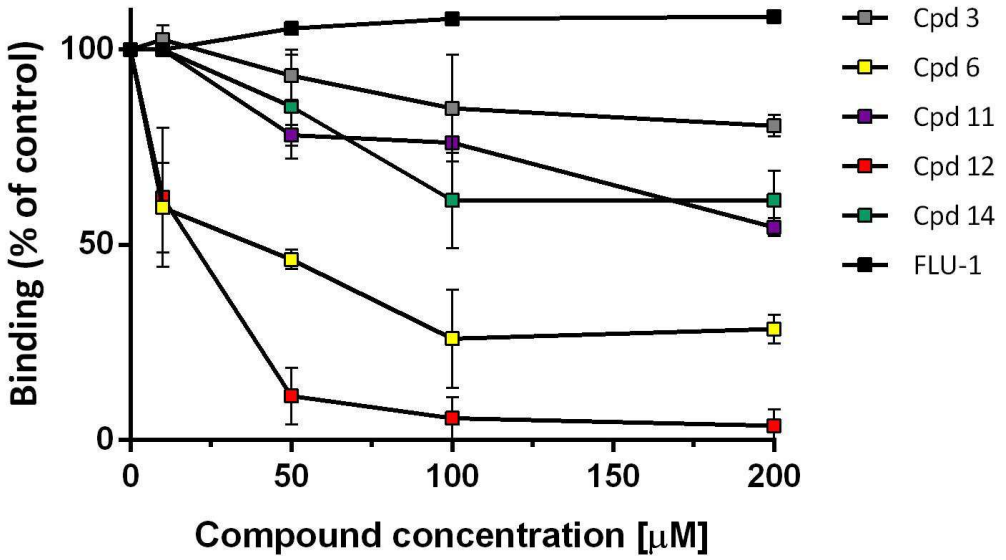

Figure 4.22. Inhibitory activity of test compounds in ELISA $E6_N$ homodimerization assays. Inhibition curves obtained for some of the hits selected in the *in silico* screening (compounds 3, 6, 11, 12, and 14), and of an unrelated protein-protein interaction inhibitor (FLU-1) as a control. Data shown represent the mean ± SD of at least two independent experiments.

4.2.3 Effects of the compounds on the viability of HPV-positive cells.

In parallel to the investigation of the *in vitro* activity of the selected small molecules, compounds cytotoxicity was measured by the MTT assay in several cell lines. Compounds were tested both on HPV-positive (Hela, SiHa, CaSki) and on HPV-negative (C33A) cervical cancer cells, and non-tumoral human cells (e.g. HFF) as controls, in order to determine the specific and non-specific cytotoxicity of each compound, respectively. Preliminarily, cell growth curves were obtained in order to determine the proper number of cells to be plated for compound testing (data not shown) and then CC_{50} values (compound concentration that causes a decrease of cell viability by 50%) were estimated. All the compounds that were inactive *in vitro* did not exhibit significant cytotoxic effect on HPV-positive cells, and those that exhibited mild cytotoxicity on Hela, SiHa and CaSki cells (such as compound 11) were also mildly cytotoxic for C33A and HFF cells (data not shown). However, compound 6 and 12 exhibited toxic effects preferentially on HPV-positive cells, with overall minor cytotoxicities on the HPV-negative cell lines tested (Figure 4.23), suggesting their ability to induce cell death in HPV-positive cells as a result of specific anti-E6 activity. In parallel, compound 3 was inactive as expected.

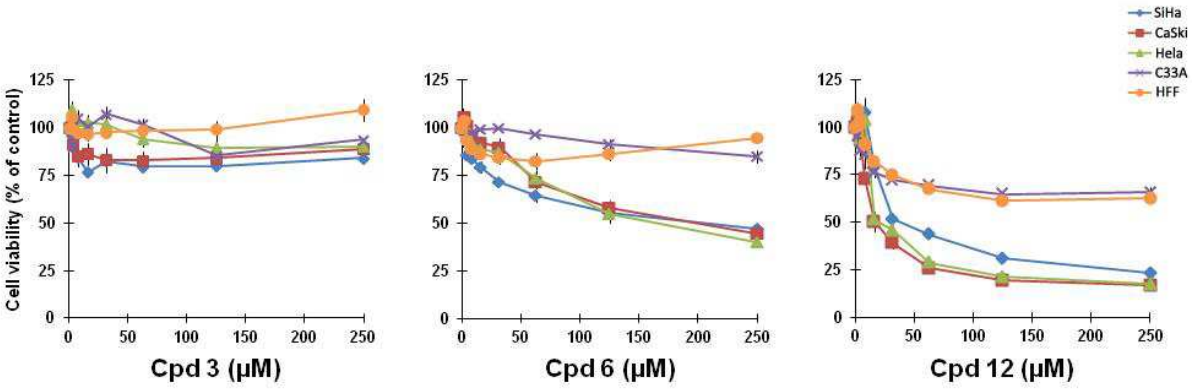

Figure 4.23. Cytotoxic effect of test compounds on the viability of HPV-positive cells. Cytotoxic effects obtained for some of the compounds selected in the *in silico* screening (compounds 3, 6, and 12) on the viability of Hela (HPV18-positive), SiHa (HPV16-positive), CaSki (HPV16-positive), C33A (HPV-negative) cervical carcinoma cells and on HFF (human foreskin fibroblast) cell line. Cytotoxicities were assessed by the MTT assay after 48 hours of treatment and compared to that of non-treated cells.

4.2.4 Compound 12 impairs the HPV16 E6-mediated degradation of p53 and enhances the downregulation of HPV16 E6.

The results presented so far suggest that two compounds – 6 and 12 – are capable of disrupting the dimerization HPV16 E6 and might potentially act against the activity of the endogenous E6 proteins expressed in HPV-positive Hela, SiHa, and CaSki cells. Thus, we sought to investigate the ability of these compounds to impair the binding between E6 and p53. However, we were not able to test these compounds in an *in vitro* E6-p53 binding assay mainly due to the difficulty in purifying wild-type full-length HPV16 E6, since the full-length protein is required to mediate the interaction with p53. Thus, we studied the ability of these two compounds to inhibit the E6-dependent degradation of p53 in transfected cells. To this aim, we transfected C33A cells with a plasmid encoding full-length untagged HPV16 E6 and then we treated the transfected cells with compounds 6, 12 and 3 (the latter used as a negative control) each at two different concentrations below their respective CC_{50} values and analyzed the endogenous levels of p53, as well as the expression of E6, by western blotting. Noteworthy, compound 12, unlike compound 6, was able to rescue p53 in transfected cells, suggesting its ability to impair the interaction between E6 and p53, which results in the inhibition of p53 degradation, while compound 3 was inactive as expected (Figure 4.24A). Furthermore, in repeated experiments we observed the downregulation of E6 protein levels following treatment with compound 12, which suggested the possible ability of this compound to induce the degradation of E6, since the levels of the internal control, i.e. actin, were not affected (Figure 4.24B).

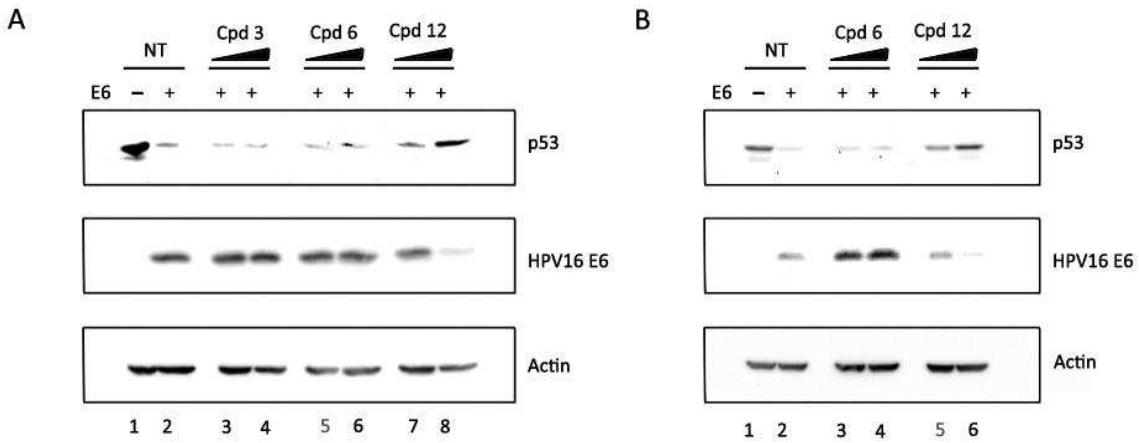

Figure 4.24. Activity of compounds 6 and 12 on the levels of p53 and E6. (A and **B)** C33A cells were transfected with empty vector (1) or with plasmid encoding splicing-defective HPV16 E6 (2 to 8). Cells were treated with DMSO (NT) or with compounds 3 (not shown in **B**) and 6 at 50 µM and 100 µM and with compound 12 at 20 µM and 50 µM. Cells were harvested and cellular lysates were analyzed by western blotting using anti-p53, anti-HPV16 E6 (N-17), and anti-actin antibodies at 48 hours post-transfection.

Thus, to test whether this compound could enhance the proteasome-dependent turnover of E6, we treated C33A cells, transfected with wild-type E6, with compound 12 in the absence or presence of proteasome inhibitor MG-132. Strikingly, we observed that E6 protein levels were rescued in cells treated with MG-132, thus suggesting the ability of compound 12 to enhance E6 degradation through the cellular proteasome machinery (Figure 4.25). Finally, to test whether compound 12 may have induced the downregulation of E6 as a result of its direct binding to the viral oncoprotein, rather than through an indirect mechanism, we transfected C33A cells with full-length wild-type E6 or mutant E6 F47R and cells were treated with compound 12. Notably, we observed that E6 downregulation was higher in cells transfected with wild-type E6 rather than in cells transfected with mutant E6 F47R, suggesting an impaired binding affinity between E6 F47R and compound 12 (Figure 4.26).

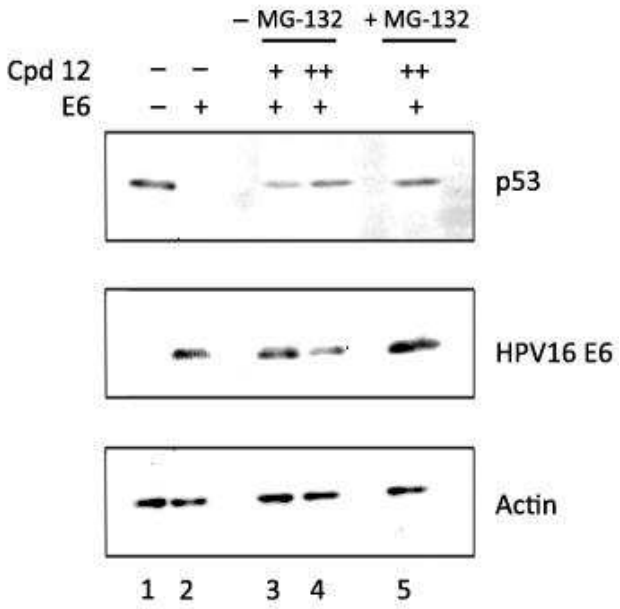

Figure 4.25. Proteasome-dependent downregulation of E6 protein levels induced by compound 12. C33A cells were transfected with empty vector (1) or with plasmid encoding splicing-defective HPV16 E6 (2 to 5). Cells were treated with DMSO or with compound 12 at 20 µM (+) and 50 µM (++) in the absence or the presence of proteasome inhibitor MG-132 (40 µM). Cells were harvested and cellular lysates were analyzed by western blotting using anti-p53, anti-HPV16 E6 (N-17), and anti-actin antibodies at 48 hours post-transfection.

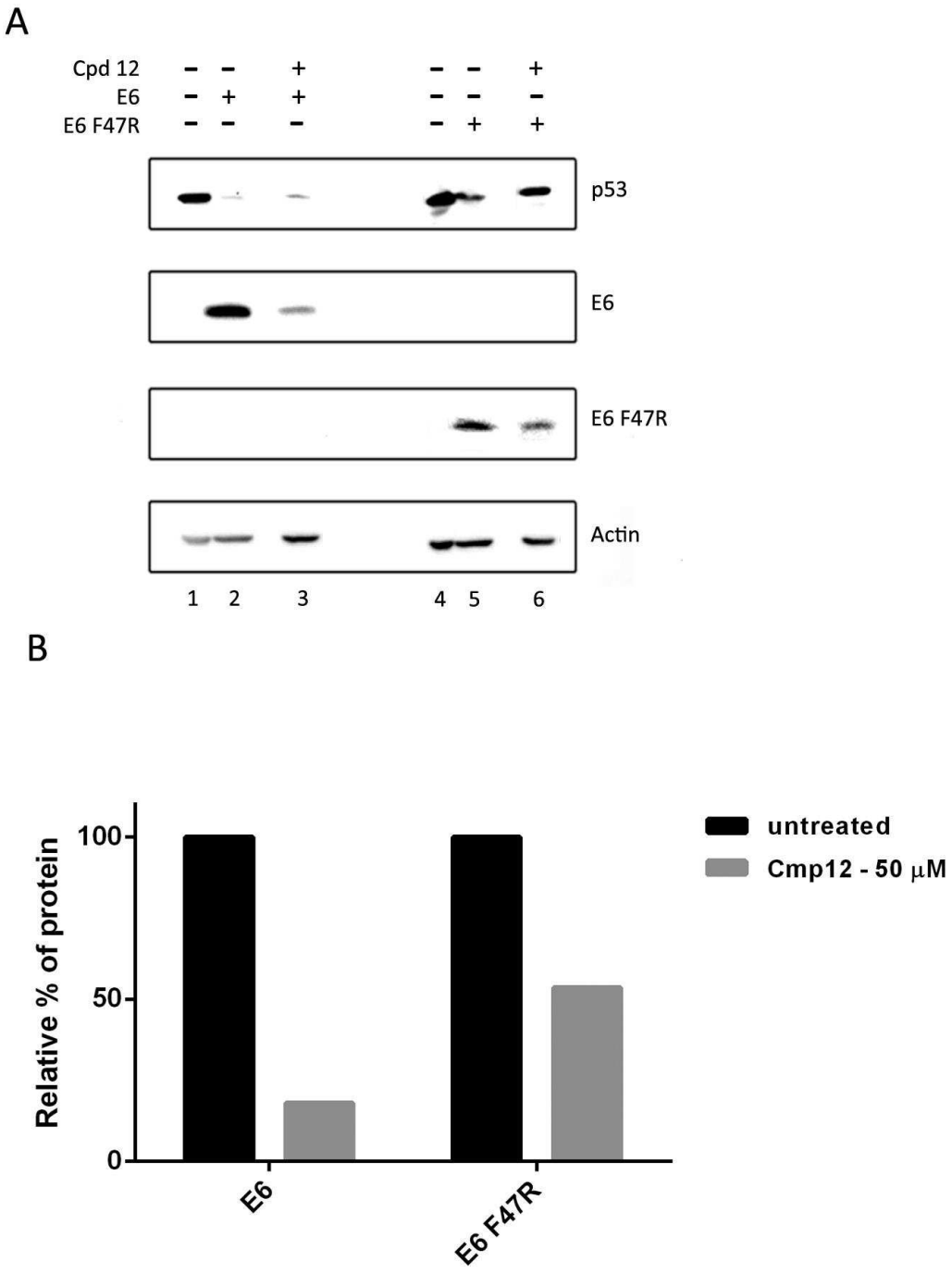

Figure 4.26. Differential affinity of compound 12 towards wild-type E6 and mutant E6 F47R. (A) C33A cells were transfected with empty vector (1 and 4) or with plasmid encoding splicing-defective HPV16 E6 (2 and 3) or splicing-defective HPV16 E6 F47R (5 and 6). Cells were treated with DMSO or with compound 12 at 50 μM. Cells were harvested and cellular lysates were analyzed by western blotting using anti-p53, anti-HPV16 E6 (N-17 for wild-type E6; C-19 for E6 F47R), and anti-actin antibodies at 48 hours post-transfection. **(B)** Quantification of E6 protein bands detected in **(A)** by western blot analysis. Bands were quantified using ImageJ Software (NIH, USA).

4.2.5 Effects of active compounds on the proliferation of HPV-positive cells.

Finally, we wanted to study the effects of these two compounds also against the proliferative capacity of HPV-positive cells. Thus, we performed both 2D clonogenic assays on plastic and 3D clonogenic assays on soft agar matrix, in order to determine the proliferation of cells after treatment with compounds 3, 6 and 12. For 2D colony formation assays, Hela, SiHa, CaSki and C33A cells, the last included as a control to verify whether the effects of the compounds are specific for E6-expressing cells, were plated and treated with the compounds for 2 weeks. Notably, compounds 6 and 12, but not compound 3, drastically reduced the number and size of colonies of Hela, SiHa and CaSki cells, while having no or minor effects on the proliferation of C33A cells at the tested concentrations of 100 and 50 µM, respectively (Figure 4.27).

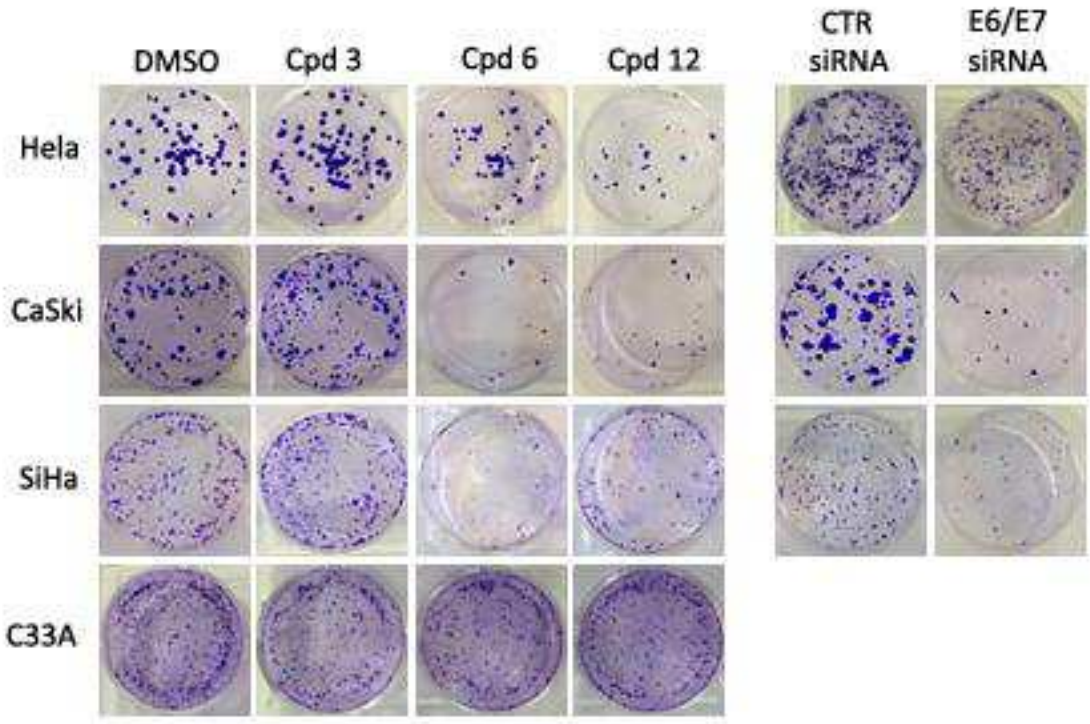

Figure 4.27. Anti-clonogenic properties of test compounds. 2D colony formation assay was used to evaluate the long-term (14 days) effects of compounds 3, 6, and 12 on Hea, CaSki, SiHa HPV-positive cervical carcinoma cell lines, compared to non-treated cells (DMSO). HPV-negative cervical carcinoma C33A cells were used as a negative control to test the specificity of compounds in targeting E6. Silencing of E6/E7 (E6/E7 siRNA) in HPV-positive cervical carcinoma cell lines, compared with scrambled siRNA (CTR siRNA), was used as a positive control (right panel).

Additionally, the inhibition of proliferation capacity of compound-6 and -12-treated cells was close to that of the positive control wherein the expression of E6 and E7 was downregulated through the use of anti-E6/E7 siRNAs, which were shown to successfully induce senescence and apoptosis due to the restoration of p53 levels [Koivusalo *et al.*, 2005]. Finally, we studied the ability of these compounds to impair the anchorage-independent growth of HPV-positive cells in soft agar colony formation assays. Noteworthy, similar results were obtained, wherein the anchorage-independent proliferation of Hela, SiHa and CaSki cells was significantly reduced upon treatment with compounds 6 and 12 for up to 8 weeks, while compound 3 exhibited almost no effect (Figure 4.28). Unfortunately, we could not include C33A cells in these assays for their inability to grow on soft agar matrices [Villanueva-Toledo *et al.*, 2014].

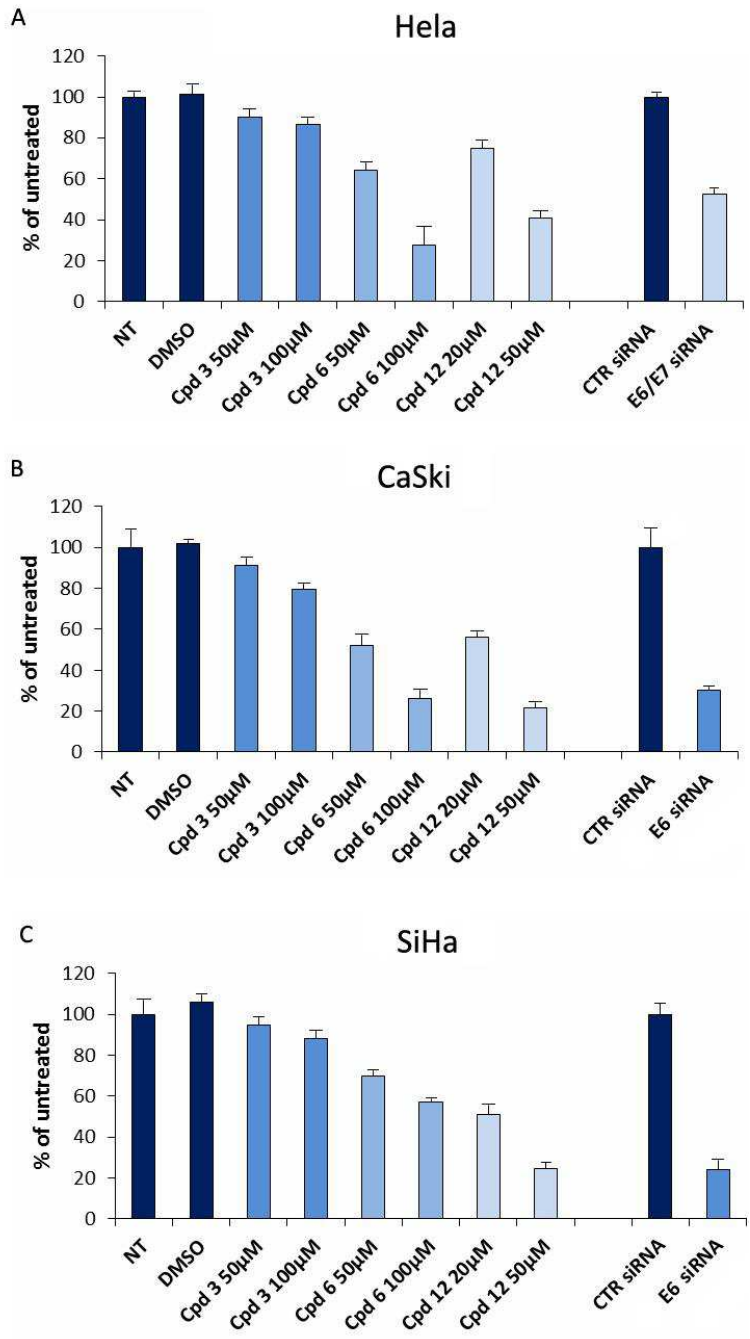

Figure 4.28. Anti-clonogenic properties of test compounds in anchorage-independent growth assays. Soft agar colony formation assay was used to evaluated the long-term (up to 2 months) effects of compounds 3, 6, and 12 on **(A)** Hela, **(B)** CaSki and **(C)** SiHa HPV-positive cell lines. Cells treated with DMSO were used as a negative control. Silencing of E6/E7 (E6/E7 siRNA), compared with scrambled siRNA (CTR siRNA), was used as a positive control (right bars).

5. Discussion and Conclusions

By the use of a cell-based technique for the detection of protein-protein interactions, i.e., Bioluminescence Resonance Energy Transfer (BRET), we studied and characterized the self-association of full-length HPV16 E6 in living cells. BRET turned out to be a potent qualitative and quantitative technique to detect protein-protein interactions in living cells. Taking advantage of the high expression levels that can be achieved by the use of HEK 293T cell line, we successfully detected the homodimerization of the N-terminal domain of E6 and a full-length E6 isoform, named E6 4C/4S, where four non-conserved cysteines on protein surface are mutated into serines, preventing E6 protein aggregation *in vitro*, albeit not impairing E6 degradative functions [Zanier *et al.*, 2010; Zanier *et al.*, 2012]. The use of a non-aggregating isoform was required, as the overexpression of YFP-tagged wild-type E6 induced the formation of nuclear foci, recently characterized as nuclear aggresomes, which are distinctive perinuclear compartments induced by the accumulation of misfolded and aggregated proteins [Stutz *et al.*, 2015]. An intrinsic limit of the BRET technique is the overexpression of the acceptor partner (i.e. the YFP-tagged protein) in order to saturate the donor partner (i.e. the RLuc-tagged protein), especially when dealing with putative weak protein-protein interactions, as higher levels of the recombinant acceptor protein is required. Indeed, E6 homodimerization was previously shown to be a weak interaction, at least *in vitro* [Zanier *et al.*, 2012]. Thus, we speculate that the inability to detect wild-type E6 homodimerization by this assay is justified by the E6-induced aggresome formation which ideally caused a loss of active, properly folded E6 molecules, hence decreasing the detectable signal of interaction. Nevertheless, the use of the non-aggregating isoform E6 4C/4S successfully prevented recombinant protein aggregation in transfected cells and resulted in a detectable interaction. Notably, the self-association signal detected for E6 4C/4S was close to the signal detected using $E6_N$ recombinant proteins at similar Y/R values, suggesting a homodimerization of E6 driven specifically by the N-terminal domain of the protein, as previously reported [Zanier *et al.*, 2012]. Most importantly, the introduction of one or two substitutions in the dimeric interface, that were previously reported to block the homodimerization *in vitro* (F47R and F47R/Y43E), effectively reduced the interaction also in transfected cells, thus confirming the specificity of the observed interaction signal. Furthermore, the quantitative analysis of $E6_N$, $E6_N$ F47R, and $E6_N$ F47R/Y43E self-associations, performed by a BRET saturation assay in HEK 293T cells, revealed that the substitution of residue 47 is sufficient to inhibit the interaction almost completely, as the binding curves of $E6_N$ F47R and $E6_N$ F47R/Y43E mostly overlap and are very close to the non-specific background.

The detection of $E6_N$ self-association in an *in vitro* ELISA-based assay further supported the occurrence of the homodimerization as a result of a direct self-interaction, ruling out the possibility of a bridging effect, where other cellular binding partners may have induced the close contact of two E6 molecules in our BRET experiments. In addition, the ELISA-based *in vitro* assay confirmed the occurring self-association of the N-terminal domains of E6 with high specificity and overall good sensitivity. Taken together, these results demonstrate the effective existence of a dimeric form of E6 in a cellular context, and although we were unable to calculate the dissociation constant (K_d), they point to a weak interaction, as previously reported [Zanier *et al.*, 2012]. This can be inferred, on the one hand, by the high expression levels of YFP-$E6_N$ required to saturate the RLuc-$E6_N$ protein in the BRET saturation assay (i.e. the very high Y/R values at which the $E6_N$ binding curve reaches the plateau) and, on the other hand, by the high amount of purified protein required to saturate the binding partner in the ELISA assay.

The importance of the hydrophobic residues of α2-helix with regard to E6 transforming activities was correlated to the ability of the viral oncoprotein to successfully degrade p53, and indeed, we confirmed the importance of this hydrophobic surface for the productive degradation of p53 in transfected cells. However, contrasting results were published about the ability of mutant E6 F47R to bind p53, and thus, whether the dimerization was really an event necessary for the degradation of p53 remained an open question. To this aim, we studied the interaction between E6 and p53 in living cells and, remarkably, mutant E6 F47R and E6 F47R/Y43E had binding capacities significantly reduced compared to wild-type E6 and thus, our data appear to be in keeping with the latest structural model of the E6/E6AP/p53 trimeric complex and explain the inability to degrade p53 as a result of an impaired binding capacity [Martinez-Zapien *et al.*, 2016].

In line with these results, we then tested whether E6 self-association and the binding of E6 to p53 could compete with each other as a result of two distinct interactions occurring on the same surface on the viral oncoprotein. Notably, in repeated experiments, we never observed a reduction of E6 self-association in the presence of exogenous p53, whereas FLAG-$E6_N$ could successfully impair the interaction between RLuc-E6 4C/4S and YFP-E6 4C/4S in the same experimental conditions. Thus, taken together, our results point to the exclusion of E6 self-association from being a protein-protein interaction required to form the protein complex which induces the degradation of p53, and suggest the involvement of E6 self-association in other molecular processes. In addition, the occurrence of these two interactions likely take place in different cellular compartments, as suggested by the inability of p53 to compete with E6 homodimerization. Indeed, p53 is a well known nuclear protein whose intracellular localization is due to the presence of different sequences important for its nuclear import [Liang and Clarke, 1999]. Furthermore, the N-terminal domain of E6, which was able to compete with E6 self-association in our BRET competition assay, localizes both in the nucleus and the cytoplasm of transfected cells. Thus, we speculate that the cytoplasmic fraction of FLAG-$E6_N$ was likely responsible for the impairment of E6 homodimerization. Although further experiments are required to study the intracellular localization of E6 dimers, oligomeric forms of E6 were already reported to localize in the

cytosol of HPV-positive cells and to target cytoplasmic cellular proteins [Garcia-Alai *et al.*, 2007(b)]. Thus, we propose a model in which nuclear E6 binds to p53 as a monomer, while cytoplasmic E6 can dimerize and interact with other cellular targets.

In order to investigate the possible role of E6 homodimerization, and in line with our aforementioned observations, we monitored the endogenous levels of another known cellular target of E6, the cytoplasmic PDZ-containing protein Scribble, following the expression of E6 in HPV-negative cell lines. Unfortunately, we failed to find a correlation between the homodimerization of the viral oncoprotein and Scribble degradation following western blot analysis of cells transfected with either wild-type E6 or dimerization defective mutants. However, we did not observe a loss of Scribble even in cells transfected with wild-type E6, a result that contrasts with previous studies reporting the E6-induced E6AP-dependent degradation of Scribble [Nakagawa and Huibregtse, 2000]. Nevertheless, some studies previously reported the E6-mediated delocalization of Scribble rather than its degradation [Choi *et al.*, 2014], and thus our results appear to be in line with these more recent observations.

The recent discovery of the crosstalk between the Hippo transducer YAP and E6 in HPV-positive cancer cells prompted us to test whether E6 dimerization could be related to YAP upregulation [He *et al.*, 2015]. Strikingly, in an attempt to monitor the endogenous levels of YAP in cells transfected with wild-type E6 or dimerization-defective E6 mutants, we observed that E6 mediates also the upregulation of TAZ, the other main transducer of the Hippo signaling cascade. Most importantly, we observed the inability of dimerization-defective E6 mutants to upregulate TAZ in the same experimental conditions, and the same result could be observed also in H1299 cells, a p53-null cell line. This, in turns, suggests that the hydrophobic core of the α2-helix of HPV16 E6 is crucial for TAZ upregulation and the mechanism does not depend on the interaction between E6 and p53, but involves another protein-protein interaction occurring on the same protein surface. We propose E6 self-association as the candidate interaction required for the upregulation of TAZ. Furthermore, Scribble is known to be a cytoplasmic scaffold protein which serves as a TAZ inhibitor and its delocalization has been already reported to induce TAZ accumulation in the nucleus [Cordenonsi *et al.*, 2011]. Thus, in line with our previous considerations, it may be worth investigating whether the cytoplasmic dimeric form of E6 induces Scribble delocalization which in turns results in the upregulation of TAZ. Indeed, further research will be conducted with the goal to investigate the precise molecular mechanisms behind this process.

The identification of a druggable pseudo-cavity around Phe47 allowed us to select several potential inhibitory small molecules by an *in silico* screening aimed at serching E6 dimerization inhibitors. Not surprisingly, the second *in silico* screening, performed against a pseudo-cavity at the E6-p53 binding sub-interface II, clearly showed the significant overlap between the two cavities. This observation resulted in the possibility to develop dual inhibitors able to disrupt simultaneously both E6 self-association and E6-p53 interaction.

Initially, we tested the inhibitory activity of the 14 selected compounds that resulted positive hits in both screenings in the ELISA $E6_N$ homodimerization assay, and we could identify two compounds, 6 and 12, that successfully inhibited E6 homodimerization with an IC_{50} of ~40 µM and ~20 µM, respectively. Furthermore, both compounds showed to be specifically cytotoxic for HPV-positive cell lines, although compound 6 showed a CC_{50} four times higher than its IC_{50} observed *in vitro*.

Starting from these initial observations, we tested the ability of compounds 6 and 12 to impair the E6-mediated degradation of p53 in cells transfected with wild-type full-length HPV16 E6. Noteworthy, compound 12, but not compound 6, was able to rescue p53 levels in transfected cells, suggesting the inhibition of E6-p53 interaction induced by compound 12. Additionally, in repeated experiments we also observed the ability of compound 12 to induce the downregulation of E6 protein levels in transfected cells, in a dose-dependent manner. Indeed, E6 is known to be degraded by the proteasome machinery within infected cells [Stewart *et al.*, 2004], and thus we investigated whether compound 12 could induce E6 degradation in a proteasome-dependent manner. Strikingly, cells treated with compound 12 in the presence of the proteasome inhibitor MG-132 showed higher E6 levels compared to those of transfected cells treated only with compound 12.
Finally, to test whether compound 12 is enhancing E6 clearance as a result of a possible direct interaction with the viral oncoprotein, cells were transfected either with wild-type E6 or dimerization-defective E6 F47R. Noteworthy, compound 12 showed a reduced capacity to downregulate the levels of E6 F47R compared to wild-type E6 in the same experimental conditions. Thus, these preliminary data suggest that compound 12 is counteracting E6 by directly binding to the viral oncoprotein, preventing the interaction and degradation of p53 and enhancing E6 degradation through the cellular proteasome machinery.

Furthermore, these results agree with the data from the MTT assays in which compound 12 was shown to be preferentially cytotoxic for HPV-positive cells. Noteworthy, also compound 6 resulted to be toxic for HPV-positive cells in the MTT assays, although this compound could not rescue p53 levels in E6-transfected cells. Thus, we wished to test the anti-proliferative activity of both compounds, 6 and 12, in 2D and 3D clonogenic assays. Surprisingly, both compound 12 and compound 6 showed anti-proliferative activity in HPV-positive cells, while producing no or minimal effect against HPV-negative cell lines. This observation further supports the idea that E6 homodimerization has a role in the oncogenic functions of E6 and heralds the prospect of developing dual inhibitors that, by interfering with both the PPIs driven by the α2-helix of the N-terminal domain of E6, could block multiple activities of the viral oncoprotein important for its transforming activities. This, on the one hand, can be explained by the anti-proliferative activity of compound 6 that we identified as an inhibitor of E6 dimerization while appearing unable to block the E6-mediated p53 degradation, and, on the other hand, by the ability of compound 12 to impair both E6 self-association and the E6-mediated degradation of p53, thus possibly representing a candidate dual inhibitor. In the future, further research will be carried out to study the anti-proliferative activity of compound 6 with regard to the oncogenic function of E6 homodimerization.

References

Ajiro, M. and Z. M. Zheng. "E6^E7, a Novel Splice Isoform Protein of Human Papillomavirus 16, Stabilizes Viral E6 and E7 Oncoproteins Via Hsp90 and Grp78." MBio 6, no. 1 (2015): e02068-14.

Amin, A. A., S. Titolo, A. Pelletier, D. Fink, M. G. Cordingley and J. Archambault. "Identification of Domains of the Hpv11 E1 Protein Required for DNA Replication in Vitro." Virology 272, no. 1 (2000): 137-50.

Ansari, T., N. Brimer and S. B. Vande Pol. "Peptide Interactions Stabilize and Restructure Human Papillomavirus Type 16 E6 to Interact with P53." J Virol 86, no. 20 (2012): 11386-91.

Auster, A. S. and L. Joshua-Tor. "The DNA-Binding Domain of Human Papillomavirus Type 18 E1. Crystal Structure, Dimerization, and DNA Binding." J Biol Chem 279, no. 5 (2004): 3733-42.

Azzolin, L., T. Panciera, S. Soligo, E. Enzo, S. Bicciato, S. Dupont, S. Bresolin, C. Frasson, G. Basso, V. Guzzardo, A. Fassina, M. Cordenonsi and S. Piccolo. "Yap/Taz Incorporation in the Beta-Catenin Destruction Complex Orchestrates the Wnt Response." Cell 158, no. 1 (2014): 157-70.

Baleja, J. D., J. J. Cherry, Z. Liu, H. Gao, M. C. Nicklaus, J. H. Voigt, J. J. Chen and E. J. Androphy. "Identification of Inhibitors to Papillomavirus Type 16 E6 Protein Based on Three-Dimensional Structures of Interacting Proteins." Antiviral Res 72, no. 1 (2006): 49-59.

Banks, L., D. Pim and M. Thomas. "Human Tumour Viruses and the Deregulation of Cell Polarity in Cancer." Nat Rev Cancer 12, no. 12 (2012): 877-86.

Barksdale, S. K. and C. C. Baker. "Differentiation-Specific Expression from the Bovine Papillomavirus Type 1 P2443 and Late Promoters." J Virol 67, no. 9 (1993): 5605-16.

Baroni, M., G. Cruciani, S. Sciabola, F. Perruccio and J. S. Mason. "A Common Reference Framework for Analyzing/Comparing Proteins and Ligands. Fingerprints for Ligands and Proteins (Flap): Theory and Application." J Chem Inf Model 47, no. 2 (2007): 279-94.

Baxter, M. K., M. G. McPhillips, K. Ozato and A. A. McBride. "The Mitotic Chromosome Binding Activity of the Papillomavirus E2 Protein Correlates with Interaction with the Cellular Chromosomal Protein, Brd4." J Virol 79, no. 8 (2005): 4806-18.

Bodaghi, S., R. Jia and Z. M. Zheng. "Human Papillomavirus Type 16 E2 and E6 Are Rna-Binding Proteins and Inhibit in Vitro Splicing of Pre-Mrnas with Suboptimal Splice Sites." Virology 386, no. 1 (2009): 32-43.

Bolatti, E. M., D. Chouhy, P. E. Casal, G. R. Perez, E. J. Stella, A. Sanchez, M. Gorosito, R. F. Bussy and A. A. Giri. "Characterization of Novel Human Papillomavirus Types 157, 158 and 205 from Healthy Skin and Recombination Analysis in Genus Gamma-Papillomavirus." Infect Genet Evol 42, (2016): 20-9.

Borbely, A. A., M. Murvai, J. Konya, Z. Beck, L. Gergely, F. Li and G. Veress. "Effects of Human Papillomavirus Type 16 Oncoproteins on Survivin Gene Expression." J Gen Virol 87, no. Pt 2 (2006): 287-94.

Bossis, I., R. B. Roden, R. Gambhira, R. Yang, M. Tagaya, P. M. Howley and P. I. Meneses. "Interaction of Tsnare Syntaxin 18 with the Papillomavirus Minor Capsid Protein Mediates Infection." J Virol 79, no. 11 (2005): 6723-31.

Bouvard, V., G. Matlashewski, Z. M. Gu, A. Storey and L. Banks. "The Human Papillomavirus Type 16 E5 Gene Cooperates with the E7 Gene to Stimulate Proliferation of Primary Cells and Increases Viral Gene Expression." Virology 203, no. 1 (1994): 73-80.

Bryan, J. T., B. Buckland, J. Hammond and K. U. Jansen. "Prevention of Cervical Cancer: Journey to Develop the First Human Papillomavirus Virus-Like Particle Vaccine and the Next Generation Vaccine." Curr Opin Chem Biol 32, (2016): 34-47.

Burd, E. M. "Human Papillomavirus and Cervical Cancer." Clin Microbiol Rev 16, no. 1 (2003): 1-17.

Burk, R. D., A. Harari and Z. Chen. "Human Papillomavirus Genome Variants." Virology 445, no. 1-2 (2013): 232-43.

Busch, C. J., B. Becker, M. Kriegs, F. Gatzemeier, K. Kruger, N. Mockelmann, G. Fritz, C. Petersen, R. Knecht, K. Rothkamm and T. Rieckmann. "Similar Cisplatin Sensitivity of Hpv-Positive and -Negative Hnscc Cell Lines." Oncotarget 7, no. 24 (2016): 35832-35842.

Camus, S., S. Menendez, C. F. Cheok, L. F. Stevenson, S. Lain and D. P. Lane. "Ubiquitin-Independent Degradation of P53 Mediated by High-Risk Human Papillomavirus Protein E6." Oncogene 26, no. 28 (2007): 4059-70.

Cavatorta, A. L., G. Fumero, D. Chouhy, R. Aguirre, A. L. Nocito, A. A. Giri, L. Banks and D. Gardiol. "Differential Expression of the Human Homologue of Drosophila Discs Large Oncosuppressor in Histologic Samples from Human Papillomavirus-Associated Lesions as a Marker for Progression to Malignancy." Int J Cancer 111, no. 3 (2004): 373-80.

Chang, J. L., Y. P. Tsao, D. W. Liu, S. J. Huang, W. H. Lee and S. L. Chen. "The Expression of Hpv-16 E5 Protein in Squamous Neoplastic Changes in the Uterine Cervix." J Biomed Sci 8, no. 2 (2001): 206-13.

Charbonnier, S., Y. Nomine, J. Ramirez, K. Luck, A. Chapelle, R. H. Stote, G. Trave, B. Kieffer and R. A. Atkinson. "The Structural and Dynamic Response of Magi-1 Pdz1 with Noncanonical Domain Boundaries to the Binding of Human Papillomavirus E6." J Mol Biol 406, no. 5 (2011): 745-63.

Chen, J. "Signaling Pathways in Hpv-Associated Cancers and Therapeutic Implications." Rev Med Virol 25 Suppl 1, (2015): 24-53.

Cherry, J. J., A. Rietz, A. Malinkevich, Y. Liu, M. Xie, M. Bartolowits, V. J. Davisson, J. D. Baleja and E. J. Androphy. "Structure Based Identification and Characterization of Flavonoids That Disrupt Human Papillomavirus-16 E6 Function." PLoS One 8, no. 12 (2013): e84506.

Choi, M., S. Lee, T. Choi and C. Lee. "Roles of the Pdz Domain-Binding Motif of the Human Papillomavirus Type 16 E6 on the Immortalization and Differentiation of Primary Human Foreskin Keratinocytes." Virus Genes 48, no. 2 (2014): 224-32.

Chong, T., D. Apt, B. Gloss, M. Isa and H. U. Bernard. "The Enhancer of Human Papillomavirus Type 16: Binding Sites for the Ubiquitous Transcription Factors Oct-1, Nfa, Tef-2, Nf1, and Ap-1 Participate in Epithelial Cell-Specific Transcription." J Virol 65, no. 11 (1991): 5933-43.

Conrad, M., V. J. Bubb and R. Schlegel. "The Human Papillomavirus Type 6 and 16 E5 Proteins Are Membrane-Associated Proteins Which Associate with the 16-Kilodalton Pore-Forming Protein." J Virol 67, no. 10 (1993): 6170-8.

Contreras-Paredes, A., E. De la Cruz-Hernandez, I. Martinez-Ramirez, A. Duenas-Gonzalez and M. Lizano. "E6 Variants of Human Papillomavirus 18 Differentially Modulate the Protein Kinase B/Phosphatidylinositol 3-Kinase (Akt/Pi3k) Signaling Pathway." Virology 383, no. 1 (2009): 78-85.

Cordenonsi, M., F. Zanconato, L. Azzolin, M. Forcato, A. Rosato, C. Frasson, M. Inui, M. Montagner, A. R. Parenti, A. Poletti, M. G. Daidone, S. Dupont, G. Basso, S. Bicciato and S. Piccolo. "The Hippo Transducer Taz Confers Cancer Stem Cell-Related Traits on Breast Cancer Cells." Cell 147, no. 4 (2011): 759-72.

Cornelissen, M. T., H. L. Smits, M. A. Briet, J. G. van den Tweel, A. P. Struyk, J. van der Noordaa and J. ter Schegget. "Uniformity of the Splicing Pattern of the E6/E7 Transcripts in Human Papillomavirus Type 16-Transformed Human Fibroblasts, Human Cervical Premalignant Lesions and Carcinomas." J Gen Virol 71 (Pt 5), (1990): 1243-6.

D'Abramo, C. M. and J. Archambault. "Small Molecule Inhibitors of Human Papillomavirus Protein - Protein Interactions." Open Virol J 5, (2011): 80-95.

Daniel, B., A. Rangarajan, G. Mukherjee, E. Vallikad and S. Krishna. "The Link between Integration and Expression of Human Papillomavirus Type 16 Genomes and Cellular Changes in the Evolution of Cervical Intraepithelial Neoplastic Lesions." J Gen Virol 78 (Pt 5), (1997): 1095-101.

Davy, C., P. McIntosh, D. J. Jackson, R. Sorathia, M. Miell, Q. Wang, J. Khan, Y. Soneji and J. Doorbar. "A Novel Interaction between the Human Papillomavirus Type 16 E2 and E1--E4 Proteins Leads to Stabilization of E2." Virology 394, no. 2 (2009): 266-75.

Davy, C. E., D. J. Jackson, K. Raj, W. L. Peh, S. A. Southern, P. Das, R. Sorathia, P. Laskey, K. Middleton, T. Nakahara, Q. Wang, P. J. Masterson, P. F. Lambert, S. Cuthill, J. B. Millar and J. Doorbar. "Human Papillomavirus Type 16 E1 E4-Induced G2 Arrest Is Associated with Cytoplasmic Retention of Active Cdk1/Cyclin B1 Complexes." J Virol 79, no. 7 (2005): 3998-4011.

De Villiers, E. M., C. Fauquet, T. R. Broker, H. U. Bernard and H. zur Hausen. "Classification of Papillomaviruses." Virology 324, no. 1 (2004): 17-27.

Desaintes, C. and C. Demeret. "Control of Papillomavirus DNA Replication and Transcription." Semin Cancer Biol 7, no. 6 (1996): 339-47.

Disbrow, G. L., I. Sunitha, C. C. Baker, J. Hanover and R. Schlegel. "Codon Optimization of the Hpv-16 E5 Gene Enhances Protein Expression." Virology 311, no. 1 (2003): 105-14.

Doorbar, J. "The Papillomavirus Life Cycle." J Clin Virol 32 Suppl 1, (2005): S7-15.

Doorbar, J., N. Egawa, H. Griffin, C. Kranjec and I. Murakami. "Human Papillomavirus Molecular Biology and Disease Association." Rev Med Virol 25 Suppl 1, (2015): 2-23.

Doorbar, J., W. Quint, L. Banks, I. G. Bravo, M. Stoler, T. R. Broker and M. A. Stanley. "The Biology and Life-Cycle of Human Papillomaviruses." Vaccine 30 Suppl 5, (2012): F55-70.

Dunne, E. F., E. R. Unger, M. Sternberg, G. McQuillan, D. C. Swan, S. S. Patel and L. E. Markowitz. "Prevalence of Hpv Infection among Females in the United States." JAMA 297, no. 8 (2007): 813-9.

Dutta, S., C. Chakraborty, A. K. Dutta, R. K. Mandal, S. Roychoudhury, P. Basu and C. K. Panda. "Physical and Methylation Status of Human Papillomavirus 16 in Asymptomatic Cervical Infections Changes with Malignant Transformation." J Clin Pathol 68, no. 3 (2015): 206-11.

Egawa, K. "Do Human Papillomaviruses Target Epidermal Stem Cells?" Dermatology 207, no. 3 (2003): 251-4.

Egawa, N., K. Egawa, H. Griffin and J. Doorbar. "Human Papillomaviruses; Epithelial Tropisms, and the Development of Neoplasia." Viruses 7, no. 7 (2015): 3863-90.

Enemark, E. J. and L. Joshua-Tor. "Mechanism of DNA Translocation in a Replicative Hexameric Helicase." Nature 442, no. 7100 (2006): 270-5.

Fera, D., D. C. Schultz, S. Hodawadekar, M. Reichman, P. S. Donover, J. Melvin, S. Troutman, J. L. Kissil, D. M. Huryn and R. Marmorstein. "Identification and Characterization of Small Molecule Antagonists of Prb Inactivation by Viral Oncoproteins." Chem Biol 19, no. 4 (2012): 518-28.

Filippova, M., M. M. Johnson, M. Bautista, V. Filippov, N. Fodor, S. S. Tungteakkhun, K. Williams and P. J. Duerksen-Hughes. "The Large and Small Isoforms of Human Papillomavirus Type 16 E6 Bind to and Differentially Affect Procaspase 8 Stability and Activity." J Virol 81, no. 8 (2007): 4116-29.

Filippova, M., H. Song, J. L. Connolly, T. S. Dermody and P. J. Duerksen-Hughes. "The Human Papillomavirus 16 E6 Protein Binds to Tumor Necrosis Factor (Tnf) R1 and Protects Cells from Tnf-Induced Apoptosis." J Biol Chem 277, no. 24 (2002): 21730-9.

Finnen, R. L., K. D. Erickson, X. S. Chen and R. L. Garcea. "Interactions between Papillomavirus L1 and L2 Capsid Proteins." J Virol 77, no. 8 (2003): 4818-26.

Fradet-Turcotte, A., C. Moody, L. A. Laimins and J. Archambault. "Nuclear Export of Human Papillomavirus Type 31 E1 Is Regulated by Cdk2 Phosphorylation and Required for Viral Genome Maintenance." J Virol 84, no. 22 (2010): 11747-60.

Frattini, M. G. and L. A. Laimins. "Binding of the Human Papillomavirus E1 Origin-Recognition Protein Is Regulated through Complex Formation with the E2 Enhancer-Binding Protein." Proc Natl Acad Sci U S A 91, no. 26 (1994): 12398-402.

Garcia-Alai, M. M., L. G. Alonso and G. de Prat-Gay. "The N-Terminal Module of Hpv16 E7 Is an Intrinsically Disordered Domain That Confers Conformational and Recognition Plasticity to the Oncoprotein." Biochemistry 46, no. 37 (2007): 10405-12.

Garcia-Alai, M. M., K. I. Dantur, C. Smal, L. Pietrasanta and G. de Prat-Gay. "High-Risk Hpv E6 Oncoproteins Assemble into Large Oligomers That Allow Localization of Endogenous Species in Prototypic Hpv-Transformed Cell Lines." Biochemistry 46, no. 2 (2007): 341-9.

Garland, S. M., S. K. Kjaer, N. Munoz, S. L. Block, D. R. Brown, M. J. DiNubile, B. R. Lindsay, B. J. Kuter, G. Perez, G. Dominiak-Felden, A. J. Saah, R. Drury, R. Das and C. Velicer. "Impact and Effectiveness of the Quadrivalent Human Papillomavirus Vaccine: A Systematic Review of 10 Years of Real-World Experience." Clin Infect Dis 63, no. 4 (2016): 519-27.

Geisen, C. and T. Kahn. "Promoter Activity of Sequences Located Upstream of the Human Papillomavirus Types of 16 and 18 Late Regions." J Gen Virol 77 (Pt 9), (1996): 2193-200.

Gewin, L., H. Myers, T. Kiyono and D. A. Galloway. "Identification of a Novel Telomerase Repressor That Interacts with the Human Papillomavirus Type-16 E6/E6-Ap Complex." Genes Dev 18, no. 18 (2004): 2269-82.

Giroglou, T., L. Florin, F. Schafer, R. E. Streeck and M. Sapp. "Human Papillomavirus Infection Requires Cell Surface Heparan Sulfate." J Virol 75, no. 3 (2001): 1565-70.

Giuliano, A. R., G. Tortolero-Luna, E. Ferrer, A. N. Burchell, S. de Sanjose, S. K. Kjaer, N. Munoz, M. Schiffman and F. X. Bosch. "Epidemiology of Human Papillomavirus Infection in Men, Cancers Other Than Cervical and Benign Conditions." Vaccine 26 Suppl 10, (2008): K17-28.

Glaunsinger, B. A., S. S. Lee, M. Thomas, L. Banks and R. Javier. "Interactions of the Pdz-Protein Magi-1 with Adenovirus E4-Orf1 and High-Risk Papillomavirus E6 Oncoproteins." Oncogene 19, no. 46 (2000): 5270-80.

Grimmel, M., E. M. de Villiers, C. Neumann, M. Pawlita and H. zur Hausen. "Characterization of a New Human Papillomavirus (Hpv 41) from Disseminated Warts and Detection of Its DNA in Some Skin Carcinomas." Int J Cancer 41, no. 1 (1988): 5-9.

Groves, I. J. and N. Coleman. "Pathogenesis of Human Papillomavirus-Associated Mucosal Disease." J Pathol 235, no. 4 (2015): 527-38.

Gu, W., L. Putral, K. Hengst, K. Minto, N. A. Saunders, G. Leggatt and N. A. McMillan. "Inhibition of Cervical Cancer Cell Growth in Vitro and in Vivo with Lentiviral-Vector Delivered Short Hairpin Rna Targeting Human Papillomavirus E6 and E7 Oncogenes." Cancer Gene Ther 13, no. 11 (2006): 1023-32.

Handa, K., T. Yugawa, M. Narisawa-Saito, S. Ohno, M. Fujita and T. Kiyono. "E6ap-Dependent Degradation of Dlg4/Psd95 by High-Risk Human Papillomavirus Type 18 E6 Protein." J Virol 81, no. 3 (2007): 1379-89.

Hasan, U. A., E. Bates, F. Takeshita, A. Biliato, R. Accardi, V. Bouvard, M. Mansour, I. Vincent, L. Gissmann, T. Iftner, M. Sideri, F. Stubenrauch and M. Tommasino. "Tlr9 Expression and Function Is Abolished by the Cervical Cancer-Associated Human Papillomavirus Type 16." J Immunol 178, no. 5 (2007): 3186-97.

He, C., D. Mao, G. Hua, X. Lv, X. Chen, P. C. Angeletti, J. Dong, S. W. Remmenga, K. J. Rodabaugh, J. Zhou, P. F. Lambert, P. Yang, J. S. Davis and C. Wang. "The Hippo/Yap Pathway Interacts with Egfr Signaling and Hpv Oncoproteins to Regulate Cervical Cancer Progression." EMBO Mol Med 7, no. 11 (2015): 1426-49.

Hebner, C. M. and L. A. Laimins. "Human Papillomaviruses: Basic Mechanisms of Pathogenesis and Oncogenicity." Rev Med Virol 16, no. 2 (2006): 83-97.

Hegde, R. S., S. R. Grossman, L. A. Laimins and P. B. Sigler. "Crystal Structure at 1.7A of the Bovine Papillomavirus-1 E2 DNA-Binding Domain Bound to Its DNA Target." Nature 359, no. 6395 (1992): 505-12.

Hindmarsh, P. L. and L. A. Laimins. "Mechanisms Regulating Expression of the Hpv 31 L1 and L2 Capsid Proteins and Pseudovirion Entry." Virol J 4, (2007): 19.

Holmgren, S. C., N. A. Patterson, M. A. Ozbun and P. F. Lambert. "The Minor Capsid Protein L2 Contributes to Two Steps in the Human Papillomavirus Type 31 Life Cycle." J Virol 79, no. 7 (2005): 3938-48.

Honda, R. and H. Yasuda. "Activity of Mdm2, a Ubiquitin Ligase, toward P53 or Itself Is Dependent on the Ring Finger Domain of the Ligase." Oncogene 19, no. 11 (2000): 1473-6.

Howie, H. L., R. A. Katzenellenbogen and D. A. Galloway. "Papillomavirus E6 Proteins." Virology 384, no. 2 (2009): 324-34.

Howley, P. M. "Warts, Cancer and Ubiquitylation: Lessons from the Papillomaviruses." Trans Am Clin Climatol Assoc 117, (2006): 113-26; discussion 126-7.

Howley, P. M. and H. J. Pfister. "Beta Genus Papillomaviruses and Skin Cancer." Virology 479-480, (2015): 290-6.

Hu, T., S. Ferril, A. Snider and M. Barbosa. "In-Vivo Analysis of Hpv E7 Protein Association with Prb, P107 and P130." Int J Oncol 6, no. 1 (1995): 167-74.

Huh, K., X. Zhou, H. Hayakawa, J. Y. Cho, T. A. Libermann, J. Jin, J. W. Harper and K. Munger. "Human Papillomavirus Type 16 E7 Oncoprotein Associates with the Cullin 2 Ubiquitin Ligase Complex, Which Contributes to Degradation of the Retinoblastoma Tumor Suppressor." J Virol 81, no. 18 (2007): 9737-47.

Huh, K. W., J. DeMasi, H. Ogawa, Y. Nakatani, P. M. Howley and K. Munger. "Association of the Human Papillomavirus Type 16 E7 Oncoprotein with the 600-Kda Retinoblastoma Protein-Associated Factor, P600." Proc Natl Acad Sci U S A 102, no. 32 (2005): 11492-7.

Huibregtse, J. M., M. Scheffner and P. M. Howley. "Localization of the E6-Ap Regions That Direct Human Papillomavirus E6 Binding, Association with P53, and Ubiquitination of Associated Proteins." Mol Cell Biol 13, no. 8 (1993): 4918-27.

Humbert, P. O., N. A. Grzeschik, A. M. Brumby, R. Galea, I. Elsum and H. E. Richardson. "Control of Tumourigenesis by the Scribble/Dlg/Lgl Polarity Module." Oncogene 27, no. 55 (2008): 6888-907.

Janknecht, R. "On the Road to Immortality: Htert Upregulation in Cancer Cells." FEBS Lett 564, no. 1-2 (2004): 9-13.

Jiang, P. and Y. Yue. "Human Papillomavirus Oncoproteins and Apoptosis (Review)." Exp Ther Med 7, no. 1 (2014): 3-7.

Jonson, A. L., L. M. Rogers, S. Ramakrishnan and L. S. Downs, Jr. "Gene Silencing with Sirna Targeting E6/E7 as a Therapeutic Intervention in a Mouse Model of Cervical Cancer." Gynecol Oncol 111, no. 2 (2008): 356-64.

Kehmeier, E., H. Ruhl, B. Voland, M. C. Stoppler, E. Androphy and H. Stoppler. "Cellular Steady-State Levels of "High Risk" but Not "Low Risk" Human Papillomavirus (Hpv) E6 Proteins Are Increased by Inhibition of Proteasome-Dependent Degradation Independent of Their P53- and E6ap-Binding Capabilities." Virology 299, no. 1 (2002): 72-87.

Kessis, T. D., R. J. Slebos, W. G. Nelson, M. B. Kastan, B. S. Plunkett, S. M. Han, A. T. Lorincz, L. Hedrick and K. R. Cho. "Human Papillomavirus 16 E6 Expression Disrupts the P53-Mediated Cellular Response to DNA Damage." Proc Natl Acad Sci U S A 90, no. 9 (1993): 3988-92.

Knapp, A. A., P. M. McManus, K. Bockstall and J. Moroianu. "Identification of the Nuclear Localization and Export Signals of High Risk Hpv16 E7 Oncoprotein." Virology 383, no. 1 (2009): 60-8.

Knight, G. L., J. R. Grainger, P. H. Gallimore and S. Roberts. "Cooperation between Different Forms of the Human Papillomavirus Type 1 E4 Protein to Block Cell Cycle Progression and Cellular DNA Synthesis." J Virol 78, no. 24 (2004): 13920-33.

Koivusalo, R., E. Krausz, H. Helenius and S. Hietanen. "Chemotherapy Compounds in Cervical Cancer Cells Primed by Reconstitution of P53 Function after Short Interfering Rna-Mediated Degradation of Human Papillomavirus 18 E6 Mrna: Opposite Effect of Sirna in Combination with Different Drugs." Mol Pharmacol 68, no. 2 (2005): 372-82.

Kruppel, U., A. Muller-Schiffmann, S. E. Baldus, S. Smola-Hess and G. Steger. "E2 and the Co-Activator P300 Can Cooperate in Activation of the Human Papillomavirus Type 16 Early Promoter." Virology 377, no. 1 (2008): 151-9.

Kumar, A., Y. Zhao, G. Meng, M. Zeng, S. Srinivasan, L. M. Delmolino, Q. Gao, G. Dimri, G. F. Weber, D. E. Wazer, H. Band and V. Band. "Human Papillomavirus Oncoprotein E6 Inactivates the Transcriptional Coactivator Human Ada3." Mol Cell Biol 22, no. 16 (2002): 5801-12.

Kuner, R., M. Vogt, H. Sultmann, A. Buness, S. Dymalla, J. Bulkescher, M. Fellmann, K. Butz, A. Poustka and F. Hoppe-Seyler. "Identification of Cellular Targets for the Human Papillomavirus E6 and E7 Oncogenes by Rna Interference and Transcriptome Analyses." J Mol Med (Berl) 85, no. 11 (2007): 1253-62.

Lambert, C. R. "Pathophysiology of Stable Angina Pectoris." Cardiol Clin 9, no. 1 (1991): 1-10.

Lee, D., H. Z. Kim, K. W. Jeong, Y. S. Shim, I. Horikawa, J. C. Barrett and J. Choe. "Human Papillomavirus E2 Down-Regulates the Human Telomerase Reverse Transcriptase Promoter." J Biol Chem 277, no. 31 (2002): 27748-56.

Lee, J. O., A. A. Russo and N. P. Pavletich. "Structure of the Retinoblastoma Tumour-Suppressor Pocket Domain Bound to a Peptide from Hpv E7." Nature 391, no. 6670 (1998): 859-65.

Liu, J. S., S. R. Kuo, A. M. Makhov, D. M. Cyr, J. D. Griffith, T. R. Broker and L. T. Chow. "Human Hsp70 and Hsp40 Chaperone Proteins Facilitate Human Papillomavirus-11 E1 Protein Binding to the Origin and Stimulate Cell-Free DNA Replication." J Biol Chem 273, no. 46 (1998): 30704-12.

Liu, Y., G. D. Henry, R. S. Hegde and J. D. Baleja. "Solution Structure of the Hdlg/Sap97 Pdz2 Domain and Its Mechanism of Interaction with Hpv-18 Papillomavirus E6 Protein." Biochemistry 46, no. 38 (2007): 10864-74.

Loregian, A., B. A. Appleton, J. M. Hogle and D. M. Coen. "Residues of Human Cytomegalovirus DNA Polymerase Catalytic Subunit Ul54 That Are Necessary and Sufficient for Interaction with the Accessory Protein Ul44." J Virol 78, no. 1 (2004): 158-67.

Ma, T., N. Zou, B. Y. Lin, L. T. Chow and J. W. Harper. "Interaction between Cyclin-Dependent Kinases and Human Papillomavirus Replication-Initiation Protein E1 Is Required for Efficient Viral Replication." Proc Natl Acad Sci U S A 96, no. 2 (1999): 382-7.

Malecka, K. A., D. Fera, D. C. Schultz, S. Hodawadekar, M. Reichman, P. S. Donover, M. E. Murphy and R. Marmorstein. "Identification and Characterization of Small Molecule Human Papillomavirus E6 Inhibitors." ACS Chem Biol 9, no. 7 (2014): 1603-12.

Mallen-St Clair, J., M. Alani, M. B. Wang and E. S. Srivatsan. "Human Papillomavirus in Oropharyngeal Cancer: The Changing Face of a Disease." Biochim Biophys Acta 1866, no. 2 (2016): 141-150.

Manzo-Merino, J., M. Thomas, A. M. Fuentes-Gonzalez, M. Lizano and L. Banks. "Hpv E6 Oncoprotein as a Potential Therapeutic Target in Hpv Related Cancers." Expert Opin Ther Targets 17, no. 11 (2013): 1357-68.

Markowitz, L. E., S. Hariri, C. Lin, E. F. Dunne, M. Steinau, G. McQuillan and E. R. Unger. "Reduction in Human Papillomavirus (Hpv) Prevalence among Young Women Following Hpv Vaccine Introduction in the United States, National Health and Nutrition Examination Surveys, 2003-2010." J Infect Dis 208, no. 3 (2013): 385-93.

Martinez-Zapien, D., F. X. Ruiz, J. Poirson, A. Mitschler, J. Ramirez, A. Forster, A. Cousido-Siah, M. Masson, S. Vande Pol, A. Podjarny, G. Trave and K. Zanier. "Structure of the E6/E6ap/P53 Complex Required for Hpv-Mediated Degradation of P53." Nature 529, no. 7587 (2016): 541-5.

Massari, S., G. Nannetti, L. Goracci, L. Sancineto, G. Muratore, S. Sabatini, G. Manfroni, B. Mercorelli, V. Cecchetti, M. Facchini, G. Palu, G. Cruciani, A. Loregian and O. Tabarrini. "Structural Investigation of Cycloheptathiophene-3-Carboxamide Derivatives Targeting Influenza Virus Polymerase Assembly." J Med Chem 56, no. 24 (2013): 10118-31.

Massimi, P. and L. Banks. "Repression of P53 Transcriptional Activity by the Hpv E7 Proteins." Virology 227, no. 1 (1997): 255-9.

Massimi, P., N. Gammoh, M. Thomas and L. Banks. "Hpv E6 Specifically Targets Different Cellular Pools of Its Pdz Domain-Containing Tumour Suppressor Substrates for Proteasome-Mediated Degradation." Oncogene 23, no. 49 (2004): 8033-9.

Massimi, P., A. Shai, P. Lambert and L. Banks. "Hpv E6 Degradation of P53 and Pdz Containing Substrates in an E6ap Null Background." Oncogene 27, no. 12 (2008): 1800-4.

McBride, A. A., H. Romanczuk and P. M. Howley. "The Papillomavirus E2 Regulatory Proteins." J Biol Chem 266, no. 28 (1991): 18411-4.

McIntosh, P. B., S. R. Martin, D. J. Jackson, J. Khan, E. R. Isaacson, L. Calder, K. Raj, H. M. Griffin, Q. Wang, P. Laskey, J. F. Eccleston and J. Doorbar. "Structural Analysis Reveals an Amyloid Form of the Human Papillomavirus Type 16 E1--E4 Protein and Provides a Molecular Basis for Its Accumulation." J Virol 82, no. 16 (2008): 8196-203.

McIntyre, M. C., M. N. Ruesch and L. A. Laimins. "Human Papillomavirus E7 Oncoproteins Bind a Single Form of Cyclin E in a Complex with Cdk2 and P107." Virology 215, no. 1 (1996): 73-82.

McLaughlin-Drubin, M. E., K. W. Huh and K. Munger. "Human Papillomavirus Type 16 E7 Oncoprotein Associates with E2f6." J Virol 82, no. 17 (2008): 8695-705.

Melendy, T., J. Sedman and A. Stenlund. "Cellular Factors Required for Papillomavirus DNA Replication." J Virol 69, no. 12 (1995): 7857-67.

Mertens, B., T. Nogueira, R. Stranska, N. Lieve, G. Andrei and R. Snoeck. "Cidofovir Is Active against Human Papillomavirus Positive and Negative Head and Neck and Cervical Tumor Cells by Causing DNA Damage as One of Its Working Mechanisms." Oncotarget, (2016).

Mesri, E. A., M. A. Feitelson and K. Munger. "Human Viral Oncogenesis: A Cancer Hallmarks Analysis." Cell Host Microbe 15, no. 3 (2014): 266-82.

Moody, C. A. and L. A. Laimins. "Human Papillomavirus Oncoproteins: Pathways to Transformation." Nat Rev Cancer 10, no. 8 (2010): 550-60.

Mullard, A. "Protein-Protein Interaction Inhibitors Get into the Groove." Nat Rev Drug Discov 11, no. 3 (2012): 173-5.

Munger, K., B. A. Werness, N. Dyson, W. C. Phelps, E. Harlow and P. M. Howley. "Complex Formation of Human Papillomavirus E7 Proteins with the Retinoblastoma Tumor Suppressor Gene Product." EMBO J 8, no. 13 (1989): 4099-105.

Munoz, N., F. X. Bosch, S. de Sanjose, R. Herrero, X. Castellsague, K. V. Shah, P. J. Snijders, C. J. Meijer and Group International Agency for Research on Cancer Multicenter Cervical Cancer Study. "Epidemiologic Classification of Human Papillomavirus Types Associated with Cervical Cancer." N Engl J Med 348, no. 6 (2003): 518-27.

Muratore, G., L. Goracci, B. Mercorelli, A. Foeglein, P. Digard, G. Cruciani, G. Palu and A. Loregian. "Small Molecule Inhibitors of Influenza A and B Viruses That Act by Disrupting Subunit Interactions of the Viral Polymerase." Proc Natl Acad Sci U S A 109, no. 16 (2012): 6247-52.

Nakagawa, S. and J. M. Huibregtse. "Human Scribble (Vartul) Is Targeted for Ubiquitin-Mediated Degradation by the High-Risk Papillomavirus E6 Proteins and the E6ap Ubiquitin-Protein Ligase." Mol Cell Biol 20, no. 21 (2000): 8244-53.

Nasseri, M., R. Hirochika, T. R. Broker and L. T. Chow. "A Human Papilloma Virus Type 11 Transcript Encoding an E1--E4 Protein." Virology 159, no. 2 (1987): 433-9.

Nguyen, C. L. and K. Munger. "Direct Association of the Hpv16 E7 Oncoprotein with Cyclin a/Cdk2 and Cyclin E/Cdk2 Complexes." Virology 380, no. 1 (2008): 21-5.

Nomine, Y., T. Ristriani, C. Laurent, J. F. Lefevre, E. Weiss and G. Trave. "Formation of Soluble Inclusion Bodies by Hpv E6 Oncoprotein Fused to Maltose-Binding Protein." Protein Expr Purif 23, no. 1 (2001): 22-32.

Ohlenschlager, O., T. Seiboth, H. Zengerling, L. Briese, A. Marchanka, R. Ramachandran, M. Baum, M. Korbas, W. Meyer-Klaucke, M. Durst and M. Gorlach. "Solution Structure of the Partially Folded High-Risk Human Papilloma Virus 45 Oncoprotein E7." Oncogene 25, no. 44 (2006): 5953-9.

Oliveira, J. G., L. A. Colf and A. A. McBride. "Variations in the Association of Papillomavirus E2 Proteins with Mitotic Chromosomes." Proc Natl Acad Sci U S A 103, no. 4 (2006): 1047-52.

Ozbun, M. A. and C. Meyers. "Characterization of Late Gene Transcripts Expressed During Vegetative Replication of Human Papillomavirus Type 31b." J Virol 71, no. 7 (1997): 5161-72.

Pereira-Suarez, A. L., M. A. Meraz, M. Lizano, C. Estrada-Chavez, F. Hernandez, P. Olivera, E. Perez, P. Padilla, M. Yaniv, F. Thierry and A. Garcia-Carranca. "Frequent Alterations of the Beta-Catenin Protein in Cancer of the Uterine Cervix." Tumour Biol 23, no. 1 (2002): 45-53.

Piccolo, S., S. Dupont and M. Cordenonsi. "The Biology of Yap/Taz: Hippo Signaling and Beyond." Physiol Rev 94, no. 4 (2014): 1287-312.

Pim, D. and L. Banks. "Hpv-18 E6*I Protein Modulates the E6-Directed Degradation of P53 by Binding to Full-Length Hpv-18 E6." Oncogene 18, no. 52 (1999): 7403-8.

Pim, D., P. Massimi and L. Banks. "Alternatively Spliced Hpv-18 E6* Protein Inhibits E6 Mediated Degradation of P53 and Suppresses Transformed Cell Growth." Oncogene 15, no. 3 (1997): 257-64.

Pim, D., P. Massimi, S. M. Dilworth and L. Banks. "Activation of the Protein Kinase B Pathway by the Hpv-16 E7 Oncoprotein Occurs through a Mechanism Involving Interaction with Pp2a." Oncogene 24, no. 53 (2005): 7830-8.

Pim, D., V. Tomaic and L. Banks. "The Human Papillomavirus (Hpv) E6* Proteins from High-Risk, Mucosal Hpvs Can Direct Degradation of Cellular Proteins in the Absence of Full-Length E6 Protein." J Virol 83, no. 19 (2009): 9863-74.

Quint, K. D., R. E. Genders, M. N. de Koning, C. Borgogna, M. Gariglio, J. N. Bouwes Bavinck, J. Doorbar and M. C. Feltkamp. "Human Beta-Papillomavirus Infection and Keratinocyte Carcinomas." J Pathol 235, no. 2 (2015): 342-54.

Ramirez, J., J. Poirson, C. Foltz, Y. Chebaro, M. Schrapp, A. Meyer, A. Bonetta, A. Forster, Y. Jacob, M. Masson, F. Deryckere and G. Trave. "Targeting the Two Oncogenic Functional Sites of the Hpv E6 Oncoprotein with a High-Affinity Bivalent Ligand." Angew Chem Int Ed Engl 54, no. 27 (2015): 7958-62.

Rampias, T., E. Boutati, E. Pectasides, C. Sasaki, P. Kountourakis, P. Weinberger and A. Psyrri. "Activation of Wnt Signaling Pathway by Human Papillomavirus E6 and E7 Oncogenes in Hpv16-Positive Oropharyngeal Squamous Carcinoma Cells." Mol Cancer Res 8, no. 3 (2010): 433-43.

Richards, R. M., D. R. Lowy, J. T. Schiller and P. M. Day. "Cleavage of the Papillomavirus Minor Capsid Protein, L2, at a Furin Consensus Site Is Necessary for Infection." Proc Natl Acad Sci U S A 103, no. 5 (2006): 1522-7.

Ristriani, T., S. Fournane, G. Orfanoudakis, G. Trave and M. Masson. "A Single-Codon Mutation Converts Hpv16 E6 Oncoprotein into a Potential Tumor Suppressor, Which Induces P53-Dependent Senescence of Hpv-Positive Hela Cervical Cancer Cells." Oncogene 28, no. 5 (2009): 762-72.

Ronco, L. V., A. Y. Karpova, M. Vidal and P. M. Howley. "Human Papillomavirus 16 E6 Oncoprotein Binds to Interferon Regulatory Factor-3 and Inhibits Its Transcriptional Activity." Genes Dev 12, no. 13 (1998): 2061-72.

Rush, M., X. Zhao and S. Schwartz. "A Splicing Enhancer in the E4 Coding Region of Human Papillomavirus Type 16 Is Required for Early Mrna Splicing and Polyadenylation as Well as Inhibition of Premature Late Gene Expression." J Virol 79, no. 18 (2005): 12002-15.

Sanders, C. M. and A. Stenlund. "Recruitment and Loading of the E1 Initiator Protein: An Atp-Dependent Process Catalysed by a Transcription Factor." EMBO J 17, no. 23 (1998): 7044-55.

Sapp, M. and P. M. Day. "Structure, Attachment and Entry of Polyoma- and Papillomaviruses." Virology 384, no. 2 (2009): 400-9.

Sarafi, T. R. and A. A. McBride. "Domains of the Bpv-1 E1 Replication Protein Required for Origin-Specific DNA Binding and Interaction with the E2 Transactivator." Virology 211, no. 2 (1995): 385-96.

Scheffner, M., B. A. Werness, J. M. Huibregtse, A. J. Levine and P. M. Howley. "The E6 Oncoprotein Encoded by Human Papillomavirus Types 16 and 18 Promotes the Degradation of P53." Cell 63, no. 6 (1990): 1129-36.

Schwartz, S. "Papillomavirus Transcripts and Posttranscriptional Regulation." Virology 445, no. 1-2 (2013): 187-96.

Shin, M. K., S. Balsitis, T. Brake and P. F. Lambert. "Human Papillomavirus E7 Oncoprotein Overrides the Tumor Suppressor Activity of P21cip1 in Cervical Carcinogenesis." Cancer Res 69, no. 14 (2009): 5656-63.

Siegel, R., J. Ma, Z. Zou and A. Jemal. "Cancer Statistics, 2014." CA Cancer J Clin 64, no. 1 (2014): 9-29.

Song, S., A. Liem, J. A. Miller and P. F. Lambert. "Human Papillomavirus Types 16 E6 and E7 Contribute Differently to Carcinogenesis." Virology 267, no. 2 (2000): 141-50.

Spangle, J. M. and K. Munger. "The Hpv16 E6 Oncoprotein Causes Prolonged Receptor Protein Tyrosine Kinase Signaling and Enhances Internalization of Phosphorylated Receptor Species." PLoS Pathog 9, no. 3 (2013): e1003237.

Stanley, M. "Immunobiology of Hpv and Hpv Vaccines." Gynecol Oncol 109, no. 2 Suppl (2008): S15-21.

Steger, G. and S. Corbach. "Dose-Dependent Regulation of the Early Promoter of Human Papillomavirus Type 18 by the Viral E2 Protein." J Virol 71, no. 1 (1997): 50-8.

Stewart, D., A. Ghosh and G. Matlashewski. "Involvement of Nuclear Export in Human Papillomavirus Type 18 E6-Mediated Ubiquitination and Degradation of P53." J Virol 79, no. 14 (2005): 8773-83.

Stewart, D., S. Kazemi, S. Li, P. Massimi, L. Banks, A. E. Koromilas and G. Matlashewski. "Ubiquitination and Proteasome Degradation of the E6 Proteins of Human Papillomavirus Types 11 and 18." J Gen Virol 85, no. Pt 6 (2004): 1419-26.

Stutz, C., E. Reinz, A. Honegger, J. Bulkescher, J. Schweizer, K. Zanier, G. Trave, C. Lohrey, K. Hoppe-Seyler and F. Hoppe-Seyler. "Intracellular Analysis of the Interaction between the Human Papillomavirus Type 16 E6 Oncoprotein and Inhibitory Peptides." PLoS One 10, no. 7 (2015): e0132339.

Suarez-Ibarrola, R., A. Heinze, F. Sanchez-Sagastegui, A. Negrin-Ramirez, R. Aguilar-Anzures, L. Xochihua-Diaz and J. O. Cuevas-Alpuche. "Giant Condyloma Acuminatum in the Genital, Perineal and Perianal Region in a Pediatric Patient. Literature Review and Case Report." Urol Case Rep 7, (2016): 14-6.

Swindle, C. S. and J. A. Engler. "Association of the Human Papillomavirus Type 11 E1 Protein with Histone H1." J Virol 72, no. 3 (1998): 1994-2001.

Talora, C., D. C. Sgroi, C. P. Crum and G. P. Dotto. "Specific Down-Modulation of Notch1 Signaling in Cervical Cancer Cells Is Required for Sustained Hpv-E6/E7 Expression and Late Steps of Malignant Transformation." Genes Dev 16, no. 17 (2002): 2252-63.

Tao, M., M. Kruhlak, S. Xia, E. Androphy and Z. M. Zheng. "Signals That Dictate Nuclear Localization of Human Papillomavirus Type 16 Oncoprotein E6 in Living Cells." J Virol 77, no. 24 (2003): 13232-47.

Thomas, M. and L. Banks. "Inhibition of Bak-Induced Apoptosis by Hpv-18 E6." Oncogene 17, no. 23 (1998): 2943-54.

Thomas, M., M. P. Myers, P. Massimi, C. Guarnaccia and L. Banks. "Analysis of Multiple Hpv E6 Pdz Interactions Defines Type-Specific Pdz Fingerprints That Predict Oncogenic Potential." PLoS Pathog 12, no. 8 (2016): e1005766.

Todorovic, B., P. Massimi, K. Hung, G. S. Shaw, L. Banks and J. S. Mymryk. "Systematic Analysis of the Amino Acid Residues of Human Papillomavirus Type 16 E7 Conserved Region 3 Involved in Dimerization and Transformation." J Virol 85, no. 19 (2011): 10048-57.

Todorovic, B., A. C. Nichols, J. M. Chitilian, M. P. Myers, T. G. Shepherd, S. J. Parsons, J. W. Barrett, L. Banks and J. S. Mymryk. "The Human Papillomavirus E7 Proteins Associate with P190rhogap and Alter Its Function." J Virol 88, no. 7 (2014): 3653-63.

Ustav, M. and A. Stenlund. "Transient Replication of Bpv-1 Requires Two Viral Polypeptides Encoded by the E1 and E2 Open Reading Frames." EMBO J 10, no. 2 (1991): 449-57.

Veldman, T., X. Liu, H. Yuan and R. Schlegel. "Human Papillomavirus E6 and Myc Proteins Associate in Vivo and Bind to and Cooperatively Activate the Telomerase Reverse Transcriptase Promoter." Proc Natl Acad Sci U S A 100, no. 14 (2003): 8211-6.

Villa, L. L., R. L. Costa, C. A. Petta, R. P. Andrade, K. A. Ault, A. R. Giuliano, C. M. Wheeler, L. A. Koutsky, C. Malm, M. Lehtinen, F. E. Skjeldestad, S. E. Olsson, M. Steinwall, D. R. Brown, R. J. Kurman, B. M. Ronnett, M. H. Stoler, A. Ferenczy, D. M. Harper, G. M. Tamms, J. Yu, L. Lupinacci, R. Railkar, F. J. Taddeo, K. U. Jansen, M. T. Esser, H. L. Sings, A. J. Saah and E. Barr. "Prophylactic Quadrivalent Human Papillomavirus (Types 6, 11, 16, and 18) L1 Virus-Like Particle Vaccine in Young Women: A Randomised Double-Blind Placebo-Controlled Multicentre Phase Ii Efficacy Trial." Lancet Oncol 6, no. 5 (2005): 271-8.

Villanueva-Toledo, J., A. Ponciano-Gomez, E. Ortiz-Sanchez and E. Garrido. "Side Populations from Cervical-Cancer-Derived Cell Lines Have Stem-Cell-Like Properties." Mol Biol Rep 41, no. 4 (2014): 1993-2004.

Vos, R. M., J. Altreuter, E. A. White and P. M. Howley. "The Ubiquitin-Specific Peptidase Usp15 Regulates Human Papillomavirus Type 16 E6 Protein Stability." J Virol 83, no. 17 (2009): 8885-92.

Wang, Y. W., H. S. Chang, C. H. Lin and W. C. Yu. "Hpv-18 E7 Conjugates to C-Myc and Mediates Its Transcriptional Activity." Int J Biochem Cell Biol 39, no. 2 (2007): 402-12.

Werness, B. A., A. J. Levine and P. M. Howley. "Association of Human Papillomavirus Types 16 and 18 E6 Proteins with P53." Science 248, no. 4951 (1990): 76-9.

Wu, D. and W. Pan. "Gsk3: A Multifaceted Kinase in Wnt Signaling." Trends Biochem Sci 35, no. 3 (2010): 161-8.

Yan, X., W. Shah, L. Jing, H. Chen and Y. Wang. "High-Risk Human Papillomavirus Type 18 E7 Caused P27 Elevation and Cytoplasmic Localization." Cancer Biol Ther 9, no. 9 (2010): 728-35.

Yang, L., I. Mohr, E. Fouts, D. A. Lim, M. Nohaile and M. Botchan. "The E1 Protein of Bovine Papilloma Virus 1 Is an Atp-Dependent DNA Helicase." Proc Natl Acad Sci U S A 90, no. 11 (1993): 5086-90.

Yoon, C. S., K. D. Kim, S. N. Park and S. W. Cheong. "Alpha(6) Integrin Is the Main Receptor of Human Papillomavirus Type 16 Vlp." Biochem Biophys Res Commun 283, no. 3 (2001): 668-73.

Yuan, C. H., M. Filippova, S. S. Tungteakkhun, P. J. Duerksen-Hughes and J. L. Krstenansky. "Small Molecule Inhibitors of the Hpv16-E6 Interaction with Caspase 8." Bioorg Med Chem Lett 22, no. 5 (2012): 2125-9.

Yuan, H., F. Fu, J. Zhuo, W. Wang, J. Nishitani, D. S. An, I. S. Chen and X. Liu. "Human Papillomavirus Type 16 E6 and E7 Oncoproteins Upregulate C-Iap2 Gene Expression and Confer Resistance to Apoptosis." Oncogene 24, no. 32 (2005): 5069-78.

Zanconato, F., M. Cordenonsi and S. Piccolo. "Yap/Taz at the Roots of Cancer." Cancer Cell 29, no. 6 (2016): 783-803.

Zanconato, F., M. Forcato, G. Battilana, L. Azzolin, E. Quaranta, B. Bodega, A. Rosato, S. Bicciato, M. Cordenonsi and S. Piccolo. "Genome-Wide Association between Yap/Taz/Tead and Ap-1 at Enhancers Drives Oncogenic Growth." Nat Cell Biol 17, no. 9 (2015): 1218-27.

Zanier, K., S. Charbonnier, A. O. Sidi, A. G. McEwen, M. G. Ferrario, P. Poussin-Courmontagne, V. Cura, N. Brimer, K. O. Babah, T. Ansari, I. Muller, R. H. Stote, J. Cavarelli, S. Vande Pol and G. Trave. "Structural Basis for Hijacking of Cellular Lxxll Motifs by Papillomavirus E6 Oncoproteins." Science 339, no. 6120 (2013): 694-8.

Zanier, K., Y. Nomine, S. Charbonnier, C. Ruhlmann, P. Schultz, J. Schweizer and G. Trave. "Formation of Well-Defined Soluble Aggregates Upon Fusion to Mbp Is a Generic Property of E6 Proteins from Various Human Papillomavirus Species." Protein Expr Purif 51, no. 1 (2007): 59-70.

Zanier, K., Y. Nomine, S. Charbonnier, C. Ruhlmann, P. Schultz, J. Schweizer and G. Trave. "Formation of Well-Defined Soluble Aggregates Upon Fusion to Mbp Is a Generic Property of E6 Proteins from Various Human Papillomavirus Species." Protein Expr Purif 51, no. 1 (2007): 59-70.

Zanier, K., A. ould M'hamed ould Sidi, C. Boulade-Ladame, V. Rybin, A. Chappelle, A. Atkinson, B. Kieffer and G. Trave. "Solution Structure Analysis of the Hpv16 E6 Oncoprotein Reveals a Self-Association Mechanism Required for E6-Mediated Degradation of P53." Structure 20, no. 4 (2012): 604-17.

Zanier, K., C. Ruhlmann, F. Melin, M. Masson, A. Ould M'hamed Ould Sidi, X. Bernard, B. Fischer, L. Brino, T. Ristriani, V. Rybin, M. Baltzinger, S. Vande Pol, P. Hellwig, P. Schultz and G. Trave. "E6 Proteins from Diverse Papillomaviruses Self-Associate Both in Vitro and in Vivo." J Mol Biol 396, no. 1 (2010): 90-104.

Zhang, Y., J. Dasgupta, R. Z. Ma, L. Banks, M. Thomas and X. S. Chen. "Structures of a Human Papillomavirus (Hpv) E6 Polypeptide Bound to Maguk Proteins: Mechanisms of Targeting Tumor Suppressors by a High-Risk Hpv Oncoprotein." J Virol 81, no. 7 (2007): 3618-26.

Zheng, L., H. Ding, Z. Lu, Y. Li, Y. Pan, T. Ning and Y. Ke. "E3 Ubiquitin Ligase E6ap-Mediated Tsc2 Turnover in the Presence and Absence of Hpv16 E6." Genes Cells 13, no. 3 (2008): 285-94.

Zheng, Z. M. and C. C. Baker. "Papillomavirus Genome Structure, Expression, and Post-Transcriptional Regulation." Front Biosci 11, (2006): 2286-302.

Zimmermann, H., R. Degenkolbe, H. U. Bernard and M. J. O'Connor. "The Human Papillomavirus Type 16 E6 Oncoprotein Can Down-Regulate P53 Activity by Targeting the Transcriptional Coactivator Cbp/P300." J Virol 73, no. 8 (1999): 6209-19.

Acknowledgments

I would like to thank my colleagues and my supervisors, prof. Giorgio Palù, for giving me the opportunity to work in the Department of Molecular Medicine, and prof. Arianna Loregian, for her guidance, encouragement and, particularly, for believing in me.

I would also like to deeply thank my family for the patience and unconditional support.

And last but by no means least, my girl Bessa for being part of all of this. Whatever was and will be, this thesis is as much yours as it is mine.